2017

Biophysical Characterization of Tear Film Biomimetics: Interactions of Major Polar Lipids and Proteins

Haley, David Alan

UNIVERSITY OF CALGARY

Biophysical Characterization of Tear Film Biomimetics: Interactions of Major Polar Lipids and Proteins

by

David Alan Haley

A THESIS

SUBMITTED TO THE FACULTY OF GRADUATE STUDIES

IN PARTIAL FULFILMENT OF THE REQUIREMENTS FOR THE

DEGREE OF MASTER OF SCIENCE

GRADUATE PROGRAM IN BIOLOGICAL SCIENCES

CALGARY, ALBERTA

NOVEMBER, 2017

Abstract

The tear film is a multilayered structure that protects the corneal epithelium from stress and damage, and allows for clear vision. A lipid layer shields the primarily aqueous portion of the tear film from the external environment. A polar lipid layer provides an interface between the aqueous layer and a thick nonpolar lipid layer. Dipalmitoylphosphatidylcholine, dipalmitoylphosphatidylethanolamine, palmitoyl-glucocerebroside, palmitoylsphingomyelin, and dipalmitoylphosphatidylserine have been previously identified as polar lipids in whole tear samples. Langmuir trough monolayer experiments were used to assess how major tear film proteins lysozyme, lactoferrin, and tear lipocalin affect the stability and elasticity of the pure lipids and lipid mixtures. Pure lipids and lipid mixtures all displayed high stability and rigidity in the tear film surface pressure range of 20 to 35 mN/m. Biologically relevant concentrations of lysozyme and lactoferrin (> 0.2 mg/mL) appeared to fluidize a quinary lipid mixture. Low concentrations of lipocalin may destabilize polar lipid films.

Preface

This thesis is original, unpublished, independent work by the author, D.A. Haley.

Acknowledgements

I am very grateful and honoured to have had the opportunity to work in Dr. Elmar Prenner's lab. He has cultivated a friendly and collaborative environment where the students help each other and work as a team. He has been a fantastic mentor to all his students, working hard to understand our career goals and tailoring our programs to best prepare us to achieve them after graduation. I am thankful to have been given the support to pursue entrepreneurship courses that have shaped what I will pursue after my program. I was also given the opportunity to travel to Ottawa and Helsinki for conferences, and those experiences were absolutely incredible. I greatly appreciate his encouragement to try different experimental techniques, although only a few ultimately contributed to this thesis.

Thank you to my committee members Dr. Sergei Noskov and Dr. Hans Vogel for sharing their valuable time with me and helping me through my program. I wish to also thank Dr. Kenneth Ng for being my internal/external examiner, and to thank Dr. Greg Moorhead for being my neutral chair.

I also thank all the past and present members of the Prenner lab for their guidance and advice. I need to specifically thank Matthew Patterson for initially training me and laying excellent foundations for this project. If I was ever stuck trouble shooting an experiment for a week, Weiam Drear would usually solve the problem in a few hours, and I'm grateful to her for giving up her time. Dr. Mark Mahadeo was an excellent lab manager, always making sure we were well stocked with supplies, and providing

valuable analyses and advice when needed, especially when we were preparing for presentations. Dr. Patrick Lai used his technical skills to help fix any equipment problems.

I owe a special thanks to the Vogel lab for proteins, guidance, and help. Dr. Zhihong Liu provided the tear lipocalin for these experiments. This work would not have been possible without him. Additionally, Dr. Gopal Ramamourthy, Dr. Mauricio Arias, and Dr. Subrata Paul were extremely helpful when I was given the opportunity to express and purify some tear lipocalin myself. I would also like to thank Dr. Rajesh Kumar and Dr. Chang-Chun Ling for their help in our attempt to synthesize OAHFAs. Although the procedure did not work like we had hoped, I am grateful for their time and expertise.

I also thank my sister Christine and brother-in-law Bryan for their encouragement. I'm especially grateful to my parents John and Sharon. I must thank them for giving me the opportunity to get my undergraduate degree. They have always been so generous and supportive of any endeavor I have undertaken. Lastly, I must thank my wife Kristy for the amazing encouragement and support she has offered during this graduate program. She has patiently supported and encouraged me through all the failed experiments and helped me to overcome the difficulties I have encountered on this journey.

Table of Contents

List of Tables

List of Figures and Illustrations

List of Symbols, Abbreviations and Nomenclature

Symbol	Definition
β	Compression or Expansion Modulus
BAM	Brewster Angle Microscopy
C-Type	Chicken or conventional lysozyme
CBS	Cerebroside
CER	Ceramide
CO	Cholesterol Oleate
DPPC	Dipalmitoylphosphatidylcholine
DPPE	Dipalmitoylphosphatidylethanolamine
FFA	Free Fatty Acids
G	Gas
GC	Glucosylcerebroside
G-Type	Goose Egg-White Lysozyme
DPPS	Dipalmitoylphosphatidylserine
HEWL	Hen Egg White Lysozyme
I-Type	Invertebrate Lysozyme
Lact	Lactoferrin
LC	Liquid Condensed Phase
LE	Liquid Expanded Phase

Lys	Lysozyme
OAHFA	(O-acyl)-ω-hydroxy fatty acid
NAG	N-acetylglucosamine
Symbol	Definition
NAM	N-acetylmuramic acid
PBS	Phosphate Buffered Saline
PC	Phosphatidylcholine
PCTF	Precorneal Tear Film
PE	Phosphatidylethanolamine
PGC	Palmitoylglucocerebroside
PHL	Unidentified Phospholipid
PL	Unidentified Polar Lipid
PLA_2	Phospholipase A_2
PS	Phosphatidylserine
PSM	Palmitoylsphingomyelin
S	Solid Phase
SM	Sphingomyelin
TG	Triglycerides
TLc	Tear Lipocalin
TLC	Thin Layer Chromatography

Chapter One: Introduction

1.1 The Tear Film

The tear film is the thin fluid layer that covers the exposed surface of the eye. It is only 3 μm thick in humans and provides a smooth surface to reduce light scattering, to provide lubrication during a blink, to protect against pathogens, and to supply moisture and nourishment to the surrounding epithelial cells [1,2]. This moist film is evident but researchers have struggled for a long time to understand its importance and complexity. The current understanding of this film is based on hundreds of years of meticulous investigation, conceptualization of nanoscale molecules and multilayered films, and advances in instrumentation. But many questions remain unanswered.

1.2 Anatomy of the Eye Related to the Precorneal Tear Film

Researchers generally differentiate portions of the tear film by whether it is covering the conjunctiva (preconjuctival tear film), or the cornea (precorneal tear film or PCTF) (figure 1.1) [3]. The latter affects vison and thus, the majority of research has focused on this part, which is also the focus of this thesis [3]. Each eye has lacrimal glands that secrete the aqueous portion of the tear film including many of the proteins [4]. Meibomian glands secrete the majority of the lipids found in the tear film [5], primarily from meibomian orifices located on the lid margin (figure 1.1) [6–8].

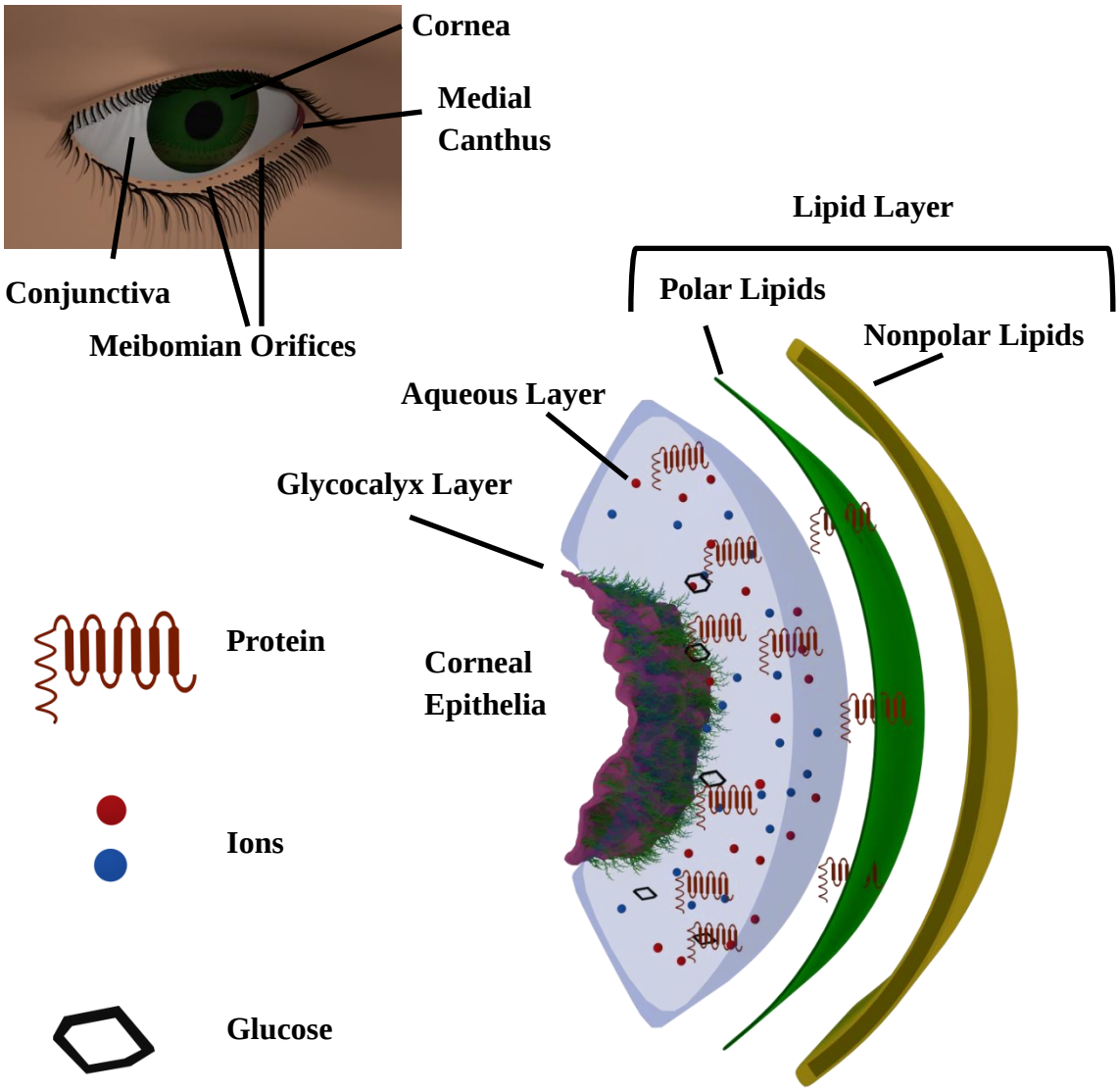

Figure 1.1 Diagram of the surface of the eye and the tear film.

1.3 Structure of the Tear Film

As first theorized by Wolff in 1946, the tear film has a glycocalyx layer covering the epithelial cells of the eye, an aqueous layer, and a lipid layer exposed to the air (figure 1.1) [9].

1.3.1 Glycocalyx Layer (also called the Mucous Layer)

The pre-corneal tear film begins where the surface of the corneal epithelial cells meet the aqueous layer, this interface is known as the glycocalyx layer [7,10]. The exposed surface membranes of many epithelial cell types of humans and other mammals have membrane protrusions that are extended with membrane-associated mucins [11], which are large, heavily glycosylated proteins [12]. Transmembrane mucins hold water near the ocular surface and help form a barrier for invading pathogens by binding with carbohydrate binding proteins [13,14]. In contrast, mucins secreted by goblet cells in the conjunctiva and the lacrimal glands, bind and eliminate debris from the tear film and provide lubrication for the epithelium of the eye during a blink [13]. The glycocalyx layer was originally called the mucus layer by Wolff; however, both secreted and membrane associated mucins are hydrophilic and negatively charged, so contemporary authors think that mucins would not form well-defined layer near the corneal epithelium [7,10,13]. They instead propose the glycocalyx layer containing membrane associated mucins and secreted mucins that are distributed throughout the aqueous layer [13].

1.3.2 Aqueous Layer

Adjacent to the glycocalyx layer is the aqueous layer, which is produced by the lacrimal glands [15]. In addition to containing mucins that lubricate the eye during a blink, the drainage of the aqueous layer allows the tear film to clear pathogens, particles, and other harmful substances [13,16].

The aqueous layer is enriched with different metabolites such as glucose [17]; it has a high protein content (up to 8 mg/mL) and contains a large variety of proteins [18]. In 2006, de Souza *et al.* identified 491 proteins whereas in 2012, Zhou *et al.* reported 1543 [18,19]. The most abundant proteins are lysozyme, lactoferrin, and tear lipocalin (formerly called tear-specific prealbumin) [20]. The most abundant ions in the tear film are Na^+ and Cl^- (>100 mmol/kg), followed by K^+ and HCO^{3-} (<50 mmol/kg), whereas Ca^{2+}, Mg^{2+}, Zn^{2+}, Mn^{2+}, and PO_4^{3-} are only found in very small amounts [21,22]. The pH of tears has been measured to be around 7.4 [23,24].

1.3.3 Lipid Layer

The lipid layer contains mostly nonpolar lipids, although an important layer of polar lipids acts as an interface between the nonpolar lipids and the aqueous layer [25]. There are also proteins that are inserted and adsorbed to the lipid layer [25]. In order to better understand the lipid layer, it is necessary to provide a brief explanation of lipids, their phase behaviour, lateral organization, and techniques used to observe these changes.

1.4 General Discussion on Lipids

1.4.1 General Lipid Structure

Lipids can be nonpolar or polar and form a large and diverse group of molecules that cellular life uses to define its structure, store energy, and for intercellular communication [26]. Polar lipids are amphipathic and have hydrophilic and hydrophobic segments (figure 1.2) [26]. They have a variety of functions, but the most important is their ability to self-assemble into barriers to form internal compartments or to separate the inside of a cell from its environment [26]. These assemblies are generally bilayer structures, but polar lipids in the tear film form a monolayer [27].

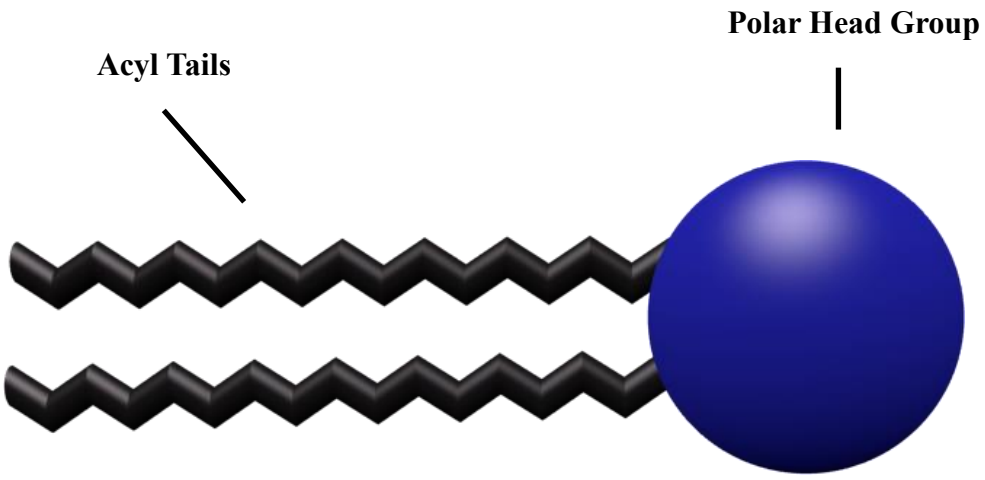

Figure 1.2 General structure of polar lipids.

Polar lipids exist in various classes that are defined by their backbone, the major groups are classified as glycerol and sphingosine based lipids (figure 1.3) [28]. The major structural differences are the hydroxyl group and an amide bond of sphingosine lipid that allow hydrogen bonding, in contrast to ester groups in glycerol lipids that do not [29]. The nonpolar acyl chains of the polar lipids can vary in length, degree of unsaturation, presence of hydroxyl groups, and chain branching; though, for the purposes of this thesis only length and saturation will be considered [28,30]. These structural differences affect the packing of the polar lipids in a monolayer, increasing or decreasing the average molecular area per lipid molecule [28]. For lipids with the same headgroup, increasing the length of the acyl chains will cause the average molecular area to decrease, with the lipids packing more closely together, and the opposite will occur for shorter acyl chains [31]. The close packing is the result of increased attractive forces between the acyl chains of adjoining lipids due to van der Waals forces [32]. The presence of double bonds in the acyl chains will increase the average molecular area per lipid, causing more relaxed packing [33]. Double bonds are normally in the cis conformation and increase average molecular areas by creating kinks, as opposed to fully saturated acyl chains that can assume a more extended, straighter conformation [34].

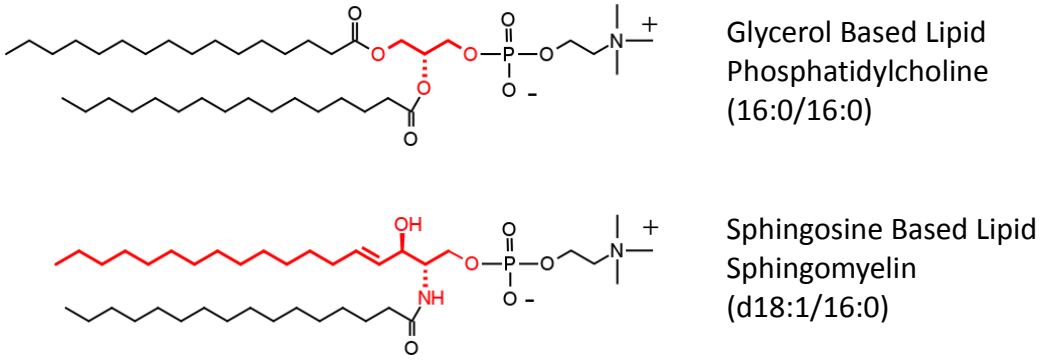

Figure 1.3 Two major classes of polar lipids, the glycerol based and sphingosine based lipids. The backbones are highlighted in red.

1.5 Tear Film Lipid Layer

1.5.1 Physical Characteristics of the Lipid Layer

The precorneal lipid layer is thought to be about 40 to 90 nm thick [1] while the polar lipid layer is around 2 to 3 nm thick [35]. The temperature of the ocular surface is ~34 °C [36]. Meibomian samples do not have a well-defined melting point, but melt over a range between 30 to 35 °C, but completely melt before 40 °C [37–40]. The surface pressure of whole tears appears to be ~26 to 29 mN/m [41] although other values have been proposed. Pulsating bubble surfactometer data vary between 27 mN/m for the largest bubble size to 37 mN/m for the smallest, suggesting that the ocular surface pressure can change during a blink [42]. Another experiment with a sessile-bubble

tensiometer showed that the tear lipids were able to reach a minimum surface pressure of ~40 mN/m and a maximum surface pressure ~50 mN/m [43].

1.5.2 Two Subphase Model of the Lipid Layer

The majority of studies concerning the composition of human tear film lipids reported mainly nonpolar lipids. The lipid layer in the tear film is generally shown as two sublayers, a nonpolar and a polar lipid layer. This two layer model was proposed by Brown and Dervichian in 1969 who argued that a polar component was necessary to allow nonpolar lipids to spread across the surface of the aqueous layer [39]. Four years later, Holly investigated how the aqueous layer adsorbed to the corneal epithelium and he diagramed how nonpolar lipids would form a lens on the air/water interface, but with the addition of polar lipids could form a two layered film at the water surface [44].

Choline and phosphate were identified as possible components of polar lipids in meibum by Linton *et al.* in 1961 [37] and Ehlers in 1965 [45]. Nicolaides *et al.* were the first to quantify that polar lipids made up ~15% of meibum lipids in 1981 [46]. In 1995, Glasgow *et al.* found that lysophosphatidylcholine co-migrated with lipids from whole tears and tear lipocalin on thin layer chromatography (TLC) [20]. Despite various authors suggesting a nonpolar and polar lipid subphase model for almost three decades, it was formally proposed by McCulley and Shine in 1997 [27]. More specifically, it is a multi-layered lipid film based on the identification of various lipid classes during their research (figure 1.4); phospholipids and cerebrosides would predominately interact with the

aqueous layer whereas triglycerides and certain wax esters could interact with the phospholipids and less polar lipids. Finally, the nonpolar wax-esters and cholesterol esters would form the outer nonpolar phase [27].

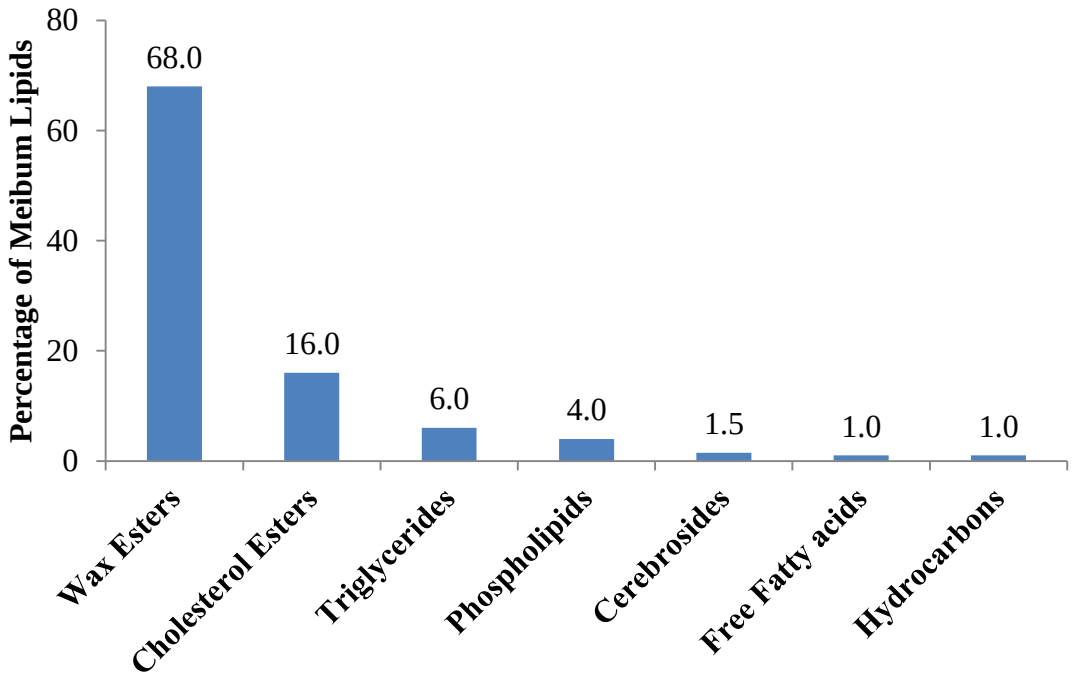

Figure 1.4 Lipid composition of meibomian secretions collected from typical volunteers. Data from McCulley and Shine [27].

1.5.3 Origin of Nonpolar Lipids in the Tear Film Lipid Layer

The nonpolar lipids are secreted by the meibomian glands, located in the upper and lower eyelids [5,9,47], onto the margin of the eyelid (figure 1.2) [48]. Small amounts

of lipids are expressed from the meibomian orifices by a milking action during each blink, but it has been observed that lipids continue to be secreted without blinking [45,49].

As meibomian lipids are expressed onto the lid margin surface, lipid reservoirs are created on both the upper and lower lids. During a blink, the lipids from both lids mix to form a combined reservoir [49]. During the up-phase of a blink the upper lid moves upwards across the eye surface and lipids from the combined lid reservoir are spread across the ocular surface although the lipid front moves from the bottom of the eye upwards [49].

1.5.4 Unknown Origin of the Polar Lipid Layer

The meibomian glands are considered as the lipid source of tear film, although researchers have found important differences between meibum and whole tear lipids [5,50]. Recent analyses show that the lipid classes in whole tears are more diverse than in meibum, and that phospholipids specifically seem to be more abundant in whole tears [5,41,50,51]. This suggests the majority of phospholipids in whole tears do not originate from the meibomian glands, and that the origin is unknown. Possible sources of the polar lipids may be the lacrimal glands, secretions from conjunctival and corneal epithelial cells, or even cellular debris from those epithelial cells [50]. Nicolaides *et al.* mentioned that the amount of polar lipids in meibum decreased if the meibomian glands were more gently expressed [46]. They did not state this, but this could suggest cellular debris.

Nagyová and Tiffany reported in 1999 that phospholipids were more abundant in whole tears than meibum, but it was only in 2013 that a different group revisited this observation [5,41]. One of the major reasons for this delay is probably the low concentrations of lipids in whole tears. The majority of studies prior to 1999 only looked at meibomian secretions [27,37–39,45,46,52–56]. Meibum can be expressed by applying pressure to the eyelid and collecting the produced excretion using some form of spatula [37]. The method is not easy, but it does produce 1 to 2 mg of meibum from each donor [37,38,53]. In contrast, gathering whole tear samples is much more difficult. Collecting tears using microcapillary tubes generally yields a maximum of 10 µL per sample [47,57,58]. In addition to the small sample volume, lipids only make up a small portion of the entire tear film, with concentrations less than a 1 µmol/ µL [57,59]. Additional difficulties are encountered with microcapillary collection because of the sensitivity of the eye. The tubes have to be used carefully, because if they touch the conjunctiva, reflex tearing will dilute the collected lipids even further [57]. In trying to increase the volume of tears collected, some researchers have stimulated reflex tearing using onion vapours, but it is not known how this affects the lipid profile of the tears [60].

One of the ways researchers have tried to improve the yield of lipids from whole tears are Schirmer strips. These filter paper strips are placed between the eyelid and the eyeball to absorb tear fluid and are normally used by doctors to assess the production of fluid [61]. Generally, Schirmer strips yield more lipids than microcapillary tubes [47]. Millar and Schuett have pointed out that this is problematic because the strips come into

contact with the meibomian orifices and multiple epithelia, which may cause lipid contamination, skewing the composition of tear lipids [50].

According to the two subphase model of the tear film lipid layer, the polar lipids are expected to form a monolayer at the interphase between the nonpolar lipids and the aqueous phase. Millar and Schuett point out that using microcapillary collection of whole tears does not allow for validation of this proposed location [50]. For this reason, whether the polar lipids are from aggregates inside the aqueous phase or from the monolayer, or both, is unknown [50]. But, a number of different *in vitro* experiments and molecular dynamic simulations support the two layer model [62].

1.5.5 Composition of Nonpolar Lipids in the Tear Film

Due to their abundance, it has been easier to study the nonpolar lipid layer of the tear film. The composition of nonpolar lipids in meibum and whole tears is similar, suggesting a common source, presumably the meibomian glands [50]. The analyses show that the majority of the nonpolar lipids are cholesterol esters and wax esters, with small amounts of (O-acyl)-ω-hydroxy fatty acids (OAHFAs) and triglycerides (table 1.1).

Table 1.1. The currently proposed composition of nonpolar lipid classes in human meibum. Data is from several studies summarized by Millar and Schuett **[50]**.

Lipid Class	**mol %**
Cholesterol Esters	30 to 45
Wax Esters	30 to 50
(O-acyl)-ω-hydroxy fatty acids (OAHFAs)	4
Triglycerides	2
Cholesterol	<0.5
Phospholipids	<0.01

The function of these nonpolar lipids is still not understood. Mishima and Maurice first found evidence that the lipid layer slowed evaporation from rabbit eyes in 1961 [63]. This hypothesis was also supported in humans by data from patients with meibomian gland dysfunction [64]. The hydrophobic nature of these lipids provides a compelling rationale, but there is a lot of variation in evaporation data [50]. Rantamäki *et al.* recently tested evaporation rates and only highly condensed films such as olive oil or behenyl alcohol were able to slow evaporation [65]. A mixture of phosphatidylcholine, cholesterol esters, triglycerides, and wax esters only slightly decreased evaporation rates [65]. Poor prevention of evaporation in model systems has been reported elsewhere, but this could mean that the model systems are lacking essential components required to reduce evaporation [3].

Recently, researchers have speculated that both, the nonpolar and polar sublayers, may not help limit evaporation, but to stabilize the tear film [50,66]. Stability is often used without being defined, but in Millar and Schuett's review and in this thesis, it refers to preventing collapse of the overall tear film [50]. Collapse of the tear film would be due to the surface pressure of the lipid-aqueous interface decreasing to the point where the tear film forms droplets instead of spreading across the ocular surface as a thin film [50]. It has been proposed that the polar lipids increase the surface pressure of the aqueous/lipid interface, and that nonpolar lipids help the polar layer to reversibly compress during a blink [66]. Additionally, the lipid layer may allow for proper drainage of the aqueous layer and prevent it from overflowing the lid margin during a blink [50].

1.5.6 Composition of Polar Lipids in the Tear Film

The composition of the polar lipid phase of the human tear film has yet to be determined, and has become a scientific controversy [67–69]. This is a challenging area of research because the small amount of sample material provides a serious analysis limitation [70]. The presence of phospholipids had been suspected since 1961 [37]. In 1995, Glasgow *et al.* identified lysophosphatidylcholine as the first polar-lipid class in the tear film [20]. This may have been a breakdown product a diacyl-phosphatidylcholine.

McCulley and Shine first quantified the polar lipid classes in 1998, and further refined the model in 2003 (figure 1.5) [56,71]. Recent studies of polar lipids in meibomian secretions have shown that the polar lipid classes identified by McCulley and

Shine are in much smaller amounts, and that OAHFAs are the most abundant polar lipid class in meibum [5,72]. However, most of the polar lipid classes identified by McCulley and Shine seem to be present in large amounts in whole tears [5,47,60,73] (figure 1.6).

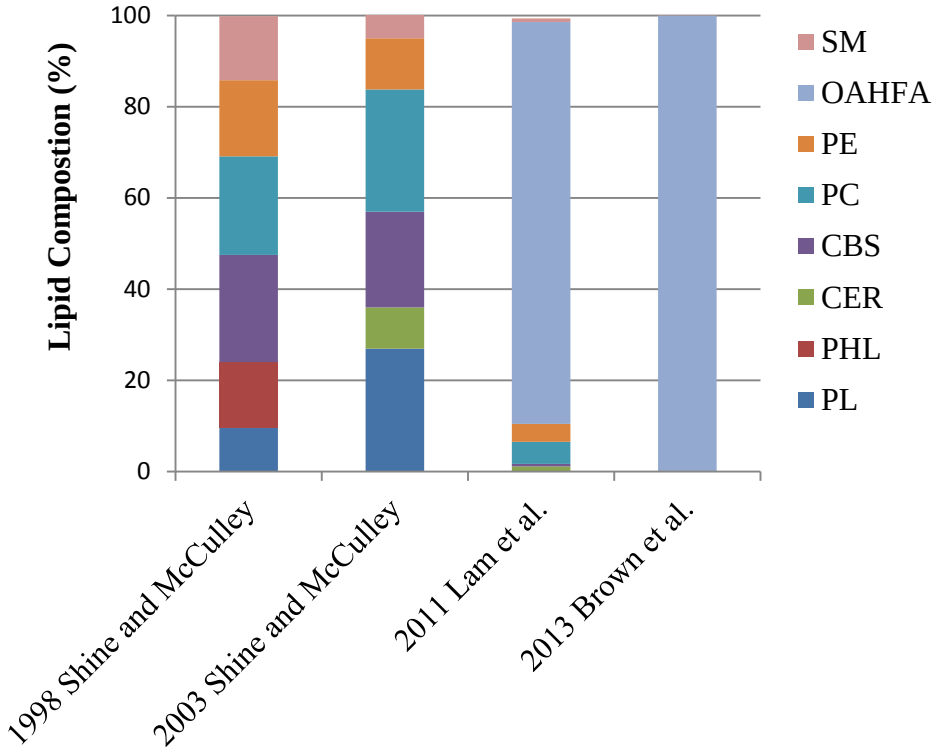

Figure 1.5 Percentage of polar lipid classes identified in meibum from various papers: sphingomyelin (SM); o-acyl ω-hydroxy fatty acids (OAHFA); phosphatidylethanolamine (PE); phosphatidylcholine (PC, including lyso-PC); cerebrosides (CBS); ceramide (CER); unidentified phospholipids (PHL); unidentified polar lipids (PL) [5,56,71,72].

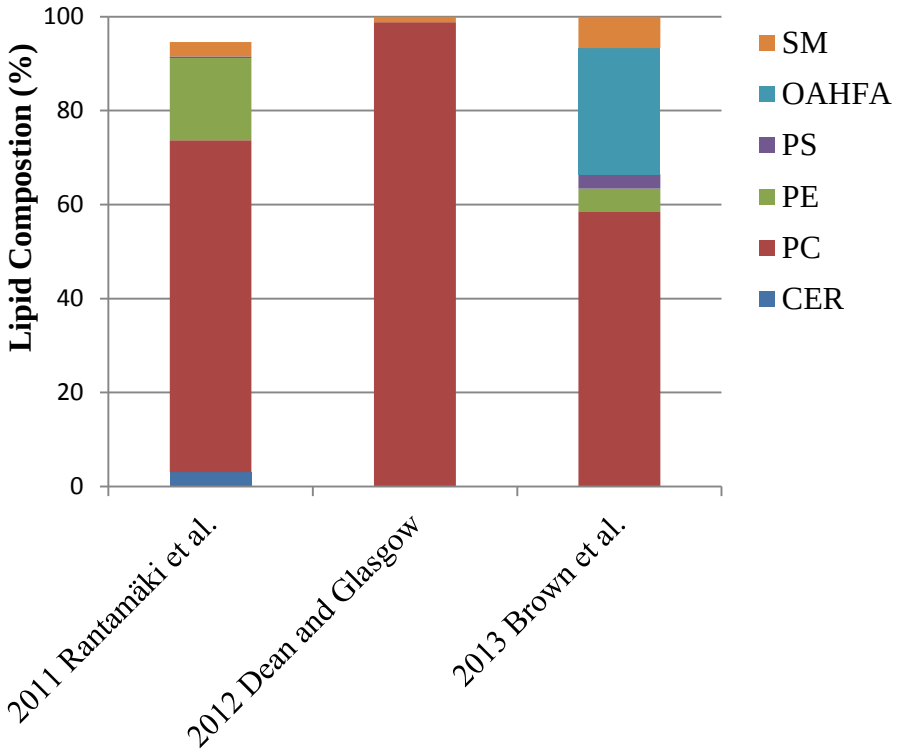

Figure 1.6. Percentage of polar lipid classes identified in whole tears from various papers: sphingomyelin (SM); o-acyl ω-hydroxy fatty acids (OAHFA); phosphatidylserine (PS); phosphatidylethanolamine (PE); phosphatidylcholine (PC); ceramide (CER) **[5,60,73]**.

Unfortunately, there is much variation between the various proposed lipid compositions [50]. This may be due to variations in collection, lipid extraction, storage, identification, and quantification methodologies. Beginning with small sample sizes, of the three most recent studies looking at whole tear lipids, Rantamäki *et al* had 30 donors, but Brown *et al.* had only 4 donors [5,73]. For whole tears, sometimes glass capillaries

were used to collect tear samples, other times Schirmer's strips [5,47,60,73]. Again, Schirmer's strips are paper strips that are generally placed between the eyeball and lower lid to absorb tears. Some researchers mentioned specifically that they attempted to avoid contacting the conjunctiva, while others did not [5,47,60,73]. Dean and Glasgow used onion vapours to stimulate tears and it is not known how this could affect the lipid composition [60]. Another key difference is the lipid extraction procedures. Rantamaki *et al.* and Dean and Glasgow used 2:1 chloroform/methanol to extract the polar lipids [60,73] and Brown *et al.* used ~3:1 methyl tert-butyl ether (MTBE)/methanol for extraction. Regarding lysolipids, only Brown *et al.* mentioned using butylated hydroxytoluene to prevent oxidation of polar lipids [5].

More recent reports stated that they did not detect phospholipids in meibum. The absence of polar lipids may be due to the samples being dissolved and stored in chloroform only; however, this was also the case for the original work by McCulley and Shine who first identified the major polar lipid classes in meibum [56,71,74,75]. The only reported difference in the lipid extraction and storage between McCulley and Shine's work and later studies was that they used lidocaine to numb the ocular surface [56,71,74,75]. Brown *et al.* used chloroform to dissolve the meibum samples and then added MTBE/methanol to extract the polar lipids, whereas the direct addition of MTBE/methanol was used for extraction of polar lipids from the large volume of water in tears [5]. Lam *et al.* was the only study to use 1:1 chloroform/methanol to extract meibomian polar lipids, and they did find small amounts of these lipids [72].

Moreover, there are differences in the analysis methods due to different internal standards used. Considering phosphatidylcholine (PC) alone, Dean and Glasgow used egg PC, Brown *et al.* used PC (19:0/19:0), and Rantamäki *et al.* used an internal library for lipid identification [5,60,73]. In addition, different chromatography instruments and methods, different mass spectrometry instruments, and ionization methods were used [5,60,73]. All these factors may contribute to the controversy of polar lipid composition.

As already mentioned, lysophosphatidylcholine (lysoPC) was an early polar lipid class identified in the tear film [20] and has been found in high abundance in more recent studies [5]. This further complicates matters. Rantamäki *et al.* suggest this is due to an abundance of phospholipase A_2 (PLA_2), an enzyme that can hydrolyze acyl chains from phospholipids [73,76].

In addition to the variation of tear film polar lipid composition due to analysis methods, there may also be differences in individual polar lipid compositions. Sullivan *et al.* used mass spectrometry to examine the differences in meibum polar lipids between men and women of different ages [77]. They found that younger men and women had increased levels of polar lipid fatty acid fragmentation products compared to older men and women [77]. In addition, using the t-test, the authors found significant differences between polar lipid profiles between men and women in general [77]. Borchman *et al.* found age related differences in the infrared spectra of meibomian secretions [78]. Unfortunately, meibomian secretions were used, which may not indicate polar lipid changes in whole tears, and sample sizes were small as Sullivan *et al.* used ~40 donors

and Borchman *et al.* used 27 donors [77,78]. Tiffany remarked in 1999 that gas-liquid chromatography traces showed much inter-donor variation [41].

More recently, Brown *et al.* did a small pilot study with 4 donors to examine differences between lipids of meibum and whole tears from day to day [79]. They used chip-based tandem mass spectrometry and found that lipid profiles were consistent from day to day, but showed large variations between individuals [79]. Moreover, Millar and Schuett noted differences in the amounts of cholesterol esters and wax esters in various studies [50]. If these abundant lipids are difficult to quantify it could be due to individual variation or inaccurate methodologies [50]. If individual variations are indeed high, it may suggest that different compositions can accomplish the same task [50]. Additionally, environmental factors may change the polar lipid composition. Robciuc *et al.* published a study where ultra-violet radiation, hyperosmolarity, and lipopolysaccharides caused human corneal epithelial cells to secrete sphingomyelinases that hydrolyze sphingomyelin to produce ceramide and phosphocholine [58]. Tobacco smoke has also been found to decrease the stability of the tear film and lowered lysozyme concentrations [80].

Phosphatidylcholine, sphingomyelin, phosphatidylethanolamine, glucocerebroside, and phosphatidylserine are polar lipid classes that have been identified in the tear film. Phosphocholine headgroups of phosphatidylcholine and sphingomyelin are large and bulky compared to phosphatidylethanolamine, so they cannot pack as closely together [31] (figure 1.7). They are zwitterionic, having an overall neutral charge,

with a negative charge on the phosphate group and a positive charge on the quaternary amine group [29]. Studies of PC indicate that the head group is tilted at a 20° to 70° angle from the plane of the monolayer [35]. The headgroup of phosphatidylethanolamine (PE) has the ability to hydrogen bond making PE more rigid [29]. Glucosylceramide is a neutral sphingolipid with a glucose moiety attached to the sphingosine [81]. In experiments with bilayers, the glucose headgroup tends to extend into the aqueous phase so that it can maximize hydrogen bonds with the surrounding water [82]. Phosphatidylserine is an anionic lipid, with negative charges on the phosphate and carboxylic acid groups, and a positive charge on the amino group [83]. Monolayers of these lipids tend to have large areas per molecule because of electrostatic repulsion, which can be reduced by cations [83].

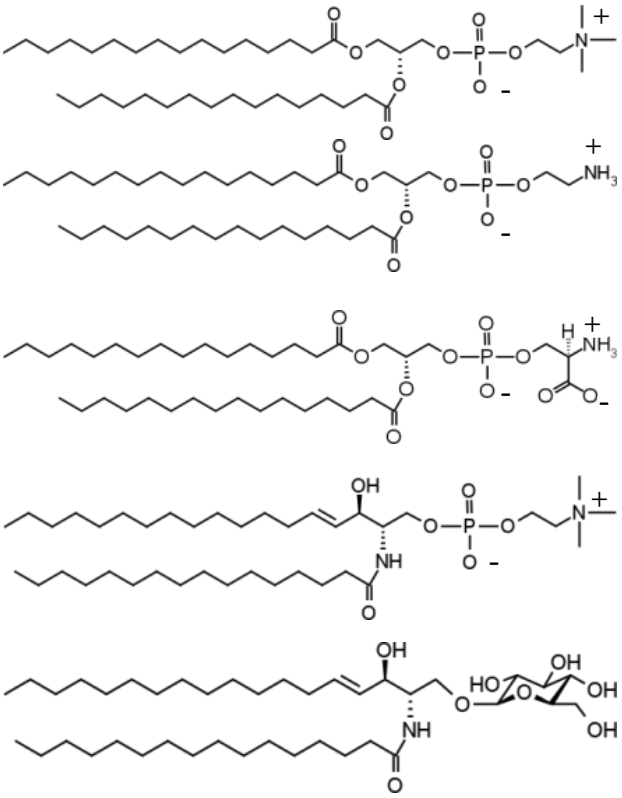

Figure 1.7. Major polar lipid classes identified in the lipid layer of the tear film: DPPC dipalmitoylphosphatidylcholine; DPPE dipalmitoylphosphatidylethanolamine; DPPS dipalmitoylphosphatidylserine; PSM palmitoylsphingomyelin; PGC palmitoylglucocerebroside.

In 2009 another lipid class was identified that makes up 2 to 5% of meibomian and whole tear lipids, (O-acyl)-ω-hydroxy fatty acids (OAHFAs) [5,47,72,84]. The OAHFAs are an interesting lipid, but more research is necessary to figure out whether they are a major polar layer lipid. One advantage proposed for OAHFAs is that they may

have longer acyl chains than those reported so far for phospholipids, allowing interactions with the nonpolar lipids to prevent them from forming micelles and vesicles during a blink [50].

1.6 Proteins of the tear film

Tear proteins are found in the aqueous layer, but also in the lipid layer, as inflections in isocycle isotherms have shown that whole tears have similar hysteresis profiles to some proteins [85]. Concentrations of lysozyme, lactoferrin, and tear lipocalin correlate with each other [86]. All three proteins have been found to be secreted by the lacrimal gland, and also can co-elute when purified with size exclusion chromatography, despite the size differences [20,87]. This may suggest some combined function [20]. These are the major proteins found in the tear film and represent 65 to 85% of the total protein in tears [88].

1.6.1 Lysozyme

Lysozyme is a common enzyme that lyses bacteria by cleaving the β (1-4) linkage between N-acetylglucosamine (NAG) and N-acetylmuramic acid (NAM) in the peptidoglycan cell wall [23,89]. More recently, the disruption of bacterial membranes has been reported, extending lysozyme's antimicrobial action to gram-negative bacteria [90]. Alexander Fleming was one of the first scientists to observe the antimicrobial action of

lysozyme in human nasal mucus, sputum, tears, saliva, and hen-egg white lysozyme (HEWL) in 1922 [91] Historically, HEWL is an important model protein as it was one of the initial proteins characterized [92]. It was the first protein to be sequenced that contained all 20 amino acids [92]. X-ray crystallography at 2 Å resolution was used to determine its 3D structure by Blake *et al.* in 1965 [93].

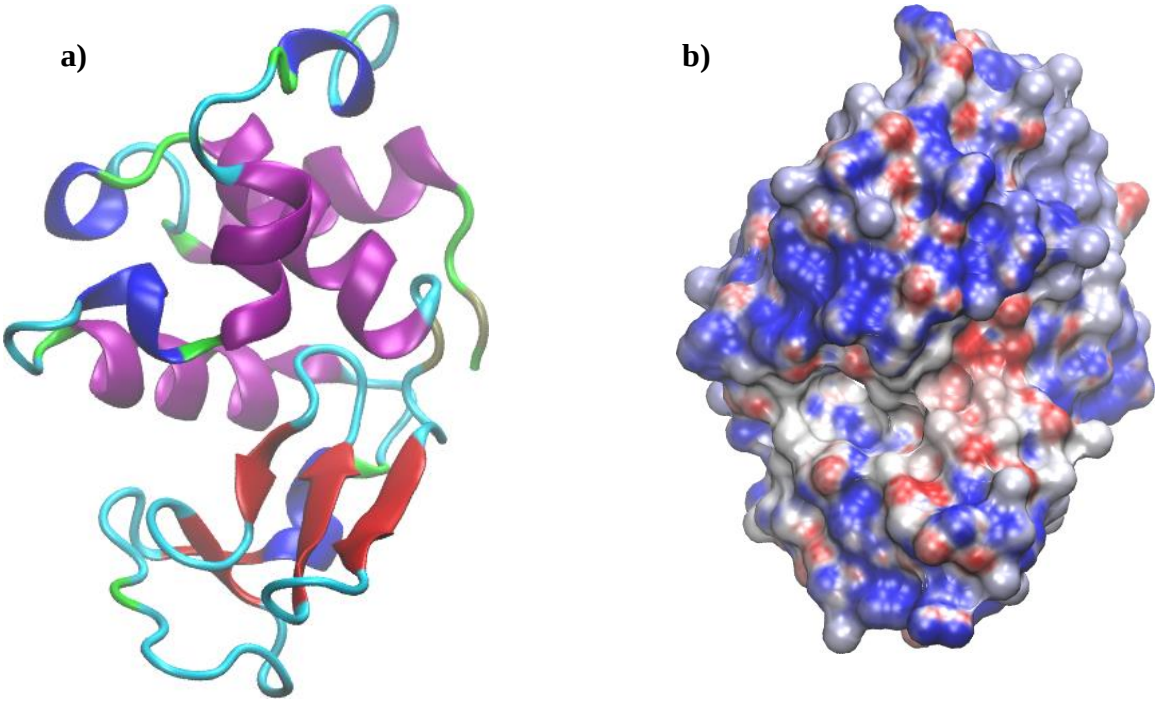

Figure 1.8. Hyman lysozyme (PDB 1REX **[94]**) visualized using VMD 1.9.3 **[95,96]** : a) cartoon representation b) electrostatic potentials calculated using PDB2PQR 2.1.1 **[97]** with the AMBER force field **[98]**, pKa calculated at pH 7.4 using PropKa **[99]**. Blue represents areas with positive charge, red with negative, and white as neutral.

There are three main types of lysozyme in the animal kingdom: c-type (chicken or conventional), g-type (goose egg-white), and i-type (invertebrate) [100]. Human lysozyme (Accession: P61626) is a c-type lysozyme and is abundantly expressed. Two g-type lysozyme genes have been found in humans, lysozyme g1 and lysozyme g2, but they are not highly expressed, nor are they expressed in the same variety of tissues as the c-type lysozyme [101]. Huang *et al.* has found lysozyme g2 RNA in human lacrimal gland tissue, but again it is in much lower abundance than the c-type [102]. In this thesis recombinant human c-type lysozyme was used.

Lysozyme has 130 amino acids once a signal peptide of 18 amino acids is cleaved [103]. C-type lysozymes generally have a molecular weights between 11 and 15 kDa [100]. It has four disulfide bonds (residues: 24 to 146; 48 to 134; 83 to 99; 95 to 113) [104]. HEWL has an isoelectric point of ~11, so at 7.4 it is positively charged [105]; however, there are some residue substitutions on the surface of human lysozyme that result in a negative patch compared to HEWL, reducing the isoelectric point to ~10 [106,107]. Lysozyme levels in tears range between 0.8 and 3.3 mg/mL, and concentrations appear to vary with age [108,109].

1.6.2 Lactoferrin

The history of lactoferrin characterization has been published in a review by Vogel [110]. According to Groves, lactoferrin (also known as lactotransferrin, P02788) was first reported by Sørensen and Sørensen in 1939 as a component of bovine milk

[111]. In 1958, Johansson identified lactoferrin in human milk, and noted that it contained iron that could not be removed using a cation exchange column at pH 6.9 [112]. Later, Groves showed that lactoferrin could reversibly bind free ferrous iron in solution, that the iron could be removed with cation exchange chromatography at the low pH of 2 [111]. In 1966, Masson *et al.* discovered lactoferrin in human tears, saliva, urine, and other external secretions as well as various internal organs [113]. As well, lactoferrin is found in high concentrations in neutrophils [114]. In the tear film it is primarily produced by the lacrimal glands and its concentration has been reported between 0.63 and 3.8 mg/mL [115,116].

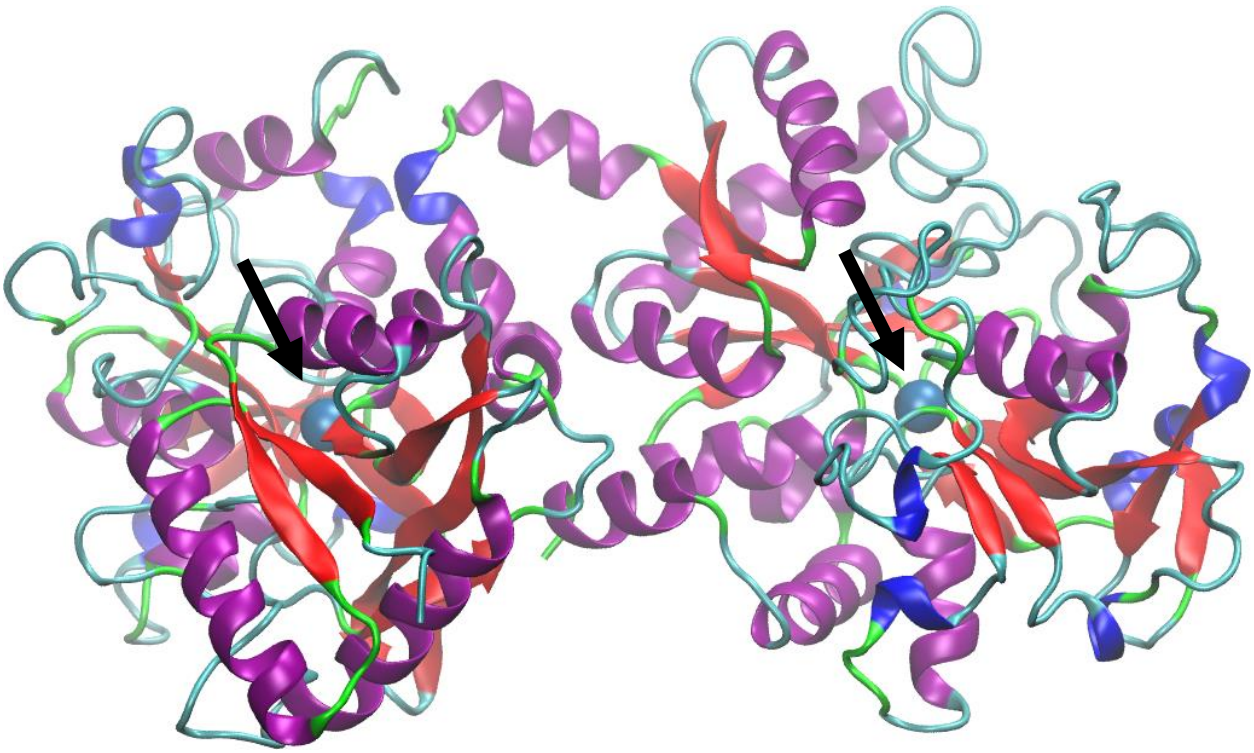

Figure 1.9. Diferric human lactoferrin (PDB 1LFG **[117]**). Visualized using VMD 1.9.3 **[95,96]**. Black arrows indicate bound iron (blue spheres).

Lactoferrin is a member of the transferrin family of proteins, and is an 80 kDa glycoprotein that contains two lobes connected by an α-helix, the first 332 residues comprise the N-lobe, and residues 344 to 703 comprise the C-lobe [118–120]. Each lobe can bind one ferric iron ion (Fe^{3+}) with a carbonate ion (CO_3^{2-}) [117,118,121] (figure 1.9). Lactoferrin can adopt two conformations, the closed iron bound (holo) and the open (apo) forms [122]. Generally, the surface of lactoferrin is positively charged whereby cationic residues are especially common in the first 30 residues of the N-terminal region and the lobe connecting helix [119] (figure 1.10).

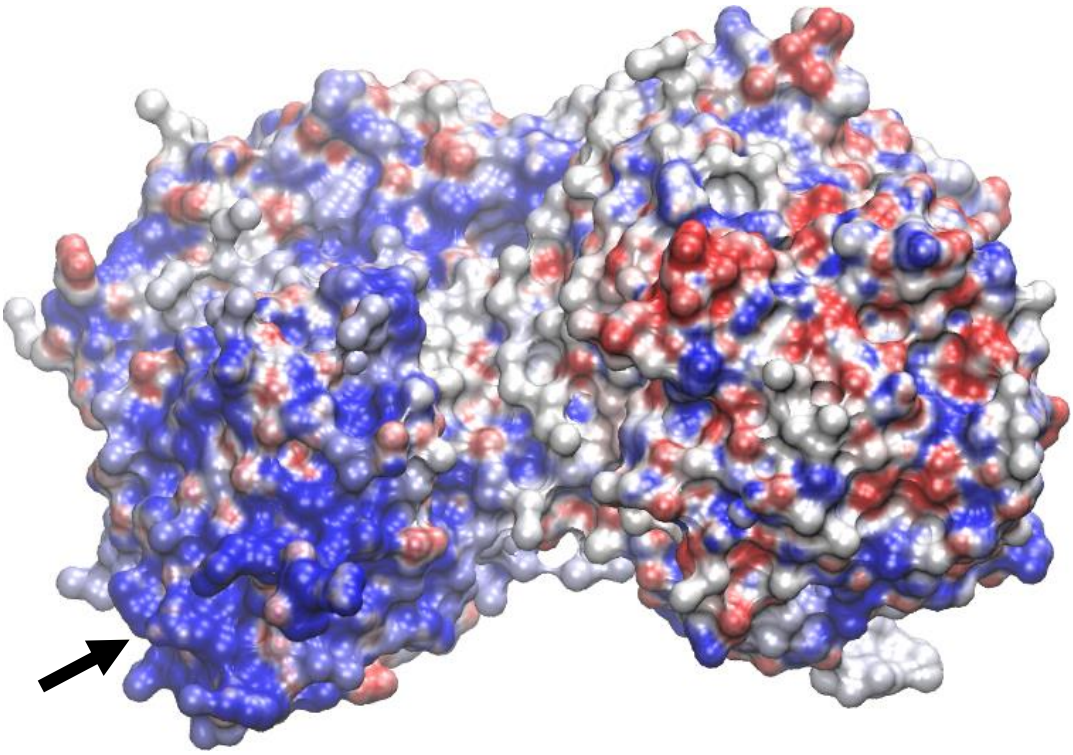

Figure 1.10 Diferric human lactoferrin (PDB 1LFG **[117]**) with surface representation of electrostatic potentials calculated using PDB2PQR 2.1.1 **[97]** with the AMBER force field **[98]**, pKa calculated at pH 7.4 using PropKa **[99]**. Visualized using VMD 1.9.3 **[95,96]**. Blue represents areas with positive charge, red with negative, and white as neutral. Black arrow points to the positively charged N-terminal region.

Antimicrobial properties of lactoferrin have been observed against a wide variety of bacteria [123] and have been attributed to its ability to tightly bind iron ($K_D \approx 10^{-22}$ M for transferrin family proteins) [120]. In 1972, Bullen *et al.* observed reduced growth of

E. coli when grown in the presence of human lactoferrin purified from milk, an effect that disappeared when iron was added in excess of the binding capacity of the protein [124]. More recently, other antimicrobial properties have been observed that are independent of iron sequestration by lactoferrin, possibly involving interactions with bacterial membranes or the internalization of the protein to act on intracellular targets [125,126].

There have been smaller peptides identified within the lactoferrin protein. The most investigated is lactoferricin, an antimicrobial peptide produced when lactoferrin is digested with pepsin [127]. In humans, this peptide is the first 47 to 49 residues of the N-terminal lobe, and has double the antimicrobial activity of intact lactoferrin [127,128]. Lactoferricin should not be present in the tear film because it normally lacks pepsin [129]. There was a preliminary study where pepsin was found in the tear film of children with laryngopharyngeal reflux disease where gastric acid from the stomach, including pepsin, was thought to reach the tear film through the nasolacrimal duct [129].

1.6.3 Tear Lipocalin

Tear lipocalin or lipocalin-1 (P31025) was originally known as tear specific prealbumin (TSP) [130]. In 1969 Bonavida *et al.* reported that the protein was only produced by the lacrimal glands [131]. The longest isoform of tear lipocalin is a 17.45 kDa protein with one disulfide bond, made up of 158 residues including an 18 residue signal peptide [132,133]. Like other lipocalins, it has a large cup-shaped cavity formed by an eight strand anti-parallel β-barrel, with one end of the barrel wider than the other

end [134]. The concentration of tear lipocalin is 1.7 to 3.6 mg/mL in the tear film [109,116].

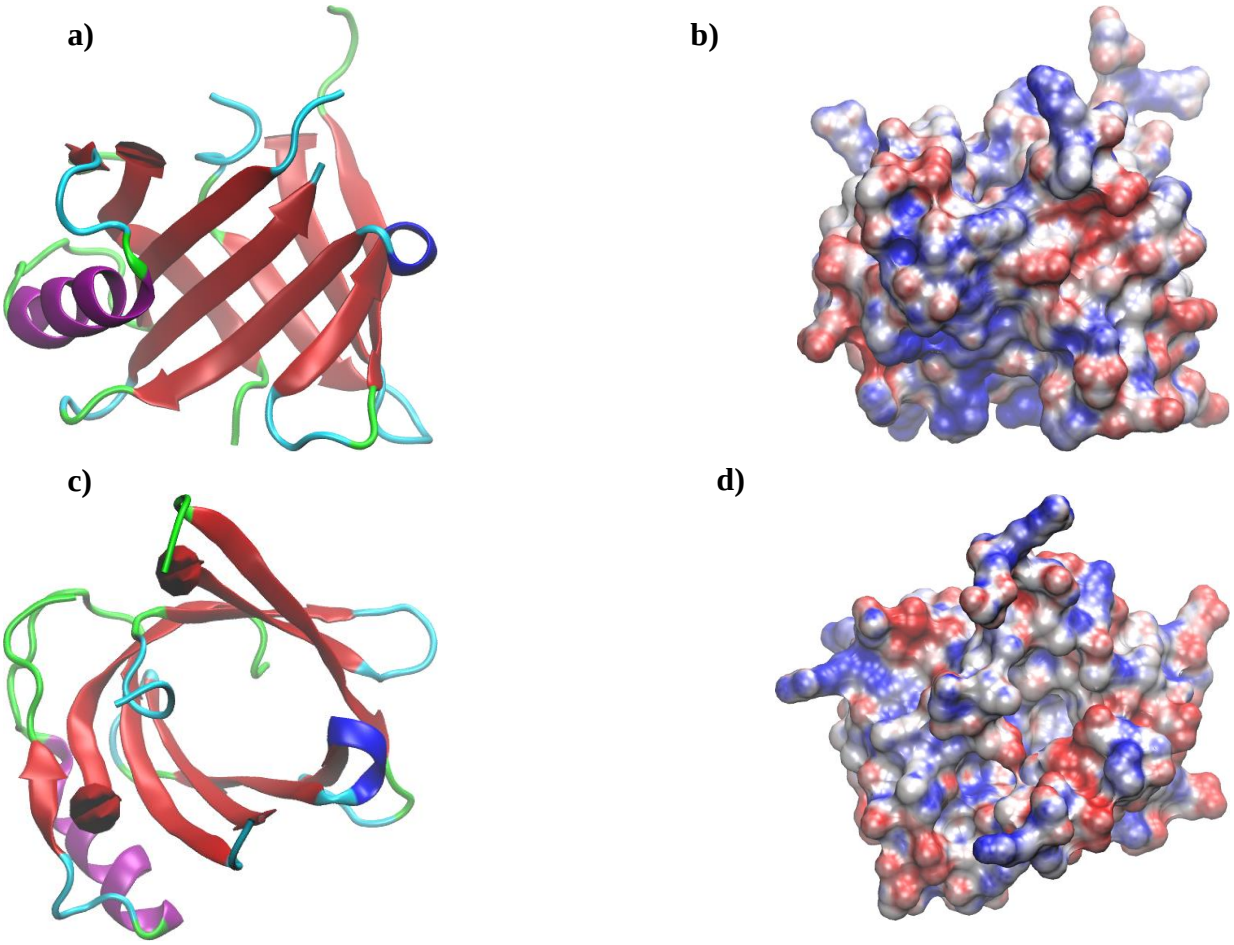

Figure 1.11. Human tear lipocalin (PDB 1XKI **[133]**) a) and c) side and top views respectively with cartoon representation b) and d) side and top views respectively with surface representation of electrostatic potential. Visualized using VMD 1.9.3 **[95,96]**. Electrostatic potentials calculated using PDB2PQR 2.1.1 **[97]** with the AMBER force field **[98]**, pKa calculated at pH 7.4 using PropKa **[99]**. Blue represents areas with positive charge, red with negative, and white as neutral.

Glasgow and Glasymov proposed that a positively charged patch of amino acid residues may be able to bind negatively charged lipids and help to stabilize the polar lipid layer [135] but the function of tear lipocalin is still not understood. Glasgow *et al.* reported that tear lipocalin was able to bind a variety of ligands, including cholesterol, fatty acids, fatty alcohols, glycolipids, and phospholipids [136]. Furthermore, Fluckinger *et al.* found that tear lipocalin can bind a diversity of siderophores, molecules used by bacteria to scavenge iron [137]. They also suggested that tear lipocalin may assist in the spreading of the lipid layer across the aqueous layer and support this process by removing lipid contamination of the glycocalyx layer that could interfere with spreading [137]. The ability of tear lipocalin to shuttle contaminating lipids interfering with the wetting of corneal epithelial cells to the lipid layer has come under scrutiny. Saaren-Seppälä *et al.* studied the lipid transfer activity of tear lipocalin with radiolabeled phosphatidylcholine from liposomes to high density lipoprotein and found no evidence of lipid transfer for phosphatidylcholine [138]. Mudgil and Millar found that holo tear lipocalin did not appear to release lipids to a meibum/aqueous interface [139]. Finally, interactions with the lipid cargo may also convey antimicrobial properties [136].

1.7 Disease States

Dry eye (also known as keratoconjunctivitis sicca) causes discomfort, inflammation, desiccation of the corneal epithelium, lowers visual acuity and function [140]. Dry eye can be classified as aqueous-deficient or evaporative [140]. Aqueous-

deficient concerns disorders of the lacrimal glands, while evaporative concerns deficiencies with meibomian secretions [140]. Often, evaporative dry eye is linked with low production or excretion of meibum itself, but polar lipids may also play a role [141]. Shine and McCulley first reported that deficiencies in PE and SM in meibum may be one cause of evaporative dry eye in 1998 [56]. In patients with evaporative dry eye syndrome, Lam *et al.* found increased amounts of phospholipids such as PC and PE [141]. Understanding how these lipids work together may give us insight into better treatment for these patients

1.8 Project Goals

Overall, this project aimed to study the interactions of the major polar lipid classes in biomimetic models with the most abundant soluble proteins found in the tear film. To accomplish this, surface pressure - area isotherms of synthetic lipids were studied with recombinant human proteins *in vitro*. There were two goals for this project. The first was to develop a reproducible assay using a Langmuir trough that allows for proteins to be injected into the aqueous subphase of polar lipid biomimetics at surface pressures found in the human tear film. This would allow for an analysis of how proteins affect the stability of these films during blinking. The second goal was to image the films during this assay with Brewster Angle Microscopy (BAM) and observe variations in the lateral arrangements of lipid and protein domains within the films.

Chapter Two: Methods

2.1 Overview of Techniques

When polar lipids are deposited on an aqueous subphase, such as the aqueous layer of the tear film, they form a single layer. The lipids can exist in different phases depending on the proximity of lipids to each other, and their molecular conformations [142]. We can infer these phases using various methods such as surface tension/pressure, surface potential, microscopy, X-ray diffraction, and X-ray/neutron reflectivity [142]. Surface pressure and microscopy were used for the experiments presented in this thesis.

2.1.1 Surface Tension

Unique properties of water can make it appear to have a "skin", where some objects can rest on the surface of a pool of water, but sink to the bottom when they penetrate the surface. Water droplets can also be seen to form spherical shapes. Surface tension is the reason for this behaviour, and it arises because water molecules at the air/water interface have less hydrogen bonds to neighbouring water molecules than in the bulk phase, due to fewer water molecules in the air near the surface (figure 2.1) [143,144]. Water molecules at the air/water interface have more potential energy than those in the bulk solution and are constantly pulled into the bulk solution [144]. The unit of surface tension (N/m) becomes clear using this description of potential energy [144].

$$\frac{J}{m^2} = \frac{N \cdot \cancel{m}}{m^{\cancel{2}}} = \frac{N}{m} \qquad \text{[Equation 2.1]}$$

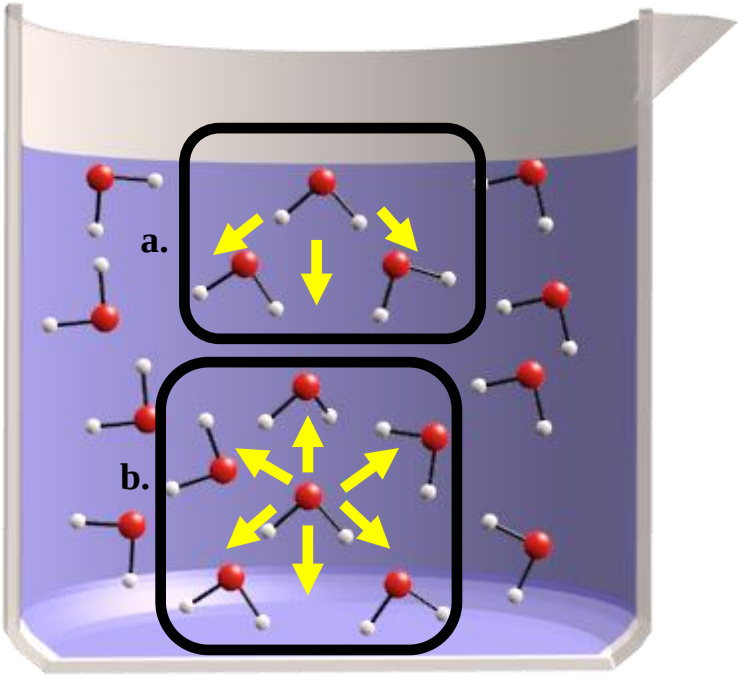

Figure 2.1. Schematic representation of the difference between attractive forces for water molecules at the a) air/water interface and b) in the bulk solution.

The spreading of a monolayer of polar lipids at the air/water interface changes the surface tension of the interface through lipid-lipid interactions and their interactions

with water molecules [143]. Surface tension experiments can be carried out using a Langmuir Surface Balance, commonly called a Langmuir Trough (figure 2.2) [142].

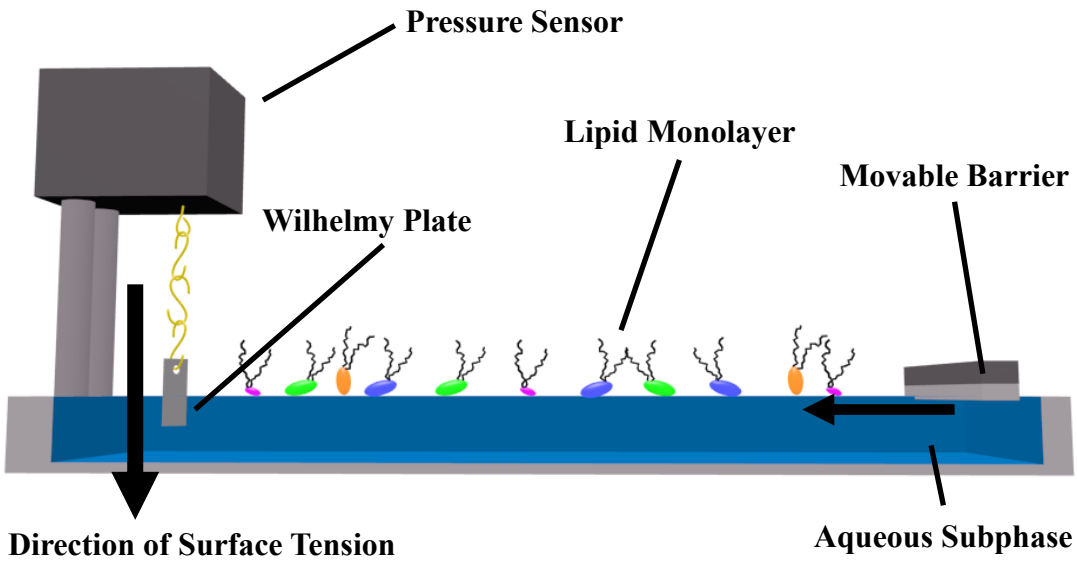

Figure 2.2. Diagram of a Langmuir surface balance (Langmuir Trough) equipped with a Wilhelmy plate.

The trough holds a subphase, and is equipped with movable barriers to manipulate the surface area of the film and a surface pressure sensor [142,143]. The setup for this thesis was the Wilhelmy plate method, where a filter paper plate is inserted into the subphase, and the downward force on the plate is measured by the attached pressure sensor, allowing the surface tension to be calculated [143]. The barrier divides the surface area of the subphase into inside and outside areas relative to the pressure sensor. The side

of the barrier in which the Wilhelmy plate is inserted into the subphase, and where lipids are normally deposited, is referred to as being inside or within the barrier. The barrier is said to be in the open position when its location maximizes the area within the barrier. The opposite holds with the minimum surface area, the barrier is in the closed position. The barrier sweeps across the surface of the subphase from open to closed positions and compresses the amphipathic lipids deposited on the inside of the barrier by corralling them into a smaller area [142,143]. The number of lipids remains the same, but lipid coverage of the surface water molecules inside the barrier increases, and this lowers surface tension [142]. Often, changes in surface pressure are reported instead of changes in surface tension [142].

$$\pi = \gamma_0 - \gamma \qquad \text{[Equation 2.2]}$$

Where π is surface pressure, γ_0 is the surface tension of the air/water interface in the absence of lipids, and γ is the surface tension of the interface in the presence of lipids [143]. As surface tension drops, surface pressure increases.

2.1.2 Phase Changes in Monolayers of Polar Lipids

We can observe changes in lipid phases using Langmuir troughs (figure 2.3). When the barrier compresses a lipid monolayer, the surface pressure of the lipid/water interface changes. Initially, lipid molecules are deposited in low amounts and occupy a

large enough area that they have few interactions with themselves and have little coverage of the aqueous subphase, this is called the gas phase (G) [142]. Since lipids in gas phase monolayers interact very little, their hydrophobic tails are free to adopt any conformation, and typically changes in surface pressure are not seen during compression of this phase [142].

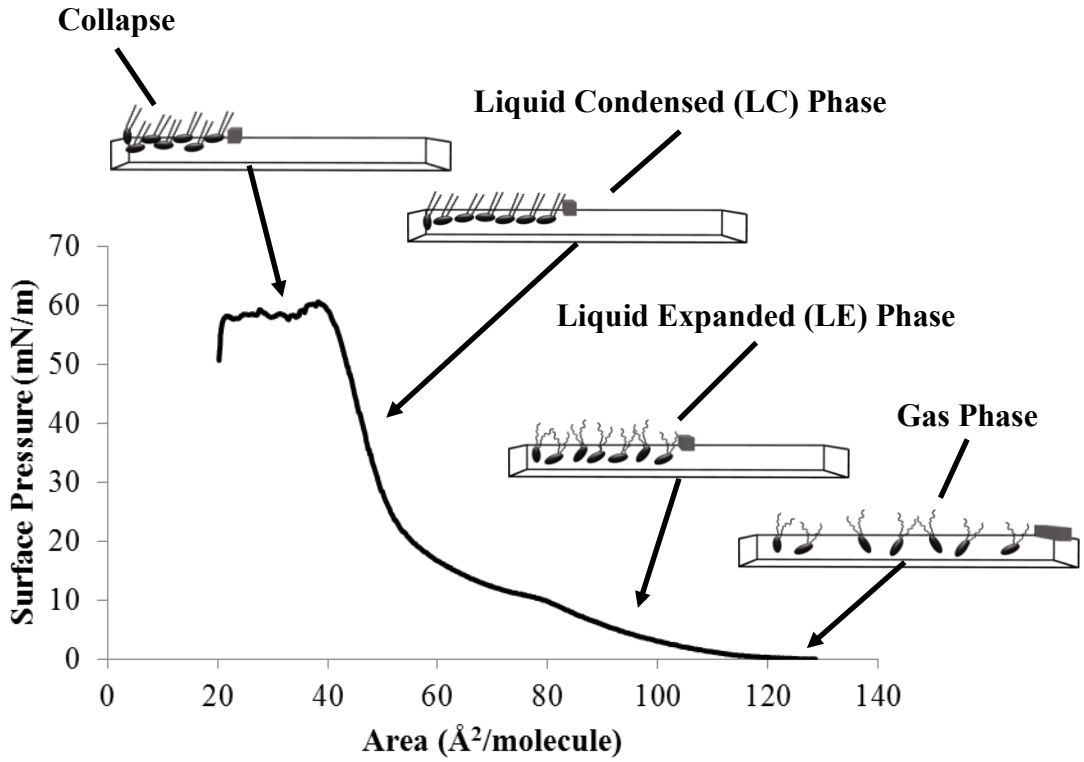

Figure 2.3. Isotherm of the change in surface pressure of DPPC with decreasing surface area, with different phases illustrated. The plateau beginning ~ 80 $Å^2$/molecule indicates phase coexistence between LE and LC phases **[145]**.

Further compression of the lipids will cause them to form a liquid-expanded (LE) phase and the surface pressure will begin to rise or take-off. The LE phase is characterized by lipids that are in contact with each other, but their hydrophobic tails can still adopt a wide variety of conformations [31]. When the lipids are compressed further, they will form a liquid condensed (LC) phase. Lipids in this phase are so close together that the tails adopt an all-trans conformation [30]. Phase changes can be seen when the slope of the isotherm changes, and near-horizontal plateaus can indicate phase coexistence, such as the LE/LC transition [145]. Unsaturated bonds create kinks that make the formation of the LC phase difficult, sometimes abolishing the phase altogether [30,142]. Continued compression of the monolayer will eventually cause it to collapse due to lipids being squeezed out of monolayer plane and forming a multilayer phase, the surface pressure will either plateau or decrease [142]. Decreases in headgroup size can shift an isotherm to smaller molecular areas because the lipids can pack more closely together, taking up less surface area [31]. Changes in the slope of the isotherm can indicate phase changes, but the slope of the isotherm itself at any particular moment can be used to provide information on the lateral compressibility of the film [143].

2.1.3 Isocycles

Isocycles can be used to compress and expand a monomolecular film and is relevant here because it was used to mimic blinking, although not nearly as fast. Two features normally present in isocycles is hysteresis between compression and expansion

isotherms, and a shift to smaller molecular areas upon successive cycles (figure 2.4). The hysteresis arises because the surface pressure at a given moleuclar area for the compression isotherm is different from the surface pressure at the same molecular area for the expansion isotherm. With DPPC for example, the expansion isotherm generally has lower surface pressures than the compression isotherm, this has been reported to be mainly caused by relaxation effects [146]. Relaxation is a term used to describe the surface pressure drop observed when the dynamic compression of a monomolecular film is stopped, and surface pressure decreases to that of a film that was compressed slowly, allowing the film to equilibrate [147]. The shift to smaller molecular areas between successive cycles can be caused by lipids leaving the plane of the monolayer and not returning upon compression, perhaps lost to the sublayer or leaking across the barrier [142,148].

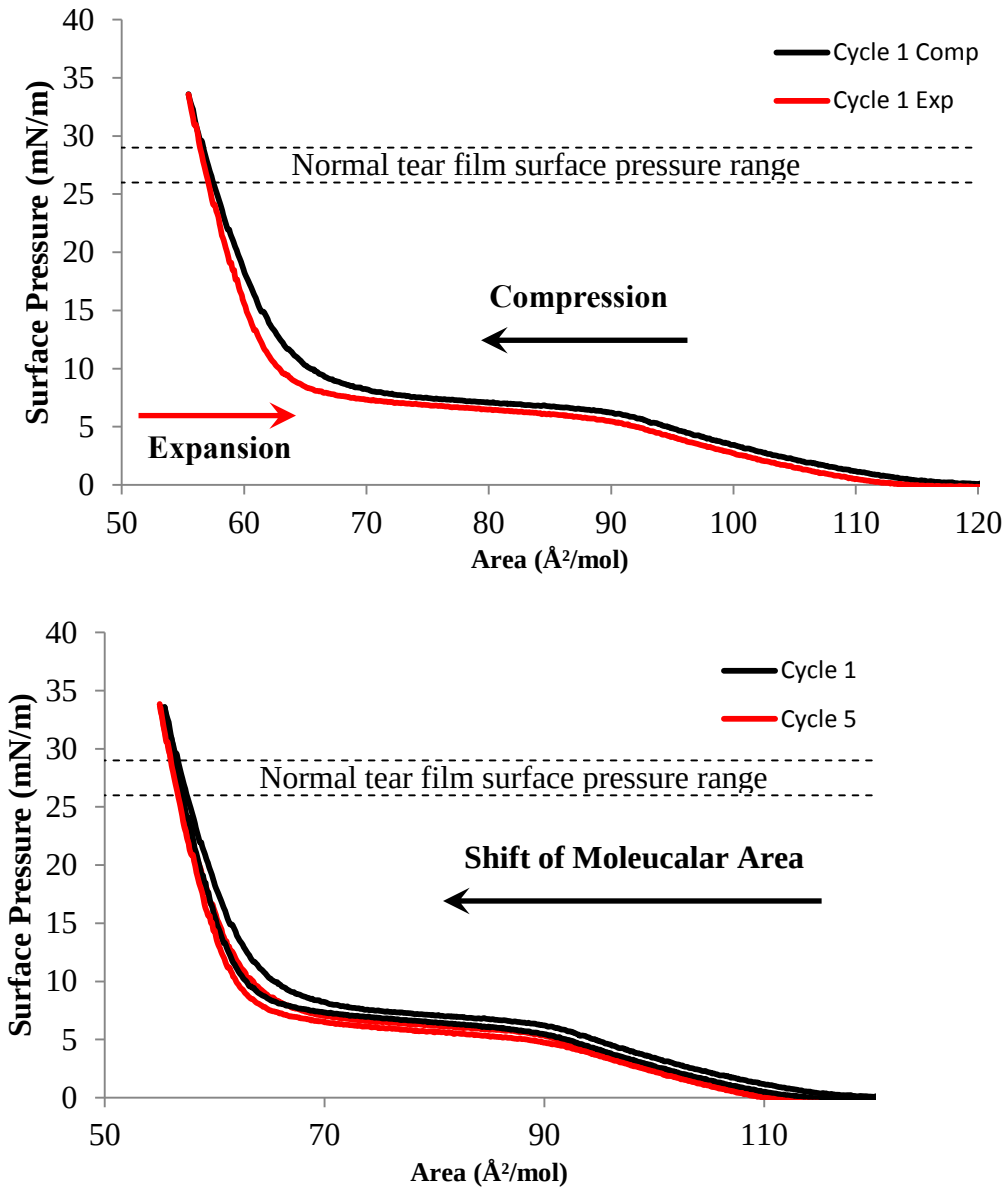

Figure 2.4. A) Schematic of hysteresis seen during isocycle experiments, and B) the shift to smaller molecular areas with successive cycles.

2.1.4 Brewster Angle Microscopy

Lateral organization of surface films can be visualized without the aid of probes using Brewster Angle Microscopy (BAM) [142] (figure 2.5). The water/air interface has a Brewster angle of 53.12°, and p-polarized light will not be reflected when it hits the interface at that angle; however, the water/lipid interface has a different Brewster angle, and this causes a reflection that can be detected and used to image the monolayer surface [142]. The images captured allow visualization of a given phase, especially for morphology, quantity, and distribution of LC domains, as well as protrusions from the plain of the monolayer [145,149].

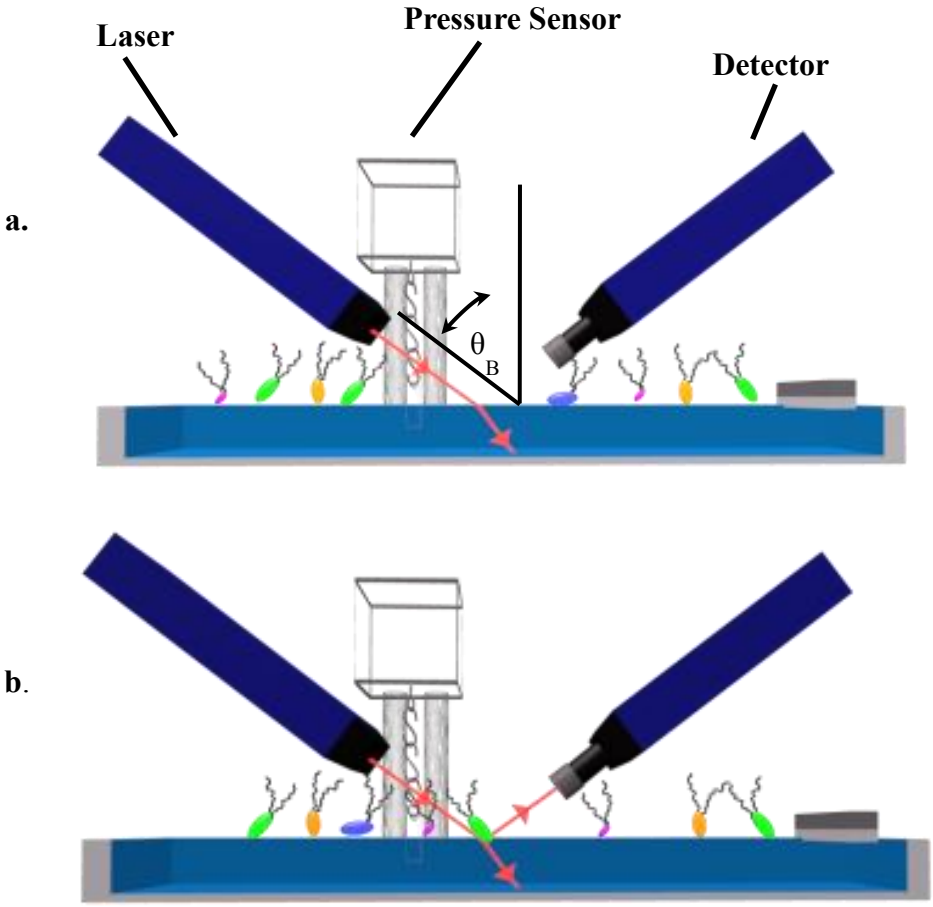

Figure 2.5. Diagram of a Brewster Angle Microscope (BAM) a) laser is incident at the Brewster angle of the air/water interface and no reflection occurs b) a lipid/water interface with a different Brewster angle causes a reflection.

2.2 Materials

2.2.1 PBS Buffer and Solvents

A 1x PBS buffer was used for all experiments and consisted of NaCl (137 mM), KCl (2.7 mM), $Na_2HPO_4 \cdot 7H_2O$ (10.1 mM), KH_2PO_4 (1.8 mM). The pH was adjusted to 7.4 and was filtered using a 1 litre bottle top filtration unit with a 2 µm filter from VWR, Radnor, PA. This buffer was chosen for previous studies in our lab because it was used in previous studies, and is currently still in use [105,139,150,151]. It has been used here for continuity with previous work. Acetone, methanol, hexane, and chloroform used in the experiments were all ACS grade.

2.2.2 Lipids

All lipids were synthetic with purity greater than 99%, purchased from Avanti Polar Lipids, Inc., Alabaster, AL (table 2.1). DPPS was the only charged lipid and was purchased as a sodium salt. Lipids were weighed using a Sartorius MC 5 Microbalance from Göttingen, Germany.

Table 2.1. Pure lipids used in experiments.

Lipid Name	Abbreviation	Molecular Weight (g/mol)	Product No.
1,2-dipalmitoyl-sn-glycero-3-phosphatidylcholine	DPPC (16:0/16:0)	734.039	850355
1,2-dipalmitoyl-sn-glycero-3-phosphatidylethanolamine	DPPE (16:0/16:0)	691.959	850705
1,2-dipalmitoyl-sn-glycero-3-phosphatidylserine	DPPS (16:0/16:0)	757.950	840037
N-palmitoyl-D-erythrosphingosylphosphorylcholine	PSM (d18:1/16:0)	703.028	860584
Glucosyl (β) Ceramide	PGC (d18:1/16:0)	700.041	860539

In addition to pure lipids, three lipid mixtures were investigated. In prior research in our lab by Patterson *et al.*, the goal was to understand the interactions of major lipid classes in a biomimetic lipid mixture based off the actual composition of polar lipids in the human tear film [152–155]. This was a quaternary mixture based off of McCulley and Shine's work, which was a molar ratio of 3 PC : 2 PE : 3 GC : 2 SM [153–156]. More research has been published that shows the polar lipid composition is still unknown [50].

For experiments reported in this thesis, the original McCulley and Shine quaternary mixture was chosen because we have an extensive data set already available from Patterson's previous work from which to build upon. Two possible differences to McCulley and Shine's system have been reported, the first was the lack of GC, the second was the presence of a small amount of PS [5,60,73]. To account for these differences, the McCulley and Shine system was altered to remove GC and include PS in another quaternary mixture in a molar ratio of 3 PC : 2 PE : 2 SM : 1 PS. Patterson's original work found interesting properties related to the incorporation of GC, so it was also decided to extend the McCulley and Shine system to include PS in a quinary mixture in a molar ratio of 3 PC : 2 PE: 3 GC : 2 SM : 1 PS.

Lipids were all weighed and transferred to glass vials using aluminum foil. The organic solvent solution used for all lipids was chloroform : methanol in a 7:3 (v/v). Pure lipids were solvated in organic solvent to 1 mM and lipid mixtures were prepared from these stocks. All lipids were dried down under argon, left in a vacuum oven overnight, and stored at -20°C until they were needed. Dried lipids were solvated to 1 mg/mL in chloroform/methanol 7:3 (v/v) for all experiments. DPPS was the only lipid that did not completely dissolve in the organic solvent. It was demonstrated that a monolayer could still be formed, but was shifted to smaller molecular areas by ~10 $Å^2$/molecule from literature values on water. Increasing the amount of methanol to a 1:1 ratio was necessary to get the DPPS to dissolve, but it also caused more DPPS to be lost to the subphase during experiments, and so this was not used. All vials, syringes, spatulas, tweezers, and

foil that came into contact with lipids were first cleaned with acetone, methanol, hexane, and chloroform to minimize lipid contamination.

2.2.3 Proteins

Most experiments used low concentrations of all three proteins. There was an additional experiment performed with varied concentrations of lysozyme and lactoferrin with the quinary lipid mixture only. For experiments with low protein concentrations, all proteins were solvated in 1 x PBS buffer to a concentration of 2.2 mg/mL, to reach a final subphase concentration of 0.01 mg/mL. Each solvated protein was used for a maximum of 12 hours. Human recombinant tear lipocalin (Accession No. P31025) was very generously provided by Dr. Liu in Dr. Vogel's lab. This tear lipocalin was expressed in *E. coli*, lyophilized, and stored at -80°C. Lyophilized human recombinant lysozyme expressed in *O. sativa* was purchased from Sigma-Aldrich Corporation, Oakville, ON. (Product No. L1667, Accession No. P61626) and stored at -80°C. Lyophilized human recombinant lactoferrin was also purchased from Sigma-Aldrich and stored at 4°C, it was expressed in rice, but the species was not listed (Product No. L4040, Accession No. P02788). This lactoferrin was partially iron saturated (0.05 to 0.10% as opposed to ≥0.10% for iron saturated lactoferrin).

For the varied protein concentration trials, it was necessary to use another supplier for lactoferrin due to the high quantity required. Those experiments used lyophilized human recombinant lactoferrin expressed in *A. niger* var. *awamori* from Agennix

Incorporated, Houston, TX. Like tear lipocalin, this was another gift from Dr. Vogel's lab. This protein was in its apo form.

2.3 Experiments and Analytical Methods

2.3.1 Surface Pressure – Area Isocycles

One 200 cm^2 (10 cm x 20 cm) side of a dual subphase Langmuir Trough with a pressure sensor was used with a one barrier set-up. The Langmuir Trough was a medium trough model made of polytetrafluoroethylene (PTFE or Teflon™) and produced by Nima Technology Ltd., Coventry, England. The bottom of the barrier that contacted the subphase was also made of PTFE. For all experiments, the minimum area was set to 30 cm^2 and the maximum area was set to 190 cm^2, and the barrier speed was 70 cm^2/min. The speed of 70 cm^2/min was chosen for all experiments to increase reproducibility during isocycles while still moving the barrier as quickly as possible. The trough was housed within a Plexiglas® cabinet to reduce exposure to air currents. All experiments were performed at room temperature of ~24°C. Before the trough was used, it would be cleaned with boiling water, and then wiped down with acetone, methanol, hexane, and chloroform. The software used was Nima 7.8.

A clean Wilhelmy 20 mm plate was hung on a PS4 model pressure sensor also from Nima Technology Ltd. The same plate would be used for all replicates in a trial, but no plate was used for more than one lipid/protein combination before being cleaned with boiling water.

A small magnetic stir bar was placed in the recessed window (normally used for microscopy) in the centre of the trough. The barrier was moved to its closed position and 109.5 mL of 1x PBS buffer subphase was added on the opposite side of the barrier from the pressure sensor. The subphase of 109.5 mL chosen as the least volume of subphase that slowed lipid leakage under the barrier. The Wilhelmy plate was lowered into the subphase. A 9 mm spacer cap was used with the pressure sensor to ensure every plate was submerged to the same amount. A 10 minute period was given to allow volatile cleaning solvents to evaporate. Of those 10 minutes, 8 minutes were given to allow any surfactants within the buffer to reach the surface of the subphase, reducing surface contamination inside of the barrier, the remaining 2 minutes was used to open the barrier and activate the magnetic stirrer. An isotherm was run to ensure the surface of the PBS subphase was clean; the barrier was swept across the surface using the barrier control feature in the software. PBS buffer has some surface activity, the subphase was considered clean as long as the surface pressure did not exceed 0.5 mN/m. A 25 µL Hamilton syringe (Avanti Polar Lipids, Inc., Alabaster, AL) was used to deposit 18 µL of 1 mg/mL lipid in organic solvent dropwise onto the subphase, and 10 minutes was allowed for the volatile solvent to evaporate. This amount of lipid was chosen so that the gas phase and collapse for each lipid film could be observed. All lipids were kept on ice during deposition, and kept at -20°C during all other times to reduce solvent evaporation.

The experiment was divided into three stages, the constant pressure stage, the constant area stage, and the isocycle stage. The constant pressure stage used the pressure

control feature to compress the lipid film to 26 mN/m, the resting surface pressure of the tear film [41]. This demonstrated the existence of a stable lipid monolayer. A target pressure of 26 mN/m was used with a gain of 2 mN/m to slow the barrier when it neared the target pressure, reducing agitation from excessive barrier movements during pressure control. After 10 minutes of pressure control, the isotherm was stopped. The time interval for pressure control was chosen as it decreased the pressure drop of DPPE films during the area control stage, this did not occur with DPPC films, but it was an attempt to make all trials more reproducible.

The second stage of the experiment was the constant area stage and involved the injection of either protein or PBS buffer as the control. The protein solution was inverted 10 times after hydration with PBS buffer to solvate. For low protein concentration experiments, 0.5 mL was drawn up using 1 mL Tuberculin Slip Tip syringe from BD, Franklin Lakes, USA. The tip of the syringe was bent so that it could inject under the barrier from the outside, and avoid disrupting the monolayer. For varied protein concentration experiments, 10 mL was drawn up using 10 mL Tuberculin Slip Tip syringe from BD, Franklin Lakes, USA. This syringe was attached to a tube that fed to a bent tip so a pump could be used to control the injection rate. The area control option of the Nima 7.8.software was activated immediately after stopping the pressure control, and the current area obtained during the pressure control was entered as the control area. One minute after starting the incubation, the protein or PBS control was carefully injected under the barrier.

For low protein concentration experiments, the injection was done manually. A pump was not used for the low concentration experiments because the tube from the syringe to the Langmuir trough would have greatly increased the amount of tear lipocalin required, which was undesirable due to the time constraints required to express and purify it. For varied protein concentration experiments, a Pump 11 Elite pump from Harvard Apparatus, Holliston, MA was used to set the rate of injection at 0.5 mL/min. For low protein concentration experiments, the injected protein volume was 0.5 mL, with a concentration of 2.2 mg/mL, giving a final subphase volume of 110 mL and a final protein concentration of 0.01 mg/mL. This low protein concertation was chosen because its surface activity could be detected in DPPE films held at 10 mN/m, but still low enough to conserve protein. For the experiments with varied concentrations of lysozyme and lactoferrin, the injected protein volume was 10 mL, with concentrations of either 0.6, 2.4, or 12 mg/mL, giving final subphase volume of 120 mL, and final protein concentrations of 0.05, 0.2, or 1 mg/mL respectively. The concentration of 1 mg/mL was the highest concentration possible for the Langmuir trough given the solubility of the proteins and represents the lower range of these proteins in the tear film [108,109,115,116]. The 0.05 and 0.2 mg/mL concentrations were chosen to investigate a concentration dependent effect. After protein injection, a 30 minute incubation period was given to allow for any pressure change to occur. The plastic BD syringes and tubes could not be cleaned with organic solvents, so they were rinsed with methanol 10 times, and then with boiling water 10 times.

Lastly, the third stage of the experiment involved a series of isocycles to mimic blinking. For low protein concentration experiments, the number of isocycles was 5, minimum surface pressure was set to 24 mN/m and the maximum surface pressure was set to 32 mN/m. This was to approximate 20 mN/m to 35 mN/m as the instrument was not responsive enough to stop immediately at the target pressures, and it always overshot or undershot desired surface pressures by a few mN/m. The number of isocycles was chosen because of the upper limit of how many blinks could be undertaken before seeing morphological changes in the interference patterns of the human tear film [157]. The surface pressure range of 20 to 35 mN/m was chosen because 25 mN/m to 35 mN/m is the current estimated surface pressure range of the tear film during a blink, and 20 mN/m is generously low enough to allow the possibility of protein insertion [41,42]. The varied protein concentration experiments were run after the low concentration experiments, and it was decided to increase the number of cycles to 20 to gather additional data.

2.3.2 Analysis of Surface Pressure – Area Data

The isotherm recorded during the constant pressure stage of each experiment was analyzed to see if a monolayer was formed. The molecular areas at 26 mN/m were analyzed, as were the isotherm profiles, and compared to literature data.

The change in surface pressure over time was calculated for the area control stage of each experiment. This was where the barrier position was held constant after injecting

the protein or PBS buffer control. The difference between the starting pressure at 5 minutes and ending pressure at 30 minutes was taken.

The isocycle data from the fourth part of the experiment was analyzed for variations in hysteresis between different systems. Two different values were calculated, a ratio of the area under the compression and expansion curves for each isocycle (reversibility), and compression modulus. Trapezoidal integration was used to calculate the area under each curve (figure 2.6, equation 2.3). If the ratio of expansion to compression areas is close to 1, then the film is more reversible. Figure 2.6 shows a more common schematic of area calculation for DPPC, with a compression isotherm beginning in gas phase. Due to the pressure ranges chosen for these experiments, the films were much more reversible than isocycles that began in the gas phase; the compression and expansion isotherms almost overlapped and were almost linear. The ends of the hysteresis loops where the barrier switched direction were not precise, so areas, slopes, and lateral compression/expansion moduli were calculated between 24 mN/m and 33 mN/m.

$$\int_1^n f(x)dx \approx \sum_{i=1}^{n} (A_{x_{i+1}} - A_{x_i}) \left(\frac{\Pi_{x_i} + \Pi_{x_{i+1}}}{2} \right) \qquad \text{[Equation 2.3]}$$

Where A is the molecular area and Π is surface pressure.

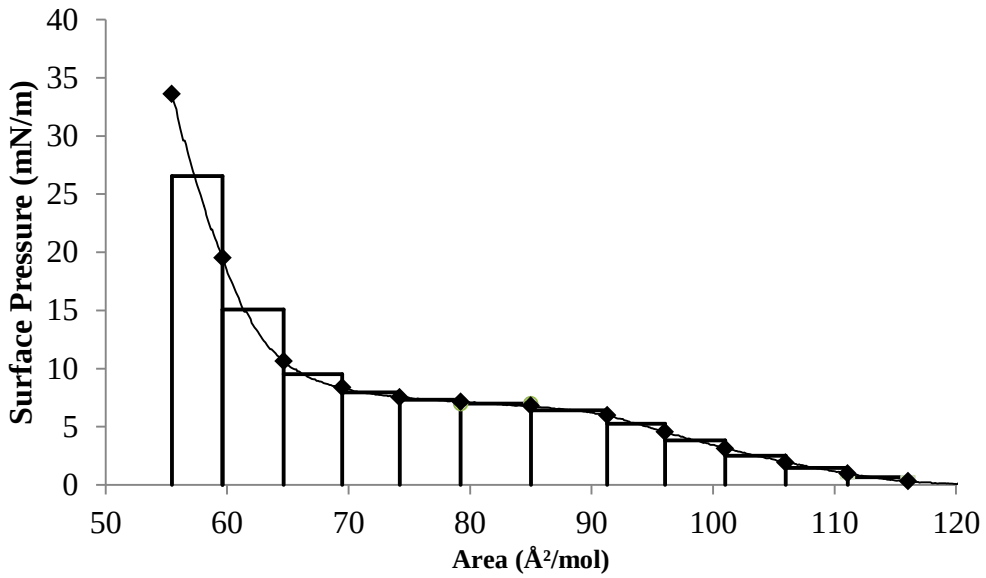

Figure 2.6. Simplified schematic of trapezoidal integration used to calculate reversibility. Actual isotherms have many more data points.

Lateral compression and expansion moduli (β) were calculated at 27.5 mN/m for each compression and expansion isocycle (equation 2.5). A single pressure was chosen to avoid artifacts caused by the barrier slowing down and speeding up near the target pressures.

$$Cs = -\frac{1}{A}\left(\frac{\partial A}{\partial \Pi}\right) \qquad \text{[Equation 2.4]}$$

$$\beta = Cs^{-1} \qquad \text{[Equation 2.5]}$$

Where Cs is lateral compressibility, A is the molecular area, and Π is surface pressure [143]. Since the isotherms were mostly linear near 27.5 mN/m, the slope was used for derivative.

2.3.3 Brewster Angle Microscopy

Brewster Angle Microscopy (BAM) was used to image the lateral organization of the various lipid only and lipid/protein systems. The trough apparatus and set-up was exactly the same as the isocycle experiments. The BAM and trough were placed on a Halcyonics anti-vibration system, and housed within a cabinet. The BAM was purchased from Accurion (BAM 601 model, Göttingen, Germany), capable of 1 μm resolution, and used a 658 nm laser. The software used to operate the BAM and capture images was EP3 View version 2.35, also from Accurion. The angle of incidence (AOI) was set to 53.120°, the polarizer (P) was set to 2°, the compensator (C) was set to 0 °, and the analyzer (A) was set to 10°. The laser intensity was set to 50%, and the focus scanner was adjusted to ~15000. Various images were captured in the constant pressure stage, while the lipids were being compressed to 26 mN/m. An image was taken at the start of the constant area stage before PBS/protein injection, immediately after injection and after 30 minutes of incubation. During the isocycle stage, images were captured at ~35 mN/m and 20 mN/m for isocycles 1 and 5. For the varied protein concentration experiments,

additional images were taken at ~35 mN/m and 20 mN/m for isocycles 10 and 20. All isotherms had to be paused while capturing images to reduce blurring of the image.

The size of the images produced were 218 x 271 μm (768 x 953 pixels). All images presented in this thesis were scaled down from their original sizes, and a region of each image was selected and magnified 2x in an inset image in the bottom right corner. Many of the images appeared quite dark due to variations in subphase height over the course of the experiments and had to be brightened. The GNU Image Manipulation Program (GIMP version 2.8.18) was used to scale, create the magnified insets, and brighten the images. A region of 180 x 180 pixels was selected for the magnification. Images were not uniformly bright, so to brighten the image, a line of pixels corresponding to the center of the magnified region was scanned across the entire width of the image. The brightest pixel was selected, and that would correspond to somewhere in an LC domain. The brightness and contrast of the entire image was adjusted up or down until the pixel's grey level was 140 ± 2 units. This process was done to provide a magnified inset for each image of similar brightness for comparison. This was not done with pure lipids DPPC, DPPE, PGC, and PSM for the lowest surface pressure shown in the pressure control stage, as no LC domains were visible. The 180 x 180 pixel selected region was scaled up 2x using cubic interpolation. The non-uniform brightness prevented the use of quantitative analysis of the images.

Chapter Three: Isotherms of Lipid-Only Films

3.1 General Chapter Overview

This chapter will present the results and discussion regarding the three stages of the experiments with lipid-only films. The three stages were the constant pressure stage, the constant area stage, and the isocycle stage. Similarities and differences based on lipid structure will be highlighted, while chapter four will discuss how the major tear film proteins affect those systems (page 84). The main purpose of these experiments was to test how proteins affect the dynamics of the lipid monolayers during blinking, as mimicked during the isocycle stage, and so that stage will be the primary focus of this thesis. The constant pressure and area stages were necessary to prepare the films for isocycles, so those results will be briefly considered. The five pure lipids will be examined first, followed by the three lipid mixtures.

3.2 Results

3.2.1 Constant Pressure Stage

The first stage of each experiment was to verify that a monolayer had formed and to bring the film to 26 mN/m, the lower surface pressure range of the human tear film [41]. This pressure was held for 10 minutes to allow the film to stabilize before the constant area stage, in order to increase reproducibility.

3.2.1.1 Pure Lipids

For DPPC, liftoff occurred at ~100 mN/m, where the system transitioned from the gas (G) phase and to the liquid expanded (LE) phase (figure 3.1). The LE-LC phase coexistence plateau began at ~78 $Å^2$/molecule and 10 mN/m and the system reached 26 mN/m at ~48 $Å^2$/molecule. DPPE and PGC had fairly similar isotherms and both lipids lacked a LE-LC phase transition plateau. They had the smallest liftoff areas at ~57 $Å^2$/molecule and areas at 26 mN/m of ~ 45 $Å^2$/molecule. For PSM, the G-LE transition occurred at ~85 $Å^2$/molecule. The LE-LC phase plateau began at ~64 $Å^2$/molecule and ~16 mN/m, and reached 26 mN/m at 50 $Å^2$/molecule. DPPS transitioned from LE to LC phase beginning at ~97 $Å^2$/molecule and 1.4 mN/m, and was compressed to ~45 $Å^2$/molecule to reach 26 mN/m.

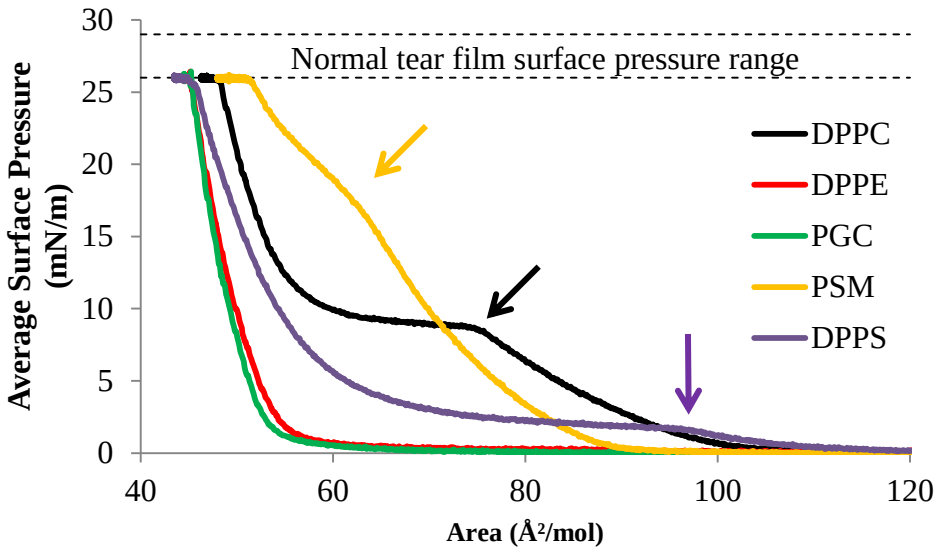

Figure 3.1. Representative surface pressure - area isotherms for individual pure lipid monolayers to 26 mN/m. Plateaus at 26 mN/m were due to pressure held at 26 mN/m for 10 minutes. Arrows indicate the beginning of plateau regions (LE – LC phase coexistence) or other slope changes.

3.2.1.2 Lipid Mixtures

The lipids that were tested individually have been reported in the past as tear film components [5,60,73,156]. Based on these studies, it was decided to investigate a quinary model with the molar composition 3 PC : 2 PE: 3 GC : 2 SM : 1 PS. The composition of polar lipids in the tear film is currently unknown, so three models were used to better capture diverse standpoints. Thus, it was decided to use an older model from Shine and McCulley that lacked DPPS, and has the molar composition 3 PC : 2 PE: 3 GC : 2 SM (DPPS (-)) [156]. Also, PGC was not identified in large amounts in recent studies, so we

decided to include another quaternary mixture that lacked PGC, this mixture had a molar ratio of 3 PC : 2 PE: 2 SM : 1 PS (PGC (-)) [5,60,73].

Isotherms from the pressure control stage for lipid mixtures show that the PGC (-) mixture shifted to higher molecular areas (figure 3.2). The DPPS (-) mixture has a LE-LC coexistence plateau beginning at 78 A^2/molecule, 1.7 mN/m, while the PGC (-) mixture has a LE-LC coexistence plateau beginning at 90.3 A^2/molecule, 1.8 mN/m. The plateau in the quinary mixture is less pronounced, but it is evident beginning at 83 A^2/molecule, 1.2 mN/m.

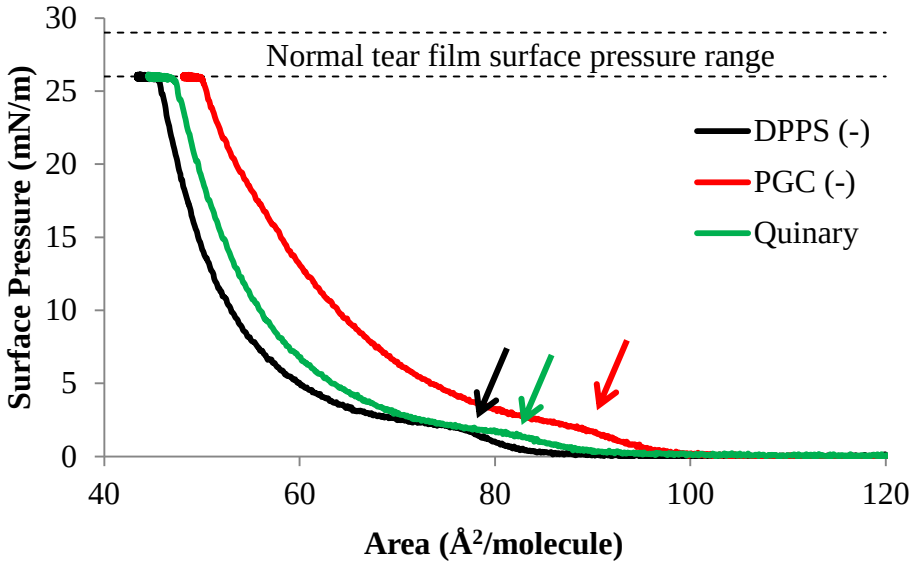

Figure 3.2. Representative area – surface pressure isotherms for two quaternary and one quinary mixed lipid monolayer. The quinary mixture molar ratio is 3 PC : 2 PE: 3 GC : 2 SM : 1 PS. The DPPS (-) quaternary mixture lacks DPPS, and the PGC (-) quaternary mixture lacks PGC. Arrows indicate the beginning of LE-LC phase existence plateaus.

3.2.2 Constant Area Stage

After the constant pressure stage of each trial, the constant area stage was started whereby the barrier was held in a fixed position. Each lipid monolayer started out at 26 mN/m, and 0.5 mL of 1x PBS buffer was injected under the barrier after 1 minute of the experimental onset. A 30 minute incubation period followed the injection. This set-up was later used for protein injection and allowed time for the proteins to diffuse throughout the subphase. A representative area control isotherm for DPPC has been provided (figure 3.3). DPPC exhibits a drop in surface pressure that becomes less severe over time, and two sets of spikes/dips in surface pressure that correspond to opening and closing the door to the Plexiglas® housing of the trough whereby the 0.5 mL of buffer was injected. The higher noise level of this curve is caused by the stir bar. The average change in surface pressure was then calculated over a 25 minute interval beginning 5 minutes after the start of the isotherm.

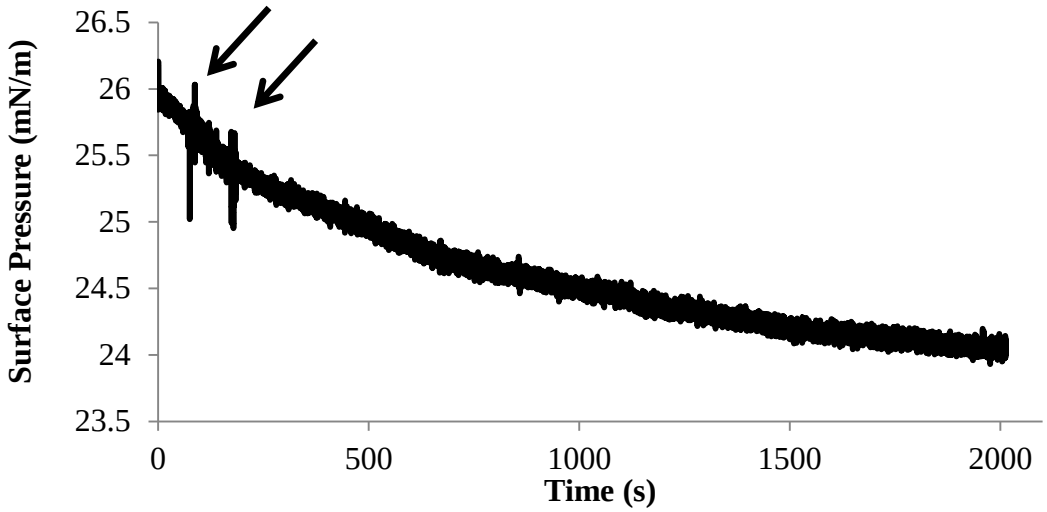

Figure 3.3 Representative isotherm for the change in surface pressure of DPPC over time. Arrows point to spikes/dips in surface pressure caused by opening and closing the door in the Plexiglas® housing to access the trough and inject PBS buffer.

3.2.2.1 Pure Lipids

All five pure lipids experience a decrease in surface pressure over the 30 minute incubation (figure 3.4). DPPE experience the least magnitude pressure drop of -0.6 mN/m, while PGC observed the highest magnitude pressure drop -2.6 mN/m. DPPS was between the two at -1.4 mN/m. DPPC and PSM experienced the most variability and so were not significantly different from the other three lipids.

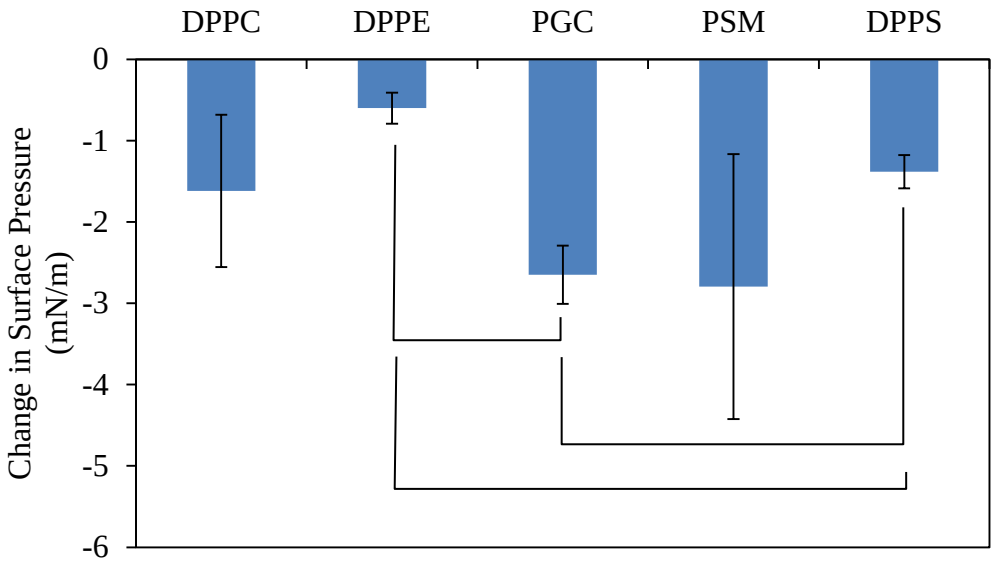

Figure 3.4. Average change in surface pressure over a 25 minute interval for five pure lipids, beginning ~3 minutes after 0.5 mL of 1 x PBS buffer had been injected under the barrier. The initial surface pressure was 26 mN/m. Error bars represent standard deviation, $n \geq 3$. Brackets indicate significant differences calculated using the t-test, $p < 0.05$.

3.2.2.2 Lipid Mixtures

Unlike pure lipids, there is no significance difference between the pressure decreases observed over the 30 minute incubation period for the lipid mixtures (figure 3.5). The mixtures appear to be most similar to pure PGC (figure 3.4), ranging from 2.8 to 2.4 mN/m for the DPPS (-) and quinary mixtures respectively. The quinary mixture may be more stable than the other two mixtures, but not significantly so.

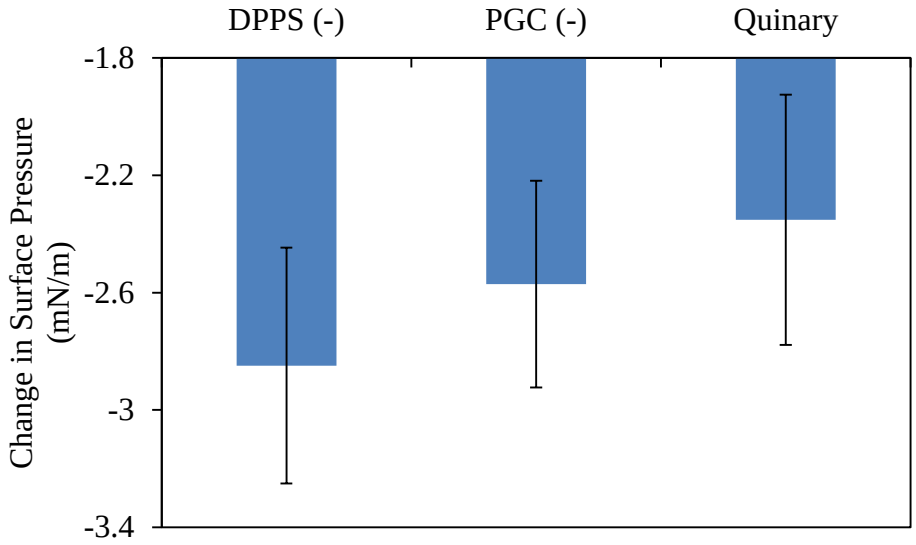

Figure 3.5. Average change in surface pressure over a 25 minute interval for three lipid mixtures, beginning ~3 minutes after 1 x PBS buffer had been injected under the barrier. The initial surface pressure was 26 mN/m. The quinary mixture molar ratio is 3 PC : 2 PE: 3 GC : 2 SM : 1 PS. The DPPS (-) quaternary mixture lacks DPPS, and the PGC (-) quaternary mixture lacks PGC. Error bars represent standard deviation, $n \geq 3$.

3.2.3 Isocycle Stage - Reversibility

After the area control stage, isocycles were performed where lipids were compressed and expanded for five cycles, between ~20 and ~35 mN/m, which are thought to be biologically relevant surface pressures for the tear film [41,42]. For reference, individual cycles from pure lipids have been provided in figure 3.6. The compression isotherms were linear, except for PSM which was slightly curved. The expansion isotherms were generally not linear. From these profiles, the compression and

expansion isotherms for DPPC and PSM overlap more than the other lipids. DPPE, PGC, and DPPS have expansion isotherms that remain at higher surface pressures than the compression isotherms for a given area.

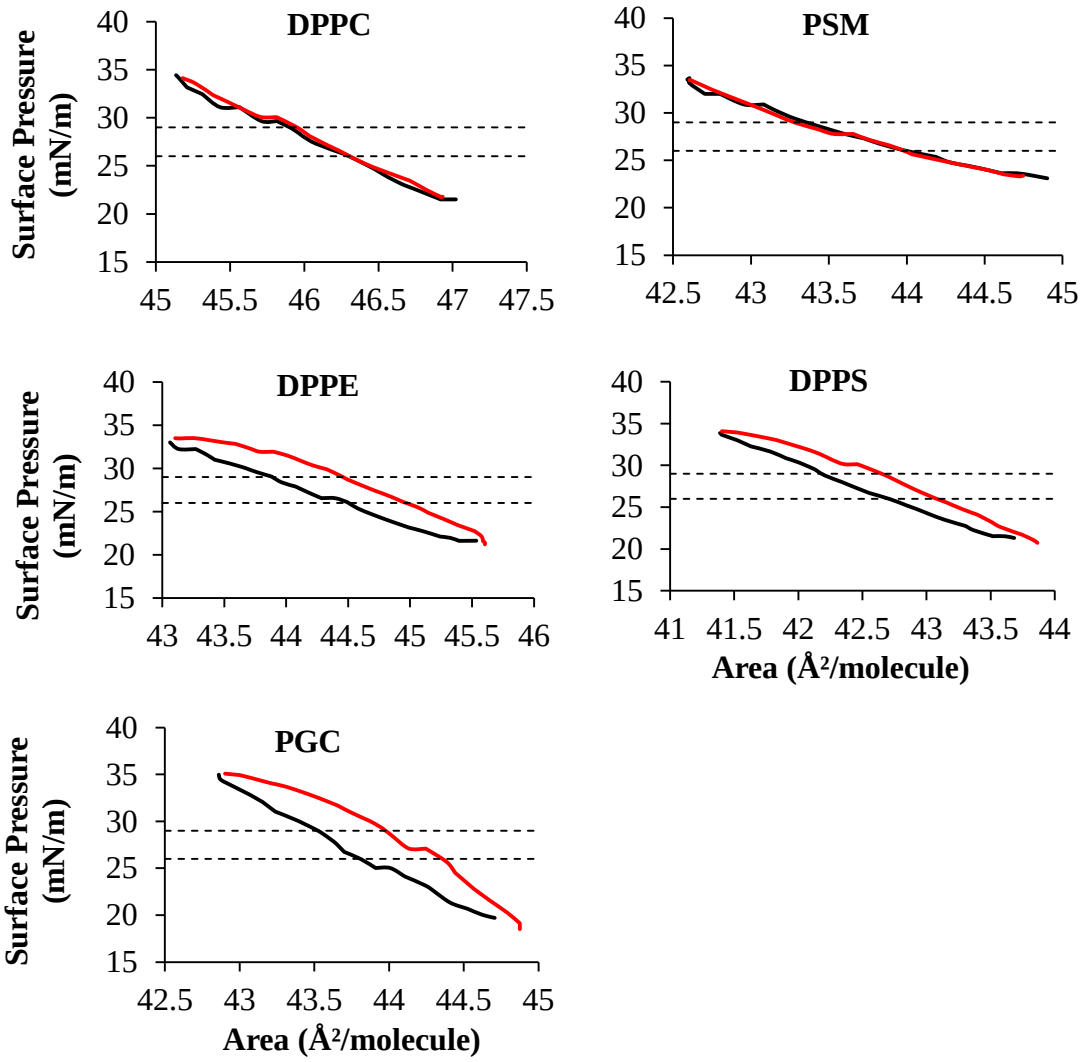

Figure 3.6. Representative compression (black) and expansion (red) isotherms during the third isocycle for pure lipids. The normal tear film surface pressure range is represented between the dotted lines.

Reversibility was calculated by dividing the area under the compression isotherm by the area under the expansion isotherm. A reversibility of 1 would mean that the expansion isotherm overlaps the compression isotherm. A reversibility of less than 1 would mean the expansion isotherm was at lower surface pressures than the compression isotherm, and a reversibility greater than 1 would mean the opposite. A range between 24 and 33 mN/m was used to keep the pressure between 20 and 35 mN/m for lipids with high compression rates. Despite the slower barrier speed of 70 cm^2/min, there was still a delay in the barrier switching direction, and that could result in the surface pressure overshooting the desired range. Cycles 1 and 5 were also omitted because of artifacts related to starting and stopping the isocycle stage. For instance, DPPE did not experience much pressure drop during the constant area stage, so it would actually begin the first cycle at a surface pressure greater than 24 mN/m, but expand below 24 mN/m, artificially increasing the reversibility for the first cycle. For the fifth cycle, the barrier seemed to slow at the end of cycle, instead of dipping past 24 mN/m as for cycles one to four. For PSM, this lead to larger molecular areas for 24 mN/m, and artificially lowered the reversibility for cycle 5.

3.2.3.1 Pure Lipids

No significant trends were seen regarding differences in reversibility between Pure lipids (figure 3.7). The reversibility seems to increase for DPPE with each successive cycle, but differences are not significant. The opposite trend appears for PGC,

but again the differences are not significant. If cycle 3 is compared between all lipids, no significant differences are seen. From the isotherm profiles in figure 3.6, you would expect the reversibility of DPPC and PGC to be close to 1, and reversibility for the other three lipids to be greater than 1. Due to the variation, it is only possible to say that reversibility is near 1.

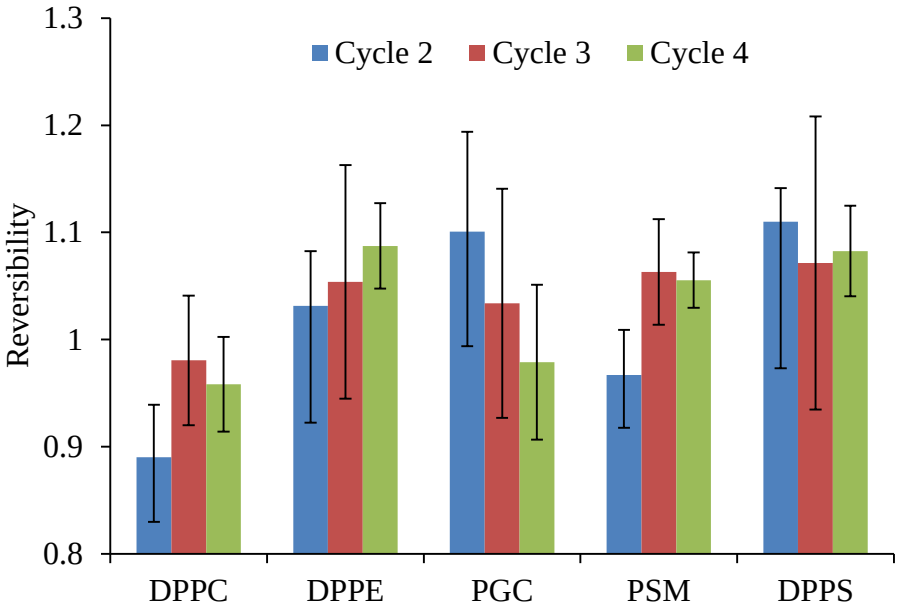

Figure 3.7. Reversibility of pure lipid isocycles, calculated for cycles 2, 3, and 4. Isocycles were roughly between 20 and 35 mN/m. Cycles 1 and 5 were omitted because of artifacts observed due to starting and stopping the isocycle stage. Error bars represent standard deviation ($n \geq 3$).

3.2.3.2 Lipid Mixtures

The isocycle stage for lipid mixtures has produced similar results to the reversibility of pure lipids, whereby no significant differences were observed (figure 3.8). Lipid mixtures all had a reversibility near 1.

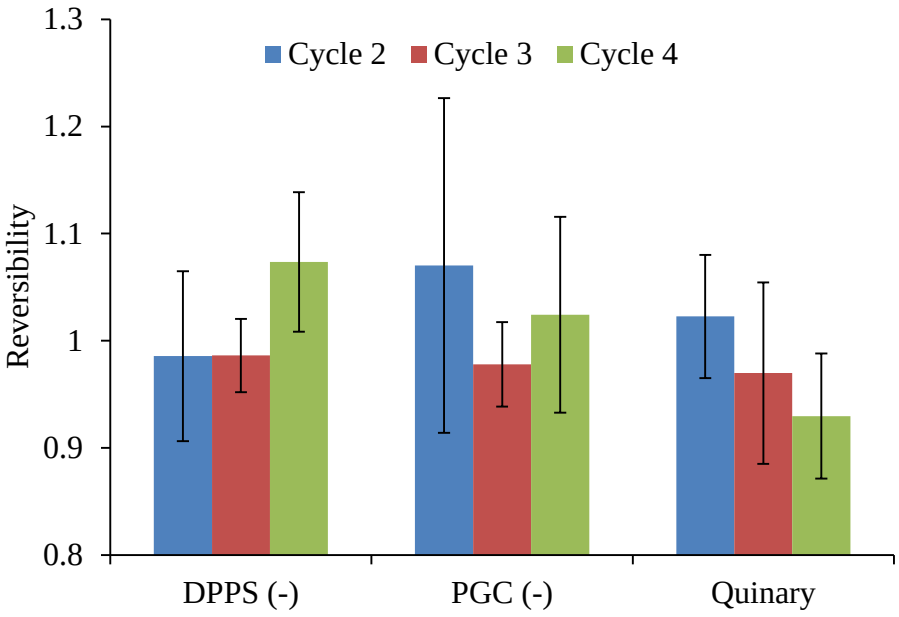

Figure 3.8. Reversibility of pure lipid isocycles, calculated for cycles 2, 3, and 4. Isocycles were roughly between 20 and 35 mN/m. Error bars represent standard deviation ($n \geq 3$). The quinary mixture molar ratio is 3 PC : 2 PE: 3 GC : 2 SM : 1 PS. The DPPS (-) quaternary mixture lacks DPPS, and the PGC (-) quaternary mixture lacks PGC.

3.2.4 Isocycle Stage - Compression and Expansion Moduli

In addition to analyzing reversibility, the compression and expansion moduli (β) were calculated at one surface pressure to allow comparison. The surface pressure of 27.5 mN/m was chosen because it was in the middle of the cycling range, furthest from maximum or minimum pressures where the barrier would switch direction. These moduli are used to assess the elastic nature of the monolayer arising from variations molecular interactions [157]. Moduli between 100 and 250 mN/m are thought to be indicative of a LC phase, and above 250 mN/m a solid phase [158].

3.2.4.1 Pure Lipids

It appears that DPPC and PGC were most likely in a solid phase, while DPPE and DPPS may have been either LC or a solid phase, and PSM was most likely in an LC phase (figure 3.9). Compression and expansion moduli within each pure lipid were similar. Table 3.1 provides a comparison to literature values. Compression moduli observed in this experiment are generally much higher than literature values.

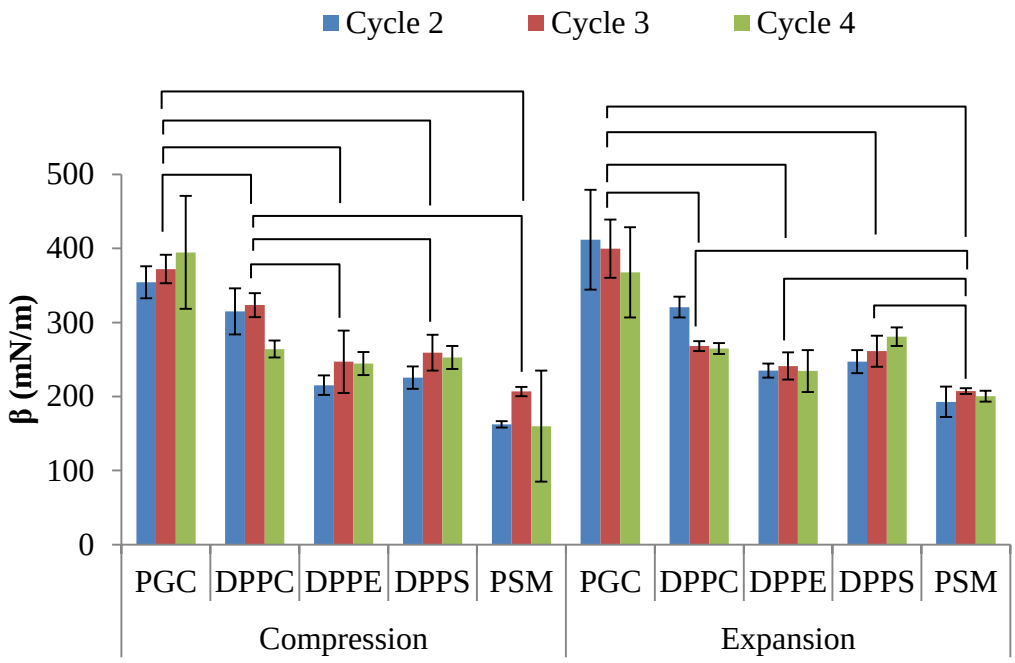

Figure 3.9. Compression and expansion moduli (β) of pure lipids calculated at ~27.5 mN/m for isocycle compression (comp) and expansion (exp) isotherms for cycles 2, 3, and 4. Isocycles were between 20 and 35 mN/m. Brackets represent significant differences that were calculated with the t-test ($p > 0.05$) for the third cycle only. Error bars represent standard deviation.

Table 3.1. Average compression moduli (β) of pure lipids calculated at ~27.5 mN/m during isocycles. Error represents standard deviation (n ≥ 3). (*) Literature values from Sakamoto *et al.* and Tae *et al.* were calculated from published isotherms and so are rough estimates only **[159,160]**.

β (mN/m) at ~27.5 mN/m			
Lipids	**Current**	**Patterson *et al.***	**Literature**
DPPC	324 ± 16	129 [154]	~170 [151], ~195 [161]
DPPE	247 ± 16	102 [154]	~85 [151]
PGC	372 ± 19	159 [154]	~300 [162]
PSM	207 ± 6	134 [154]	~ 80 (*) [160]
DPPS	259 ± 24	N/A	~140 (*) [159], ~158 [163]

3.2.4.2 Lipid Mixtures

The compression and expansion moduli for lipid mixtures were generally similar (figure 3.10). No consistent trends were observed.

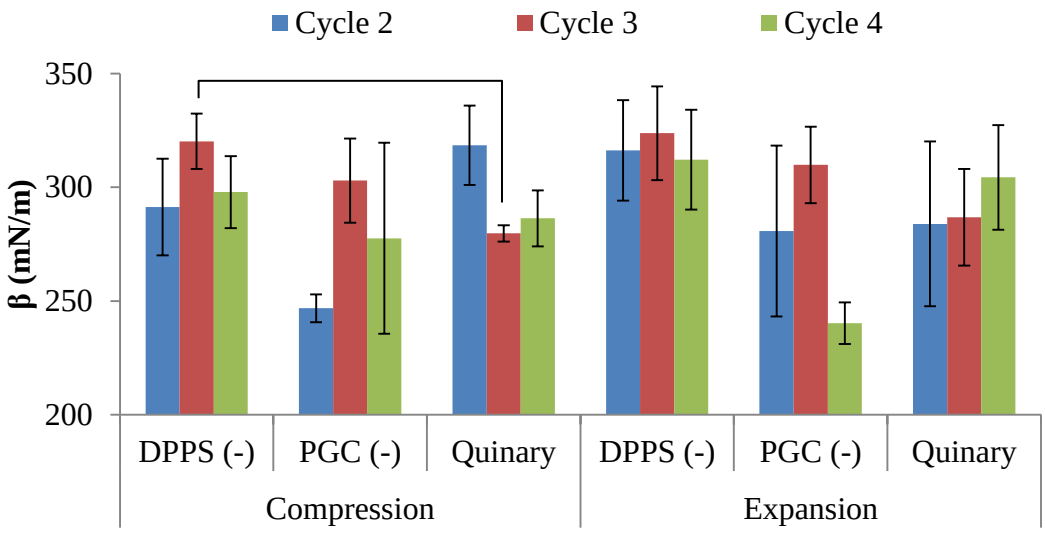

Figure 3.10. Compression and expansion moduli (β) of lipid mixtures calculated at ~27.5 mN/m for isocycle compression (comp) and expansion (exp) isotherms for cycles 2, 3, and 4. Isocycles were roughly between 20 and 35 mN/m. The quinary mixture molar ratio is 3 PC : 2 PE: 3 GC : 2 SM : 1 PS. The DPPS (-) quaternary mixture lacks DPPS, and the PGC (-) quaternary mixture lacks PGC. Brackets represent significant differences that were calculated with the t-test, $p < 0.05$. Significance was calculated using the t-test between each lipid pair for compression or expansion for cycle 3 only. Error bars represent standard deviation.

3.3 Discussion

3.3.1 Constant Pressure Stage

3.3.1.1 Pure Lipids

Results from this stage for DPPC, DPPE, PGC, and PGC were compared to values from Patterson *et al.*, a recent publication which contained similar experiments [155]. Generally, all four lipids occupied similar molecular areas at 26 mN/m, and had similar profiles to Patterson *et al.*, as were the LE-LC phase transition plateaus of DPPC and PSM.

Average molecular areas at liftoff were not compared because of the range of values in the literature, due to a variety of experimental differences and the lower accuracy of surface pressure measurements in the G-LE transition [164]. DPPC was consistent with the literature regarding the molecular area at 26 mN/m and the general isotherm profile [151,165].

DPPE and PGC had the smallest molecular areas at 26 mN/m. DPPE was consistent with the existing literature [151,165]. Compared to DPPC, PSM, and DPPS this is expected for DPPE because it has the smallest headgroup of the five lipids, a primary amine [166]. In bilayers, it has been shown that DPPE can form both intra- and intermolecular hydrogen bonds, and it is thought to have similar behavior in monolayers [166,167]. The tails are mostly in an all-trans conformations from low surface pressures according to measurements from frequency-resolved sum frequency generation vibrational spectroscopy (SFG-VS) [168].

That PGC and DPPE would be so similar may seem strange because the glucosyl moiety on PGC is quite bulky. But unlike DPPC, DPPE, and PSM, the glucosyl moiety on PGC is highly hydrophilic, and in bilayers has been shown to extend from the lipid/water interface more than the other lipids, whose headgroups are predominantly parallel to the plane of the monolayer [169,170]. Only one additional study could be found of PGC, unfortunately, differences in buffer composition and temperature shift that isotherm to lower molecular areas and cannot be compared to the results presented here [162].

Despite the similar headgroups of PSM and DPPC, the sphingosine backbone PSM has significant effects on the isotherm profile. The large standard deviation for PSM was because it is extremely sensitive to drop size during deposition, resulting in lipid being easily lost to the subphase. PSM was not as widely studied as DPPC, DPPE, or DPPS, and so one of the few experiments found matched results despite being run on a 20 mM Tris buffer subphase, pH 7.4, with 130 mM NaCl [160]. Kuikka *et al.* also had similar results despite using a pure water subphase [171]. The kink seen in the current isotherm is the start of the LE-LC phase coexistence region according to results from Patterson *et al.*, but is steeper compared to Kuikka *et al.* [154,171], likely due to a faster compression rate.

When compared to DPPC, PSM molecules at low surface pressures were more tightly packed and the average molecular area was smaller. This was mostly due to the intermolecular hydrogen bonds between the NH group in PSM to the hydroxyl oxygen or

phosphate oxygen of neighboring molecules [172]. This hydrogen bond network in PSM increases the ordering of the hydrophobic tails and decreases molecular areas compared to DPPC when the lipids are in the LE phase [172]. The LE-LC phase transition for DPPC begins at ~10 mN/m, lower than the same transition for PSM, which begins at ~16 mN/m (page 58). PSM may have a higher transition due to the unsaturated bond in the sphingosine backbone, which is lacking in DPPC. The DPPC monolayer was more ordered after the LE-LC transition than PSM, so the DPPC became more condensed and achieved smaller molecular areas than PSM. One possible explanation for this effect in addition to the presence of the double bond, is that the hydrogen bond network in PSM holds the molecules in positions that do not allow for optimal packing at surface pressures between 10 and 26 mN/m [173].

At physiological pH, DPPS has a negative charge on the phosphate and a positive charge on the primary amine on the serine moiety, but it also has another negative charge on the carboxylic acid group of the serine moiety, giving the headgroup an overall negative charge [174]. The current results have a LE-LC phase coexistence plateau which is absent for some of the literature isotherms for PBS buffer [159,163], but present for others [175]. Temperature is likely the reason for the differences with the LE-LC phase coexistence plateau. Room temperature was not controlled during these experiments, and on hotter days would shift the LE-LC plateau to higher pressures and lower molecular areas, making it visible [176].

3.3.1.2 Lipid Mixtures

Isotherms of PGC (-) from the constant pressure stage were shifted to higher molecular areas than DPPS (-) and the quinary mixture. PGC individually had a similar compression isotherm to DPPE, indicating that the orientation of the headgroup into the subphase allows it to be compressed to smaller molecular areas than the other three pure lipids. The complete lack of PGC increases the amounts of DPPC and PSM, which have much larger cross-sectional areas.

The 3 PC : 2 PE: 3 GC : 2 SM (DPPS (-)) mixture has been investigated by Patterson *et al.* [154]. The molecular areas at 26 mN/m were similar [154]. There is a LE-LC phase coexistence plateau that that is missing in the work from Patterson *et al.* [154]. Like with DPPS, this is likely due to an increase in room temperature shifting the plateau to smaller molecular areas and higher surface pressures [176].

3.3.2 Constant Area Stage

All lipids experienced a drop in surface pressure from the initial pressure of 26 mN/m, some lipids had less of a pressure drop and were therefore more stable. It appears that the most complex mixtures may be more resistant to pressure drop over time and could provide a more stable matrix for the tear film at physiological pressures. However, the differences were not significant. The pressure decline or relaxation is common with lipid isotherms. It is observed after films have been compressed at a rate where lipids cannot explore lower energy conformations and are not in an equilibrium state [177,178]. Evaporation was a part of the observed pressure drop, but it is not a primary factor. The

pressure decline experienced by a subphase lacking a monolayer and solely caused by evaporation was less than any pure lipid or lipid mixture studied here (data not shown). The processes that lead to this pressure decrease are still being investigated, and I have not found specific structural explanations. A detailed analysis of possible theoretical mechanisms is beyond the scope of this thesis as this stage was only used to provide comparison when proteins were later injected into the subphase, discussed in chapter four (page 84). Protein insertion would be indicated if the magnitude of pressure decline is reduced, abolished, or an increase in surface pressure is seen [138].

3.3.3 Isocycle Stage – Reversibility

The reversibility of pure lipids seen here were higher than those observed by Patterson *et al.*, likely due to differences in experimental set-up [155]. In those experiments, the isocycles were carried out by compressing the film to within 15 mN/m of collapse, and then expanding the film to maximum area of the trough (0 mN/m) [155]. In the current set-up, the focus was to cycle films near biologically relevant surface pressures. As mentioned earlier, the compression rate of 96 cm^2/min was used instead of the current 70 cm^2/min, and a stir bar was used in the current experiments [155]. The pronounced hysteresis seen in Patterson *et al.* isocycles is not present here [155]. Primarily, pure lipids from Patterson *et al.* had a reversibility of less than 0.9 and DPPE had reversibility of less than 0.85 [155]. The reversibility for DPPE seen here was closer to 1. So it seems that either lipids have high reversibility if cycled within biologically

relevant surface pressures, or that the time allowed during the area control stage increased the lipid reversibility. It is likely that lipids became more tightly packed when the LC domains were not allowed to dissipate completely by expanding to 0 mN/m. Moreover, it seems that the dynamic cycling behaviors of these lipids at biologically relevant surface pressures are similar under our current experimental settings, despite structural differences. Such behavior would be beneficial for films *in vivo* as film stability would not be significantly affected by variations in lipid composition.

Regarding lipid mixtures, DPPS(-) was the most complex studied by Patterson *et al.* and the reversibility was < 0.85 [155]. It seems that all three mixtures in this assay have very high reversibility between 20 and 35 mN/m, which would be relevant for its function under physiological pressures. No significant differences were observed, so regardless of the different lipid-lipid interactions that may be occurring in each film, it does not seem to affect the reversibility in a way that can be detected with this assay.

3.3.4 Isocycle Stage – Compression and Expansion Moduli

Results from Patterson *et al.* during continuous compression from gas phase to 26 mN/m showed that every lipid except DPPS – which was not studied – were all in LE phase [154]. Like with reversibility, this experimental set-up appears to have rigidified the monolayers. Again, this is probably due to preventing the expansion of the films to the point where LC domains would dissolve.

In the results from Patterson *et al.*, PSM and DPPC had compression moduli that were much more similar versus than the current results [154]. PGC and PSM are quite different, despite their ability to hydrogen bond. The hydrogen bonding network of PSM did not cause it to be highly rigid like PGC. Literature compression moduli approach current results only when using a slow quasi-static compression (2 cm^2/min) [162].

When looking at mixed lipids, the current results for the compression modulus for the DPPS (-) mixture was around 300 mN/m, much more rigid than previous results for the same mixture, which was ~80 mN/m [154]. There appear to be no literature studies on the compression moduli of polar lipids extracted from whole tears, this makes sense given the extremely small sample sizes. Kulovesi *et al.* studied mixtures of PC, PE, free fatty acids, triglycerides, and cholesterol esters and they found various two and three component mixtures never increased beyond 90 mN/m, but like previous studies from Patterson *et al.*, these compression isotherms began in the gas phase [66]. So even with lipid mixtures, this assay causes them to become very rigid by not expanding the film to 0 mN/m, where the LC phases would dissipate.

While these films have become quite rigid, it is important to discuss what happens to the polar lipid layer in the presence of nonpolar lipids. Important insight has been gained regarding the understanding of the molecular interactions between polar and nonpolar lipid classes using monolayer experiments, and biomolecular simulations have been used to provide additional insight. A thorough review from Cwiklik summarizes this work [62]. Kulovesi *et al.* used Langmuir monolayer studies to investigate eggPC, and

eggPC mixed with nonpolar lipids including free fatty acids (FFA), cholesterol oleate (CO), triglycerides (TG) (eggPC/FFA/CO/TG 60:20:10:10 mol%) [179]. The authors found that the polar/nonpolar mixture was more fluid between 20 and 35 mN/m than eggPC alone [179].

Molecular dynamics simulations by Kulovesi *et al.*, Telenius *et al.*, and Wizert *et al.* all show that neutral lipids interdigitate with the hydrophobic tails of polar lipids [179–181]. Kulovesi *et al.* revealed that the carboxylic acid group of the FFAs was near the glycerol backbone of PC [179] , and Telenius *et al.* showed that neutral lipids decrease the order of phospholipid chains [180] . Lastly, the simulation by Wizert *et al.* showed that inverse micelles could be formed in the nonpolar lipid layer during a blink [181] (figure 3.11). This is a very interesting finding in that it represents the possibility for a polar lipid reservoir established within the nonpolar layer during compression, and reincorporated back into the polar film during expansion [181]. The lipid films examined in this thesis were quite rigid, but *in vivo*, nonpolar lipids may play a role in fluidizing the monolayer.

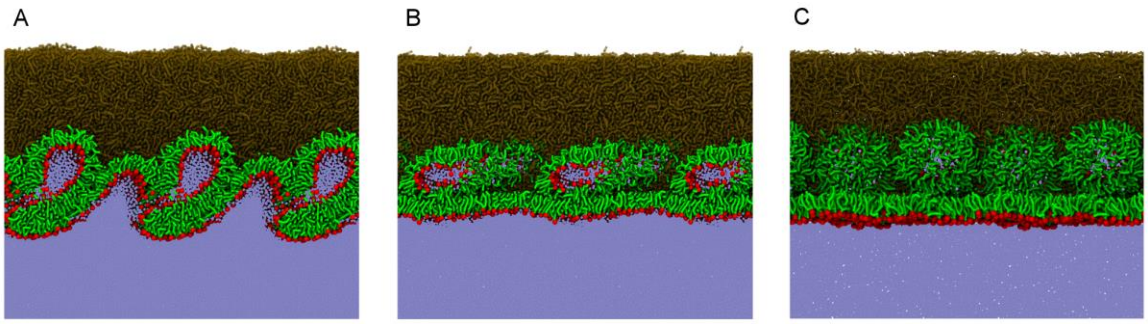

Figure 3.11. Images from Wizert *et al.* during a simulation of a polar and nonpolar lipid model of the tear film lipid layer during a blink: A) initial formation of inverse micelles with compression B) continued compression causing reorganization of the micelles and C) micelles during expansion of the film [181]. Water beads are blue, nonpolar lipids are brown, polar lipid headgroups are red, and the acyl chains of polar lipids are green. © **Wizert et al.** Wizert A, Iskander DR, Cwiklik L. Organization of Lipids in the Tear Film: A Molecular-Level View. Roccatano D, editor. PLoS ONE. 2014 Mar 20;9(3):e92461. Image url: https://doi:10.1371/journal.pone.0092461.g008, licensed under CC BY 4.0.

3.4 Conclusions

Each experiment has three stages, a constant pressure stage, a constant area stage and an isocycle stage. The pressure control stage was used to verify that a monolayer had been formed by compressing each lipid monolayer to 26 mN/m, the surface pressure found in whole tears [41]. The results from the pressure control stage indicate that monolayers of pure DPPC, DPPE, PGC, PSM, and DPPS have been formed. Lipid

mixtures where then investigated. One quinary lipid mixture with a molar ratio of 3 PC : 2 PE: 3 GC : 2 SM : 1 PS, and two quaternary mixtures were investigated, one that lacked DPPS (DPPS (-)) and one that lacked PGC (PGC (-)).The PGC (-) was shifted to higher molecular areas due to the presence of PGC, which has a small molecular area.

The characterization of the films under area control stage was necessary for later experiments, to allow proteins time to insert or adsorb to the monolayer, and thus a negative control for the lipid films. DPPE seemed to have the least magnitude in pressure drop, but PGC had the most. The results from the area control stage for lipid mixtures mostly resembled results for pure PGC. No statistical differences between lipid mixtures were seen in the area control stage, although the quinary mixture may be more stable than the two quaternary mixtures.

During the isocycle stage, five cycles were carried out to expand and compress each lipid film between 20 and 35 mN/m, the theoretical pressure range for the tear film [41,42]. Reversibility and compression/expansion moduli (β) were used to analyze the cycles. There were no detectible differences in the reversibility of the isocycles between pure lipids or lipid mixtures.

The compression/expansion moduli were calculated at 27.5 mN/m. High values for compression modulus indicate that a film is fairly rigid, where lower values indicate a more fluid film. All pure lipids were fairly rigid compared to typical values found in the literature. There were no significant differences seen between lipid mixtures regarding compression moduli during the isocycle stage. *In vivo*, the polar lipid layer in the tear

film is almost always intact when the eye is open. Thus, the limited range of expansion pursued in this thesis may be a better mimic of the biological situation; however, nonpolar lipids may have a role in fluidizing the polar lipid layer.

Chapter Four: Behavior of Lipid Monolayers after Protein Injection

4.1 General Chapter Overview

After having presented and discussed the results for lipid-only films in chapter three, chapter four will focus of the effects of lysozyme, lactoferrin, and tear lipocalin on the five pure lipids and three lipid mixtures. All eight lipid films were screened with a low final protein concentration of 0.01 mg/mL. This concentration was chosen due to the constraint of having to express and purify tear lipocalin. An additional experiment was performed with varying concentrations of lysozyme and lactoferrin with the quinary lipid mixture, so that higher protein concentrations could be explored. Tear lipocalin was not used for the varied protein concentration experiments. With the current expression protocol, it would take 4 to 5 months to prepare enough lipocalin to test with one lipid. Proteins were not injected until the constant area stage, so results of the preceding constant pressure stage will not be reviewed again. Refer to chapter three for an analysis of the constant pressure stage (pages 56 and 73).

4.2 Results

4.2.1 Constant Area Stage

4.2.1.1 Pure Lipids with Low Protein Concentrations

The same setup discussed for the lipid-only control experiments was repeated for the lipid and low protein concentration systems. After the constant pressure stage of each

trial, the barrier was held in a fixed position for the constant area stage. The experiments for each pure lipid or lipid mixture began at 26 mN/m, before 0.5 mL of lysozyme, lactoferrin, or tear lipocalin was injected under the barrier after1 minute of incubation. All three proteins were human recombinant, each was solvated in 1 x PBS buffer, and the final subphase protein concentration was 0.01 mg/mL after injection. The area was fixed for 30 minutes to allow for protein dispersion throughout the subphase; the change in pressure was calculated from 5 to 30 minutes (figure 4.1). The lipid-only (PBS control) experiments analyzed in chapter three are included here for comparison.

The pressure drop observed during the area control stage for lipid-only films was again detected for all pure lipids with each injected protein (figure 4.1). No significant differences were seen between control experiments and the three proteins for DPPC, PGC, and PSM. For DPPE, the drop in pressure observed with the injection of tear lipocalin (-1.1 mN/m) was significantly greater than the PBS control (-0.60 mN/m) and lactoferrin (-0.36 mN/m). For DPPS, the drop in pressure for tear lipocalin (-1.8 mN/m) was significantly greater than that of lysozyme (-1.4 mN/m) or lactoferrin (-1.3 mN/m). Tear lipocalin also seemed to decrease pressure more than the control and the other proteins for DPPC and PSM, but the change was not significant.

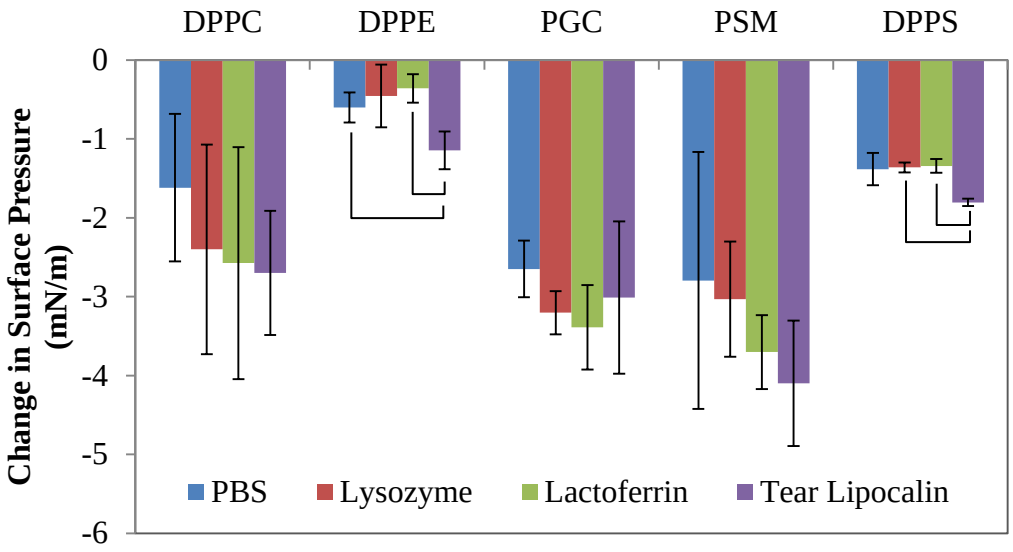

Figure 4.1. Average change in surface pressure over a 25 minute interval for five single pure lipids, after 0.5 mL of 1 x PBS buffer or protein solution had been injected under the barrier. The initial surface pressure was 26 mN/m, and the final subphase protein concentration was 0.01 mg/mL. Brackets indicate significant differences calculated using the t-test ($p < 0.05$), and error bars represent standard deviation ($n \geq 3$).

4.2.1.2 Lipid Mixtures with Low Protein Concentrations

Three lipid mixtures were tested with each protein at low concentrations. As with the pure DPPE and DPPS lipids, tear lipocalin again showed a reduction in surface pressure for the DPPS (-) mixture (molar ratio: 3 PC: 2 PE : 3PG : 2 SM) and PGC mixture (-) (molar ratio: 3PC : 2 PE : 2 SM : 1 PS) (figure 4.2). For DPPS (-), the decrease for lipocalin (-4.2 mN/m) was significant compared to the PBS control (-2.84 mN/m) and lysozyme (-2.1 mN/m). For the PGC (-) mixture, the decrease in surface

pressure for lipocalin (-3.1 mN/m) was not significant compared to the PBS control (-2.6 mN/m), but was significant compared to lysozyme (-2.13 mN/m) and lactoferrin (-1.8 mN/m). No significant change in surface pressure was observed between the PBS control and any of the injected proteins for the quinary mixture (molar ratio: 3 PC : 2 PE : 3PG : 2 SM : 1 PS).

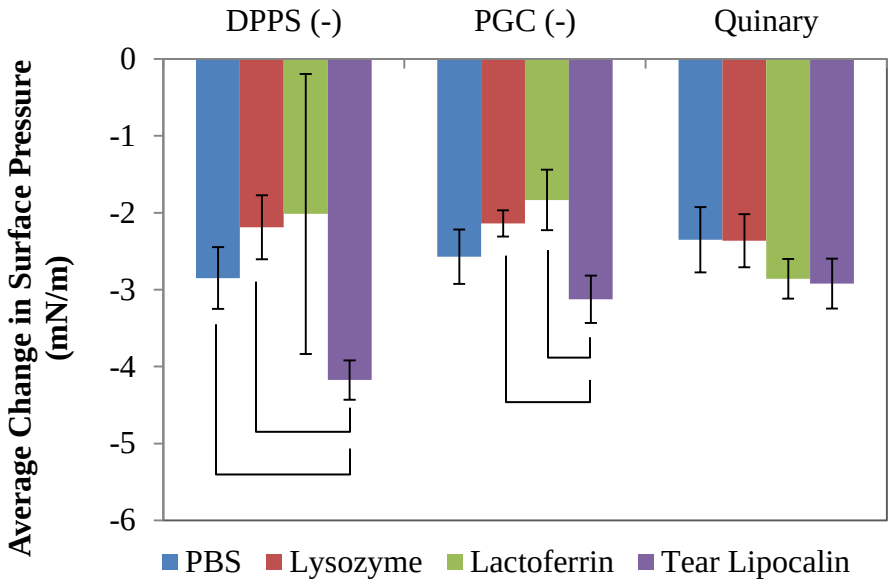

Figure 4.2. Average change in surface pressure over a 25 minute interval for three lipid mixtures , after 0.5 mL of 1 x PBS buffer or protein solution had been injected under the barrier. The quinary mixture had a molar ratio of 3 PC : 2 PE : 3 GC : 2 SM : 1 PS, the other two quaternary mixture each lacked one lipid found in the quinary mixture. DPPS (-) lacked DPPS, and PGC (-) lacked PGC. The initial surface pressure was 26 mN/m, and the final subphase protein concentration was 0.01 mg/mL. Brackets indicate significant differences calculated using the t-test ($p < 0.05$), and error bars represent standard deviation ($n \geq 3$).

4.2.1.3 Quinary Lipid Mixture with Varied Protein Concentrations

After reviewing a recent paper that showed that HEWL with a final concentration of 2 mg/mL, the midrange concentration of that found in the tear film [108,109], could change the rheological properties of whole tear lipids without changing the surface pressure [43,182], it was decided to perform an additional experiment varying the protein concentrations with the quinary lipid mixture with the addition of lysozyme and lactoferrin. The experimental protocol was identical to the low concentration experiments with a couple of exceptions. Instead of an initial subphase volume of 109.5 mL with 0.5 mL injected volume, the initial subphase volume was 110 mL, with 10 mL of buffer or protein solution injected. An injected volume of 10 mL had to be used due to solubility constraints of lysozyme and lactoferrin. The initial subphase volume could not be lowered to accommodate the larger injection volume because it would cause surface film leakage under the barrier. Due to the large volume being injected, and large of amount of protein available, a pump was used to provide a constant rate of injection at 0.5 mL/min. Final subphase protein concentrations of 0.05, 0.2, and 1 mg/mL were used. The lactoferrin used for these experiments was not from Sigma Aldrich, but from Agennix Incorporated, where appropriate quantities were generously provided by the Vogel lab.

A pressure drop was again seen for all concentrations of lysozyme and lactoferrin (figure 4.3), as with the low concentration experiments (figure 4.2). The average magnitude of the pressure drop was similar, from 1.4 to 2.6 mN/m for both proteins. For lysozyme, there were no significant differences at any concentration whereas a significant

difference was seen for lactoferrin, between the 0.05 mg/mL (1.4 mN/m) and 0.2 mg/mL (2.1 mN/m) whereas the variation observed for the 1 mg/mL lactoferrin was too large.

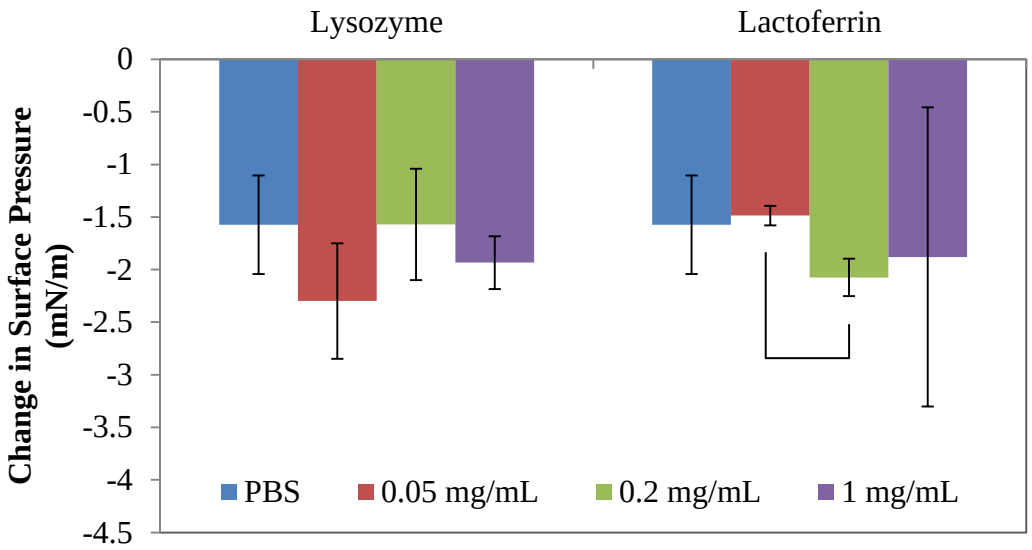

Figure 4.3. Average change in surface pressure over a 25 minute interval for the quinary lipid mixture with different concentrations of lysozyme and lactoferrin injected. 10 mL of 1 x PBS buffer or protein solution was injected. The quinary mixture had a molar ratio of 3 PC : 2 PE : 3 GC : 2 SM : 1 PS. The initial surface pressure was 26 mN/m, and the final subphase protein concentration was 0.05, 0.2, or 1 mg/mL. Brackets indicate significant differences calculated using the t-test ($p < 0.05$), and error bars represent standard deviation ($n \geq 3$).

4.2.2 Isocycle Stage – Reversibility

4.2.2.1 Pure Lipids with Low Protein Concentrations

After the constant area stage, the surface films were compressed and expanded for five cycles, between ~20 and ~35 mN/m. As mentioned previously, this is thought to be the biologically relevant surface pressure range for the tear film during a blink [41,42]. The first and fifth cycles were again omitted due to potential artifacts discussed previously (page 66). Reversibility was again calculated by dividing the area under the compression isotherm by the area under the expansion isotherm. Reversibility of 1 means that the expansion and compression isotherms overlap. Reversibility of less than 1 means the expansion isotherm was at lower surface pressures than the compression isotherm, and reversibility greater than 1 means the opposite.

Generally, there were no differences for any pure lipid with any of the three proteins injected into the subphase (figure 4.4). Reversibility ranged from 0.87 with DPPE/lactoferrin to 1.1 for a number of systems. The only significant difference was with DPPS, between the control (1.1) and lysozyme (0.97) for cycle 4. No trends are evident, other than a large variance for lactoferrin injected under DPPE films.

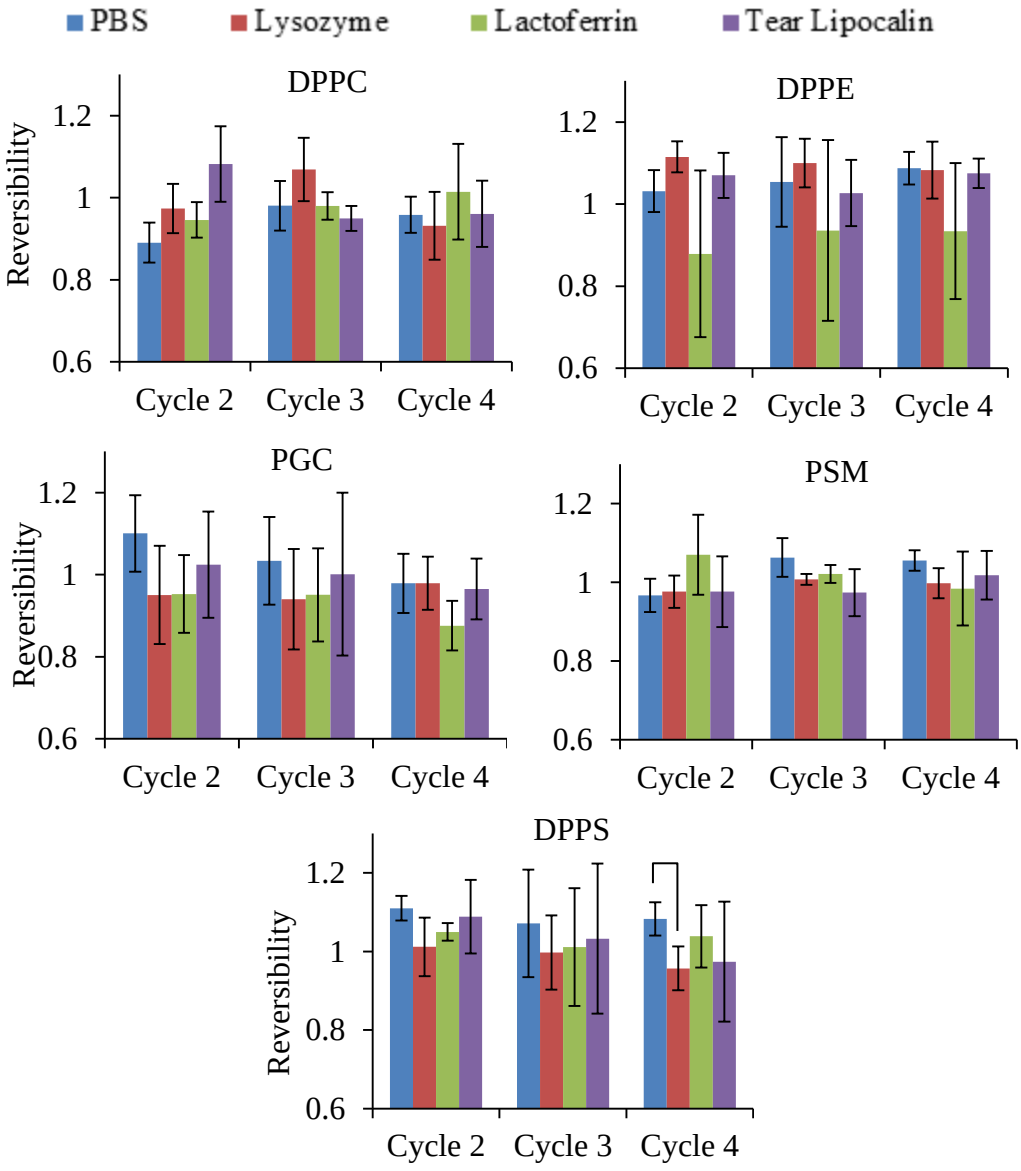

Figure 4.4. Average reversibility for five pure lipids during isocycles. Cycling commenced 30 minutes after the injection of PBS buffer or protein (0.01 mg/mL final subphase concentration). Monolayers were at ~26 mN/m during injection. Brackets indicate significant differences calculated using the t-test ($p < 0.05$), error bars represent standard deviation ($n \geq 3$).

4.2.2.2 Lipid Mixtures with Low Protein Concentrations

Reversibility for the lipid mixtures did not appear to be affected (figure 4.5). When injected into the subphase of the DPPS (-) mixture, lysozyme had significantly higher reversibility (1.1) than lactoferrin (1.0) for cycle 4 only. No trends are seen in reversibility for any mixture.

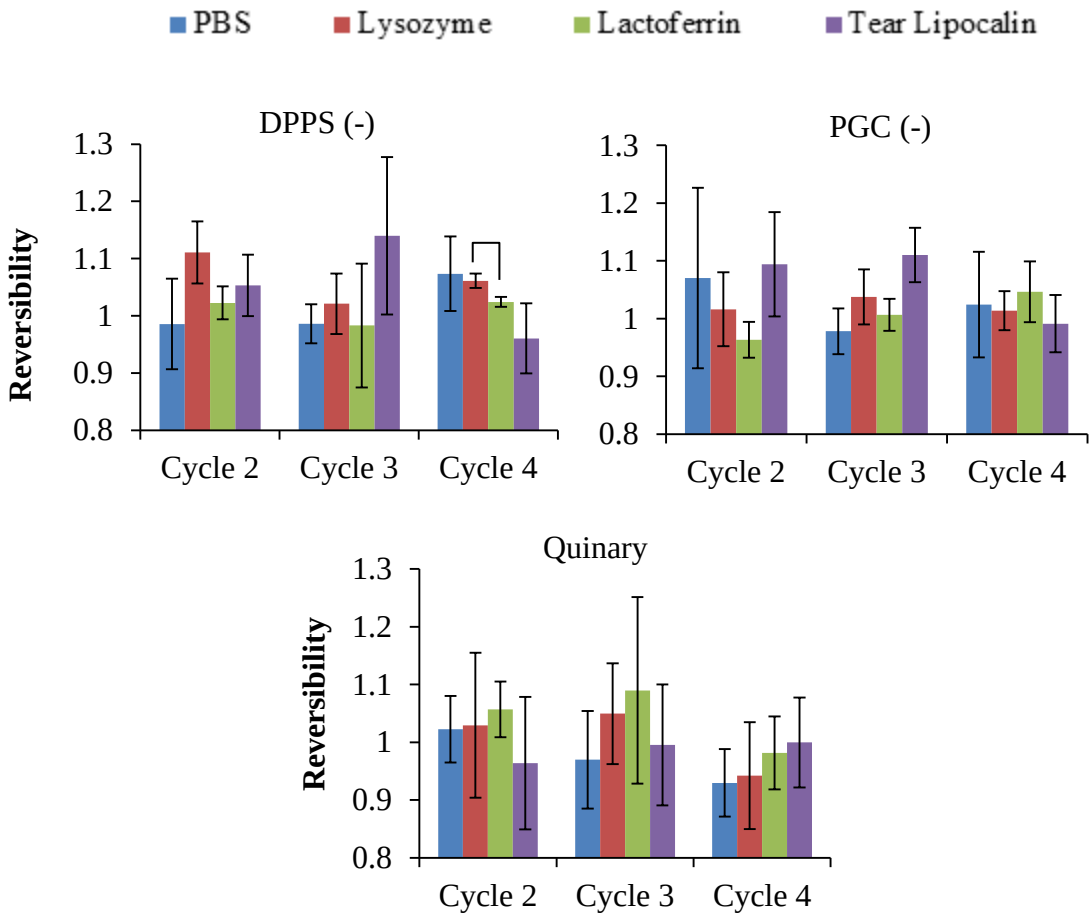

Figure 4.5. Average reversibility for three lipid mixtures during isocycles. DPPS (-) was a quaternary mixture with a molar ratio of 3PC : 2PE : 3GC : 2SM. PGC (-) was a quaternary mixture with a molar ratio of 3PC : 2 PE : 1 PS. The quinary mixture had a molar ratio of 3 PC : 2 PE : 3 GC : 2 SM : 1 PS. Cycling commenced 30 minutes after 0.5 mL of 1 x PBS buffer or protein solution had been injected. Monolayers were at ~26 mN/m during injection. Final subphase protein concentration was 0.01 mg/mL. Brackets indicate significant differences calculated using the t-test ($p < 0.05$), and error bars represent standard deviation ($n \geq 3$).

4.2.2.3 Quinary Lipid Mixture with Varied Protein Concentrations

Unlike the low protein concentration experiments, it was decided to cycle the films 20 times to see if any changes would occur over time, as low concentration experiments appeared fairly stable over 5 cycles. Few significant differences in reversibility were observed for the lactoferrin, and for the first 12 cycles of lysozyme (figure 4.6). Only the control reversibility (1.0) of cycle 18 was significantly different than 0.05 mg/mL lysozyme (0.9). There were some other significant differences for lysozyme, but they did not amount to any trend. The control reversibility seemed to be lower than the protein reversibility for the first 8 cycles, but not significantly so.

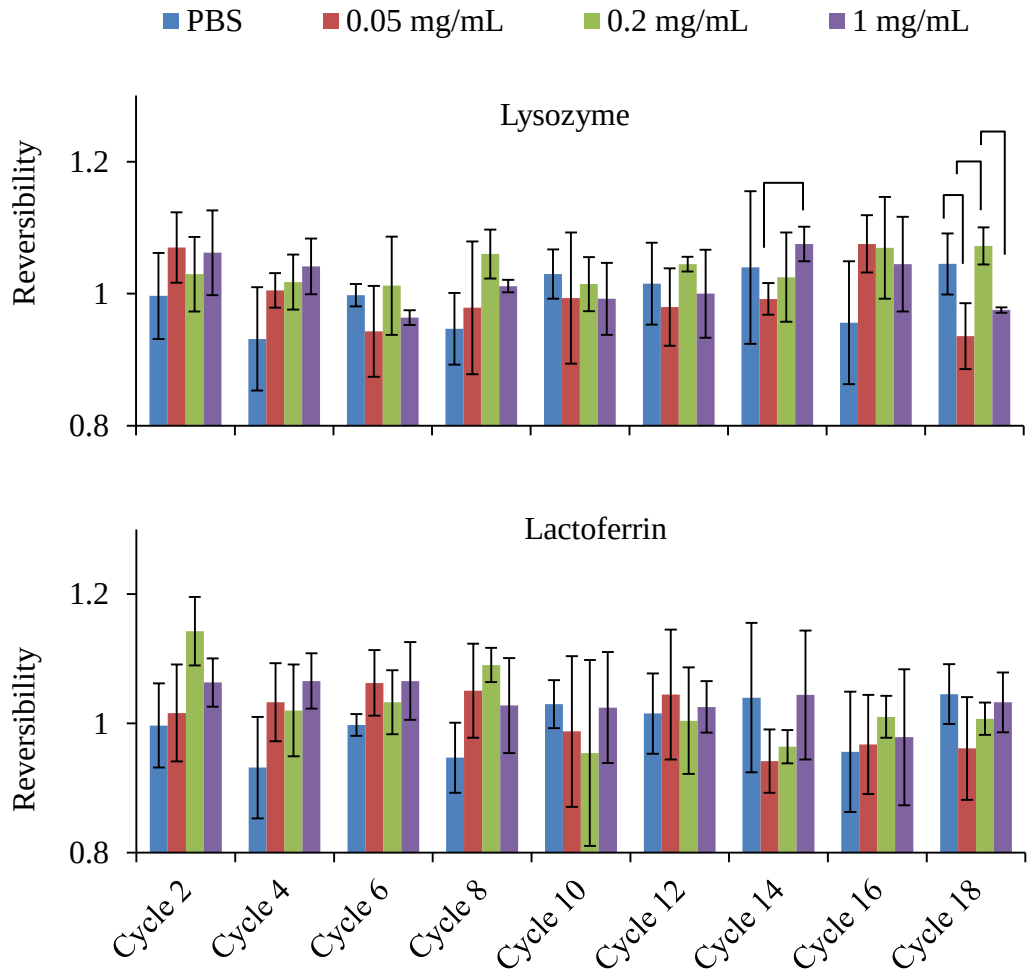

Figure 4.6. Average reversibility for the quinary lipid mixture (3 PC : 2 PE : 3 GC : 2 SM : 1 PS molar ratio) with varying concentrations of lysozyme and lactoferrin. Cycling commenced 30 minutes after 10 mL of 1 x PBS buffer or protein solution had been injected under the barrier at a starting pressure of ~26 mN/m. All proteins were solvated in PBS. Final subphase protein concentrations were 0.05, 0.2, and 1 mg/mL. Brackets indicate significant differences calculated using the t-test ($p < 0.05$) and error bars represent standard deviation ($n \geq 3$).

4.2.3 Isocycle Stage – Compression and Expansion Moduli

4.2.3.1 Pure Lipids with Low Protein Concentrations

Compression and expansion moduli (β) were again calculated at one surface pressure to allow comparison. The surface pressure of 27.5 mN/m was chosen because it was in the middle of the cycling range, furthest from maximum or minimum pressures where the barrier would switch direction. These moduli were used to detect changes in the elastic nature of the monolayer due to the presence of proteins [157].

Significant differences between control and proteins were observed for DPPC, but no trends persisted during all cycles. There was a subtle reduction in both moduli in the PBS control starting with the expansion in cycle three (figure 4.7). This reduction was significant compared to lactoferrin and tear lipocalin during compression and expansion, and only expansion for lysozyme. All three proteins seemed to maintain the moduli more consistently over the last three isotherms. No significant changes in moduli are seen for DPPE or PGC with any of the proteins (figure 4.8 and figures 4.9, respectively). PSM also seemed to have a slightly overall reduced moduli for the PBS control compared to lactoferrin and lysozyme (figure 4.10) Lastly, no trends were seen with DPPS (figure 4.11).

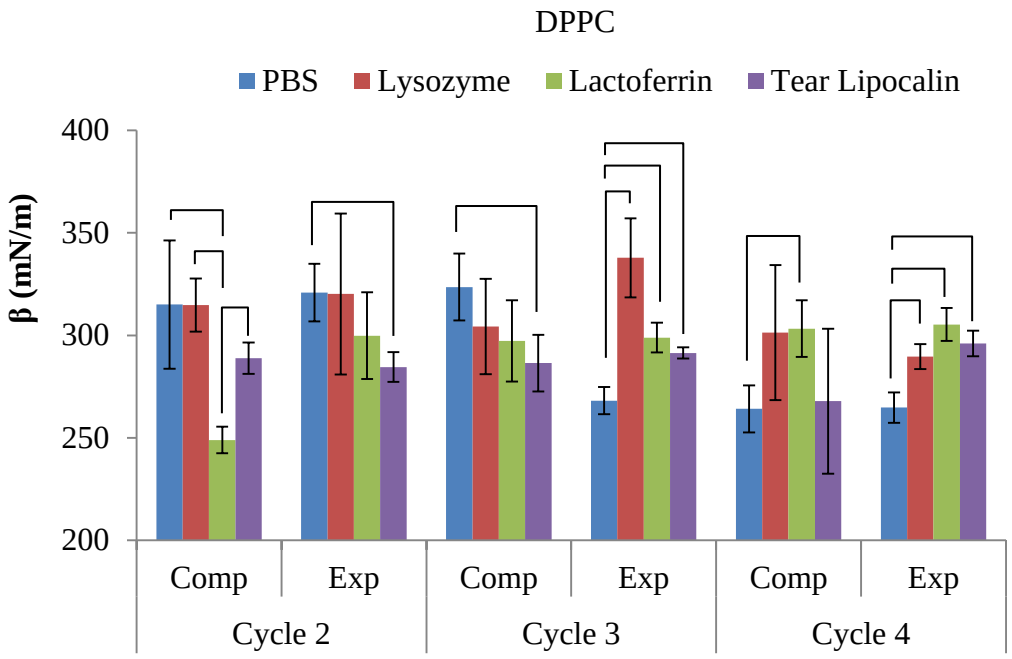

Figure 4.7. Average compression (Comp) and expansion (Exp) moduli for DPPC during isocycles. Cycling commenced 30 minutes after 0.5 mL of 1 x PBS buffer or protein solution had been injected under the barrier at a starting pressure of ~26 mN/m. All proteins were solvated in PBS buffer and the final subphase concentration was 0.01 mg/mL. Brackets indicate significant differences calculated using the t-test ($p < 0.05$), and error bars represent standard deviation ($n \geq 3$).

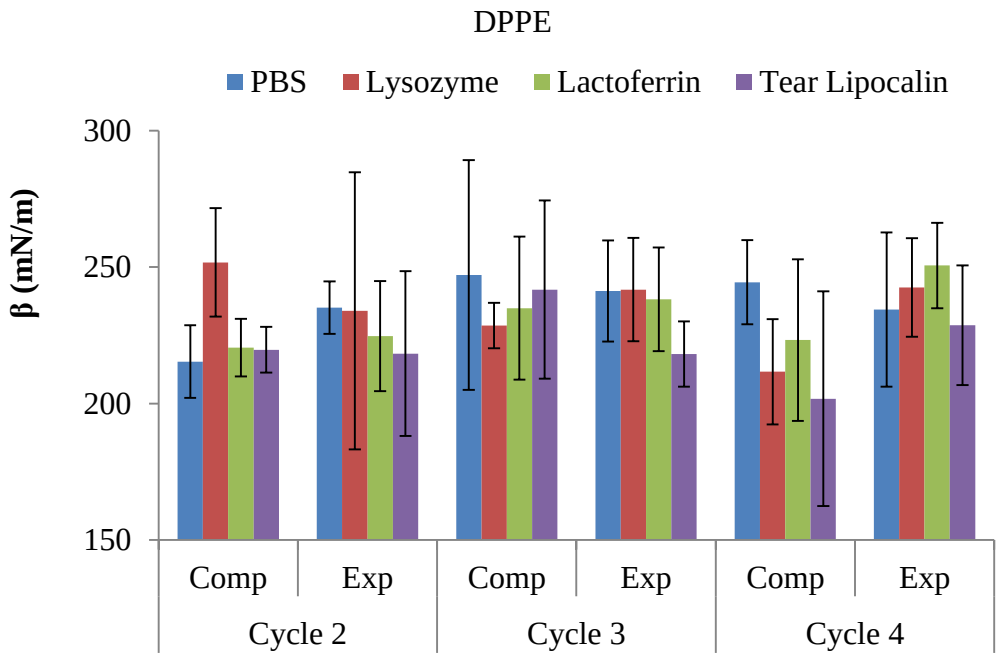

Figure 4.8. Average compression (Comp) and expansion (Exp) moduli for DPPE during isocycles. Cycling commenced 30 minutes after 0.5 mL of 1 x PBS buffer or protein solution had been injected under the barrier at a starting pressure of ~26 mN/m. All proteins were solvated in PBS buffer and the final subphase concentration was 0.01 mg/mL. The significance of the differences were calculated using the t-test ($p < 0.05$), but none were significant. Error bars represent standard deviation ($n \geq 3$).

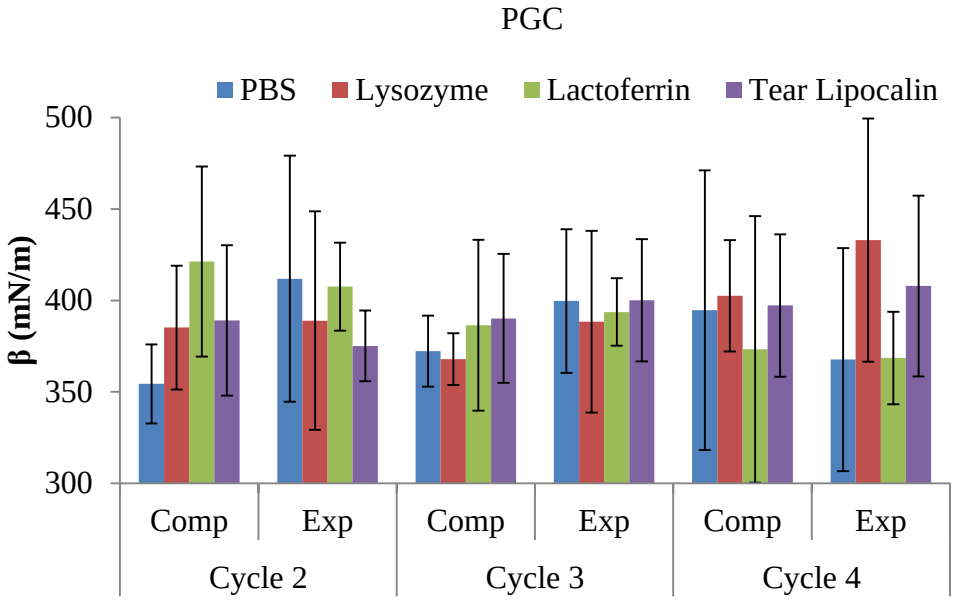

Figure 4.9. Average compression (Comp) and expansion (Exp) moduli for PGC during isocycles. Cycling commenced 30 minutes after 0.5 mL of 1 x PBS buffer or protein solution had been injected under the barrier at a starting pressure of ~26 mN/m. All proteins were solvated in PBS buffer and the final subphase concentration was 0.01 mg/mL. The significance of the differences were calculated using the t-test ($p < 0.05$), but none were significant. Error bars represent standard deviation ($n \geq 3$).

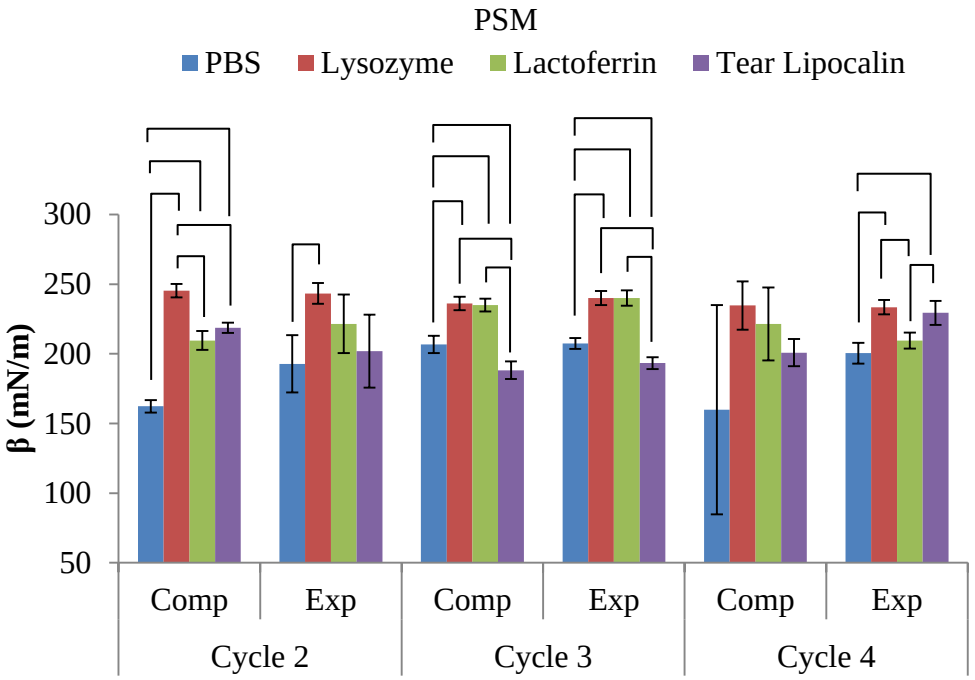

Figure 4.10. Average compression (Comp) and expansion (Exp) moduli for PSM during isocycles. Cycling commenced 30 minutes after 0.5 mL of 1 x PBS buffer or protein solution had been injected under the barrier at a starting pressure of ~26 mN/m. All proteins were solvated in PBS buffer and the final subphase concentration was 0.01 mg/mL. Brackets indicate significant differences calculated using the t-test ($p < 0.05$), and error bars represent standard deviation ($n \geq 3$).

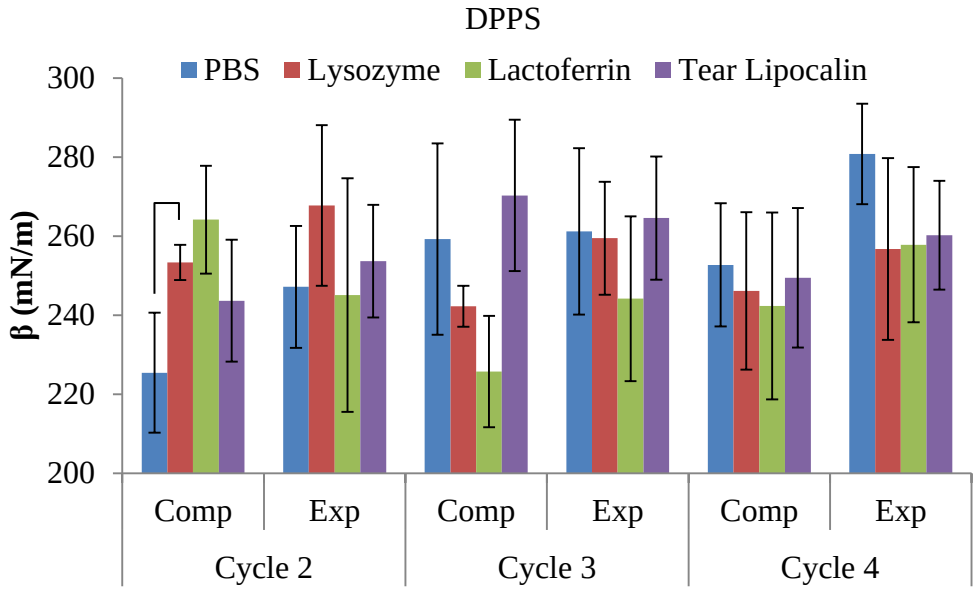

Figure 4.11. Average compression (Comp) and expansion (Exp) moduli for DPPS during isocycles. Cycling commenced 30 minutes after 0.5 mL of 1 x PBS buffer or protein solution had been injected under the barrier at a starting pressure of ~26 mN/m. All proteins were solvated in PBS buffer and the final subphase concentration was 0.01 mg/mL. Brackets indicate significant differences calculated using the t-test ($p < 0.05$), and error bars represent standard deviation ($n \geq 3$).

4.2.3.2 Lipid Mixtures with Low Protein Concentrations

Expansion and compression moduli for lipid mixtures have some minor trends. The compression moduli of the DPPS (-) mixture with tear lipocalin was significantly less than lysozyme for cycles 3 and 4, but not significantly less than the PBS control (figure 4.12). Lactoferrin had a significantly lower compression modulus than tear

lipocalin for cycle 2 only, and this trend was reversed for cycles 3 and 4, but not significantly so. There were no significant differences seen for the expansion isotherms for the DPPS (-) isocycles.

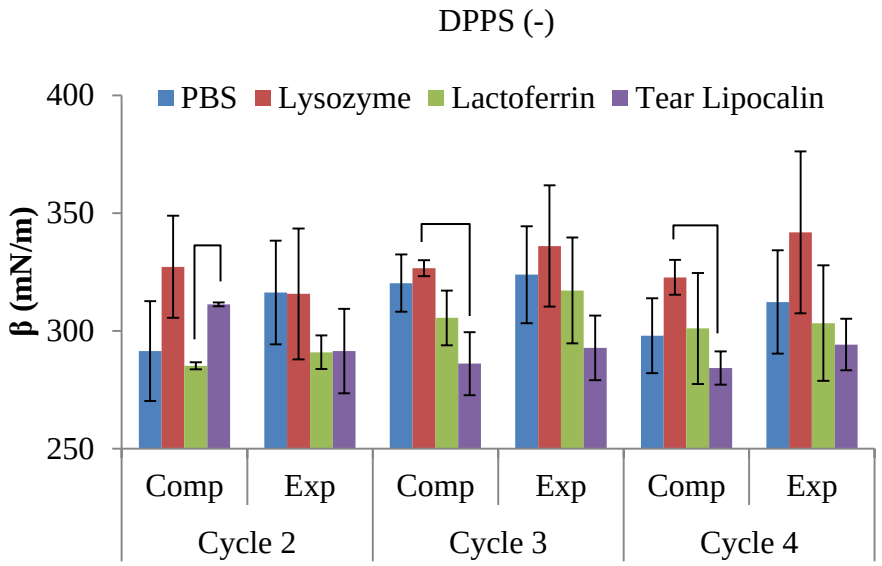

Figure 4.12. Average compression (Comp) and expansion (Exp) moduli for a quaternary lipid mixture (DPPS (-) molar ratio of 3 PC : 2 PE : 3: GC : 2 SM) during isocycles. Cycling commenced 30 minutes after 0.5 mL of 1 x PBS buffer or protein solution had been injected under the barrier at a starting pressure of ~26 mN/m. All proteins were solvated in PBS buffer and the final subphase concentration was 0.01 mg/mL. Brackets indicate significant differences calculated using the t-test ($p < 0.05$), and error bars represent standard deviation ($n \geq 3$).

There were a number of significant differences seen for the PGC (-) mixture, but they did not lead to any trends (figure 4.13). Compared to the PBS control, compression and expansion moduli for the proteins would sometimes be higher or lower. The compression moduli for lactoferrin were generally lower than the other proteins, but not the PBS control. Sometimes the moduli would be significantly lower for either lysozyme or tear lipocalin, but this was not consistent.

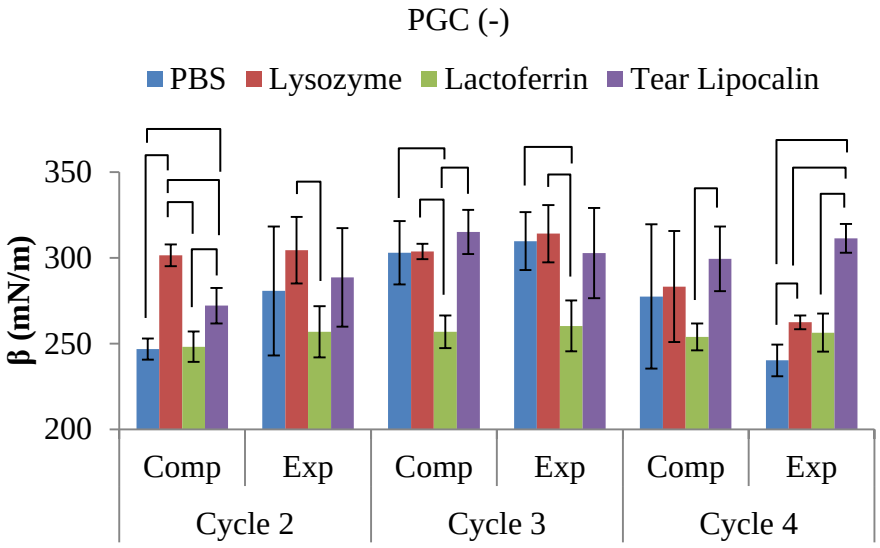

Figure 4.13. Average compression (Comp) and expansion (Exp) moduli for a quaternary lipid mixture (PGC (-) molar ratio of 3 PC : 2 PE : 2 SM : 1 PS) during isocycles. Cycling commenced 30 minutes after 0.5 mL of 1 x PBS buffer or protein solution had been injected under the barrier at a starting pressure of ~26 mN/m. All proteins were solvated in PBS buffer and the final subphase concentration was 0.01 mg/mL. Brackets indicate significant differences calculated using the t-test ($p < 0.05$), and error bars represent standard deviation ($n \geq 3$).

No trends were seen with the quinary lipid mixture (figure 4.14). Cycle 3 had compression moduli that were significantly higher for lysozyme than for the PBS control or the other proteins. Both compression and expansion moduli for the quinary mixture

appeared to be more consistent than either the DPPS (-) or PGC (-) mixtures (figures 4.12 and 4.13).

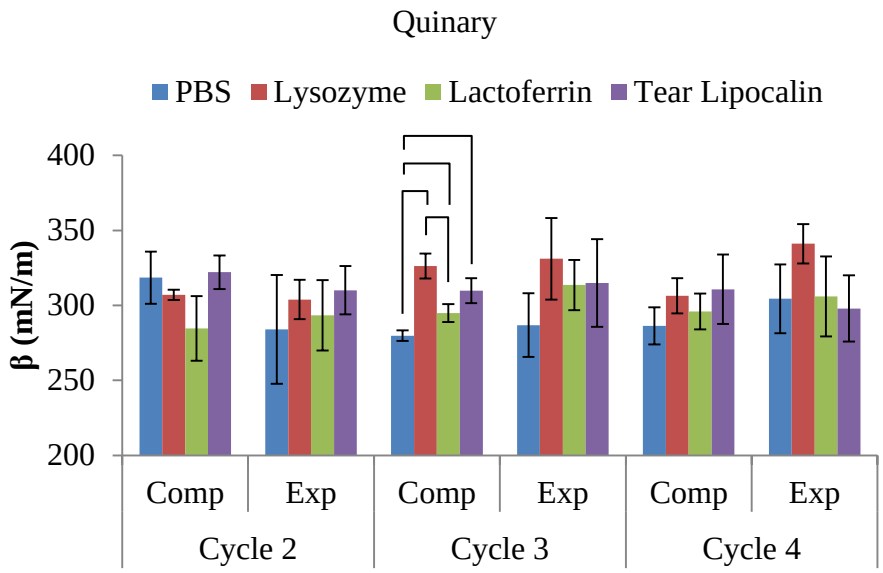

Figure 4.14. Average compression (Comp) and expansion (Exp) moduli for the quinary lipid mixture (molar ratio of 3 PC : 2 PE : 3: GC : 2 SM :1 PS) during isocycles. Cycling commenced 30 minutes after 0.5 mL of 1 x PBS buffer or protein solution had been injected under the barrier at a starting pressure of ~26 mN/m. All proteins were solvated in PBS buffer and the final subphase concentration was 0.01 mg/mL. Brackets indicate significant differences calculated using the t-test ($p < 0.05$), and error bars represent standard deviation ($n \geq 3$).

4.2.3.3 Quinary Lipid Mixture with Varied Protein Concentrations

Increasing the lysozyme and lactoferrin concentrations had a significant effect on the compression and expansion moduli of the quinary lipid mixture (figures 4.15 and 4.16). Compression and expansion moduli for both proteins are generally symmetrical. For lysozyme cycles 10 and 19, the control was significantly higher than the 0.05 mg/mL proteins, but not 0.2 mg/mL concentrations. The 1 mg/mL lysozyme decreased the moduli more than the two lower lysozyme concentrations and the control for the first 15 cycles, and lower than the control cycles 16 to 19 (figure 4.17). Lactoferrin decreased the compression and expansion moduli significantly more for all protein concentrations compared to lysozyme. The effect was especially pronounced for 1 mg/mL lactoferrin for the first 7 cycles, but then the difference between lactoferrin concentrations diminishes for cycles 8 to 19.

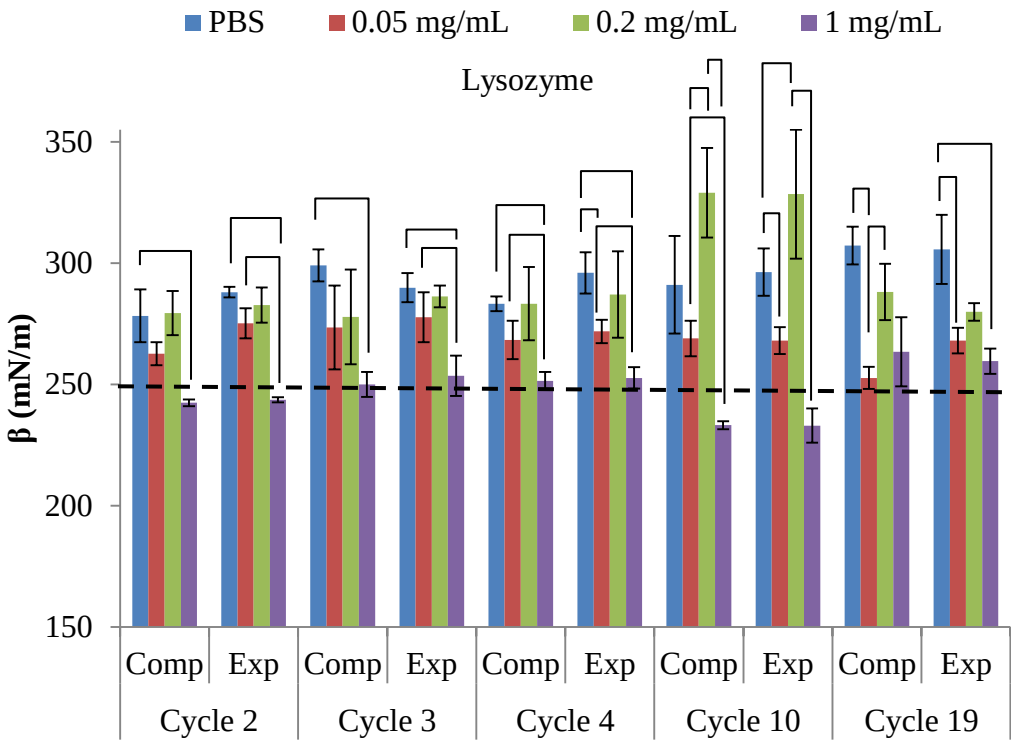

Figure 4.15. Average compression (Comp) and expansion (Exp) moduli for the quinary lipid mixture (molar ratio of 3 PC : 2 PE : 3: GC : 2 SM :1 PS) during selected isocycles with varying lysozyme concentrations. Cycling commenced 30 minutes after 10 mL of 1 x PBS buffer or protein solution had been injected under the barrier at a starting pressure of ~26 mN/m. All proteins were solvated in PBS buffer, and the final subphase concentrations were 0.05, 0.2, and 1 mg/mL. Dotted lines distinguish between moduli characteristic of the LC (<250 mN/m) and S phases (>250 mN/m) **[158]**. Brackets indicate significant differences calculated using the t-test (p value < 0.05). Error bars represent standard deviation ($n \geq 3$).

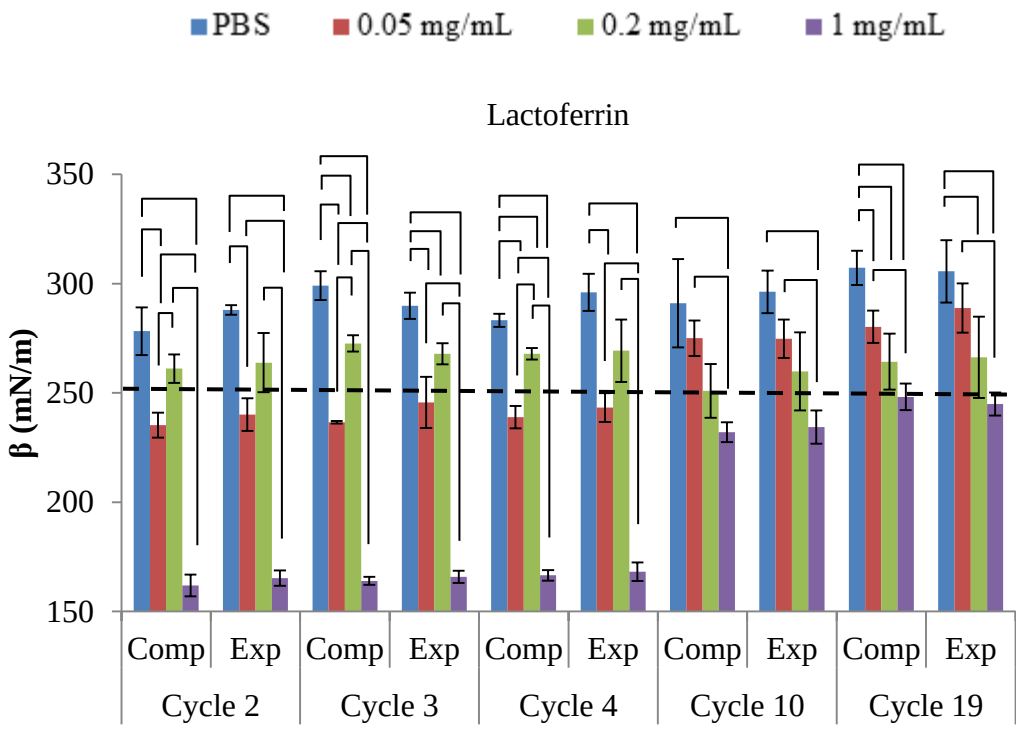

Figure 4.16. Average compression (Comp) and expansion (Exp) moduli for the quinary lipid mixture (molar ratio of 3 PC : 2 PE : 3: GC : 2 SM :1 PS) during selected isocycles with varying lactoferrin concentrations. Cycling commenced 30 minutes after 10 mL of 1 x PBS buffer or protein solution had been injected under the barrier at a starting pressure of ~26 mN/m. All proteins were solvated in PBS buffer, and the final subphase concentrations were 0.05, 0.2, and 1 mg/mL. Dotted lines distinguish between moduli characteristic of the LC (<250 mN/m) and S phases (>250 mN/m) **[158]** Brackets indicate significant differences calculated using the t-test (p value < 0.05). Error bars represent standard deviation (n ≥ 3). Error bars represent standard deviation (n ≥ 3).

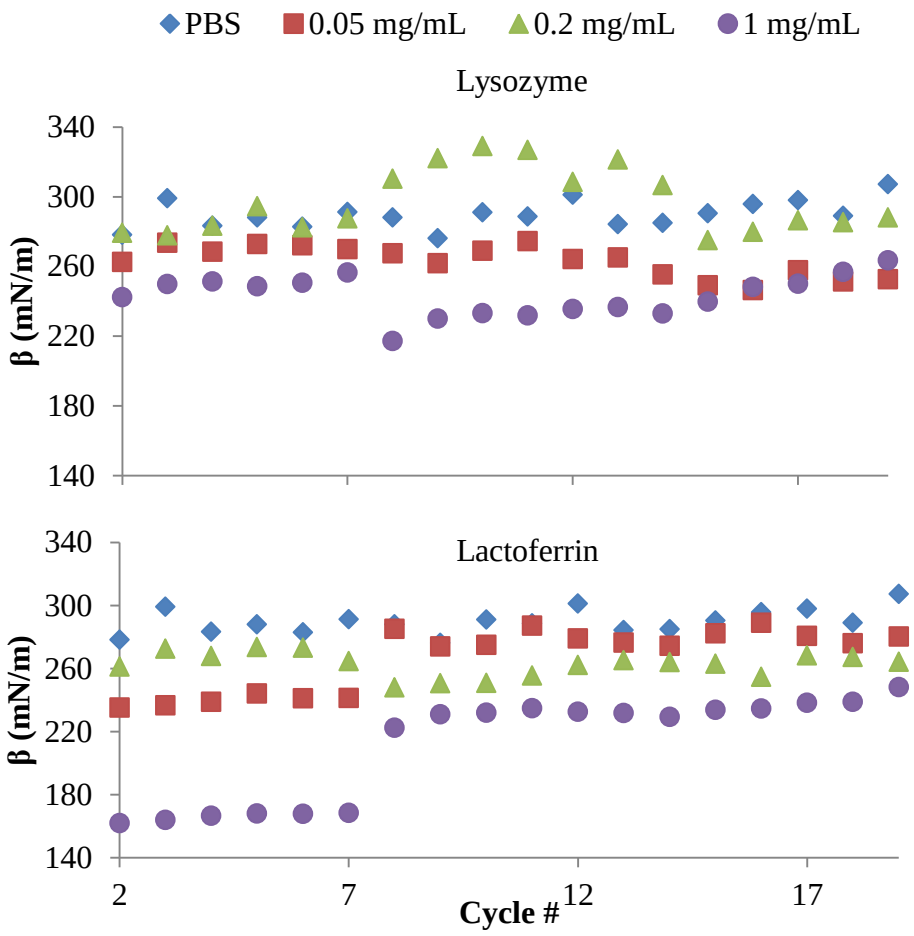

Figure 4.17. Average compression moduli for the quinary lipid mixture (molar ratio of 3 PC : 2 PE : 3: GC : 2 SM :1 PS) during isocycles, with varying protein concentrations. Cycling commenced 30 minutes after 10 mL of 1 x PBS buffer or protein solution had been injected under the barrier at a starting pressure of ~26 mN/m. All proteins were solvated in PBS buffer, final subphase concentrations were 0.05, 0.2, and 1 mg/mL. No error bars or significance differences were presented here to reduce the complexity of the figure.

4.3 *Discussion*

4.3.1 General Background on Lipid/Lysozyme Interactions

There are studies that specifically look at interactions between lipid monolayers and lysozyme, lactoferrin, and tear lipocalin that will be addressed. But much of our understanding of the process by which lysozyme binds to lipid membranes comes from research with liposomes or supported bilayers, often to explore its antimicrobial effects on negatively bacterial membranes. These lipid models allow for techniques that can monitor the thermodynamics of binding and protein structural changes that are more difficult observe with monolayers. These studies are lacking for lactoferrin and tear lipocalin, and so this is specific to lysozyme. Hen Egg White Lysozyme (HEWL) was primarily used. We do need to keep in mind the differences between HEWL and human lysozyme, as shown by the *E. coli* produced inhibitor Ivyp1 interacting more strongly with HEWL than human lysozyme [106]. Human lysozyme has an isoelectric point near ~10 [107], while HEWL has a more positively charged surface and an isoelectric point near ~11 [105].

Monolayer, liposome, and supported bilayer experiments have resulted in a proposed four step mechanism for HEWL binding to lipid membranes, but has a degree of complexity that depends on the concentration of the protein [183–186] (figure 4.18). First, the protein is attracted to the liposome surface through electrostatic attraction, which depends on the percentage of anionic lipids that attract the positive charges of

HEWL at pH 7.4, and the ionic strength of the solvent [105,183,185–189]. Second, once adsorbed to the liposome surface, the protein begins to change conformation due to the negative charge of the liposome interfering with electrostatic interactions within the protein [183,184,186]. Third, the lateral organization of lipids begins to change, and negatively charged lipids may be concentrated in the vicinity of the protein [183,185,186,190]. Fourth, changes in membrane lipid organization leads to further protein conformational changes, leading to the insertion of hydrophobic residues into the membrane [183–185,189]. Lysozyme can display wholly peripheral binding at extremely low concentrations [184]. Studies using smaller cationic peptides, sometimes derived from lysozyme or lactoferrin, show the vital importance of arginine and tryptophan residues necessary for electrostatic interaction and insertion into the membrane respectively [126]. Peptides with a high number of tryptophan residues have an enhanced ability to insert into membranes [126].

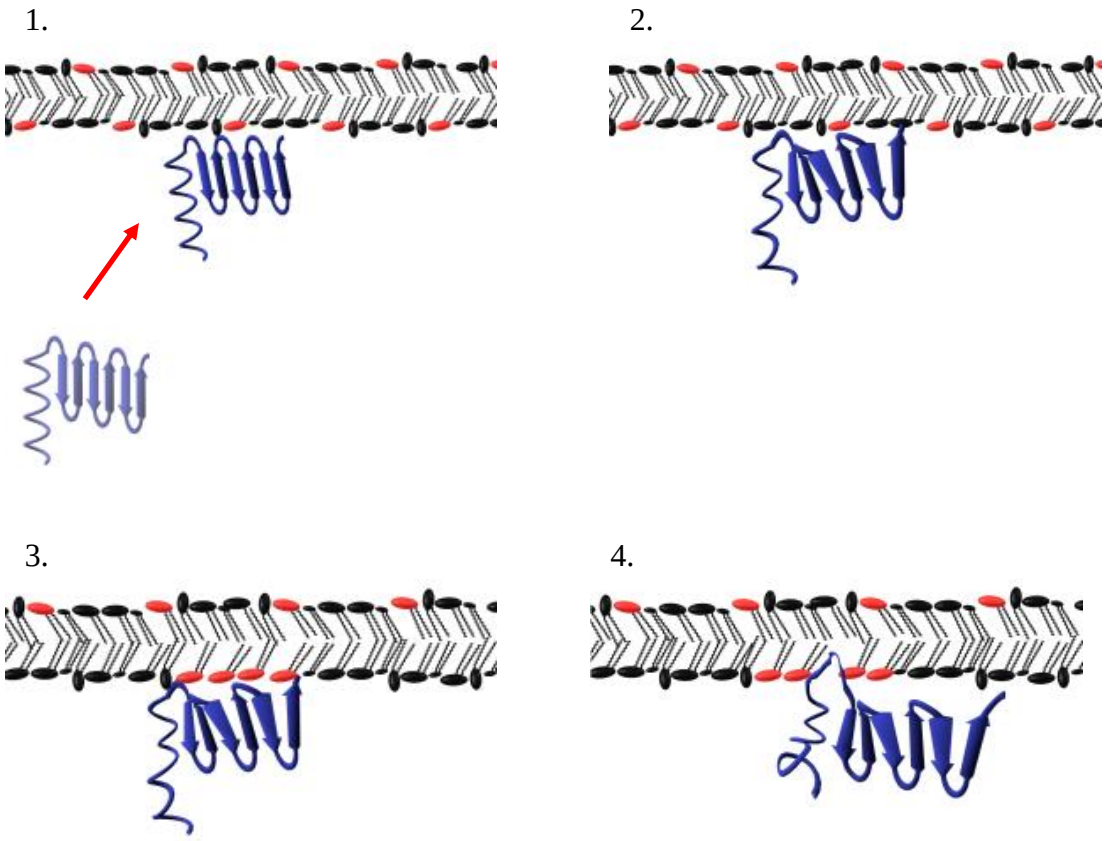

Figure 4.18. Schematic representation of stages involved in lysozyme insertion into a liposome: 1) anionic lipids (red) attract positively charged lysozyme (blue) to a membrane [105,183,185–189] 2) protein begins to change conformation due to liposome charge [183,184,186] 3) anionic lipids cluster near the protein [183,185,186,190] 4) protein further denatures and partial insertion of hydrophobic residues occurs [183–185,189].

Unlike lysozyme, the interactions of whole lactoferrin with liposomes or other vesicles have not been investigated to the same extent. Much of the research focused on lactoferricin, a cationic antimicrobial peptide produced when the first 49 residues of lactoferrin are cleaved with pepsin [126,128,191,192]. It has been suggested that lactoferricin region of the intact lactoferrin protein can pull the entire protein across bacterial membranes and into the cells, and so may be responsible for the initial electrostatic interaction [125,126].

4.3.2 Constant Area Stage

4.3.2.1 Pure Lipids with Low Protein Concentrations

That all lipids experienced a drop in surface pressure after protein injection indicates that proteins were not inserting into the monolayers to a detectable extent, in which case surface pressure would be maintained or increased [138]. There have been previously reported injection studies using surface pressure to study the insertion of lysozyme, lactoferrin, and tear lipocalin into monolayers of polar lipids found in the lipid layer of the tear film. Hen egg white lysozyme (HEWL) or human recombinant lysozyme, which is overall positively charged at pH 7.4 [105], could not penetrate into DPPC, DPPE, or PSM films at 20 mN/m or higher [105,152,193]. Arnold *et al.* reported that HEWL (0.01 mg/mL) did not insert into monolayers of PS at pH 7.4 held at 28 mN/m [194]. Mudgil *et al.* showed that steric hindrance may be more important than

electrostatic interactions for determining whether a protein can insert into a polar lipid film [193]. Indeed, lysozyme (unspecified type) was also unable to insert into monolayers of PS with a large percentage of stearic (18:0) and oleic (18:1) acyl chains [193]. This result is compelling because insertion was not evident despite the packing disruption caused by an unsaturated acyl tail, and a PS headgroup having an electrostatic attraction to lysozyme, insertion was not evident. Regarding PGC, only Patterson studied the insertion of human recombinant lysozyme and found that it inserted at 20 mN/m, but not at 30 mN/m [152]. It appears the surface pressure of pure lipid films in this experiment did not drop enough to allow for insertion of lysozyme.

Protein insertion is not just a function of surface pressure alone, but also of time scale. Marsh reported that lipids in monolayers between 30 and 35 mN/m were in a similar state to those same lipids in bilayers [195]. Lysozyme is able to insert into bilayers if conformational changes occur. It was found that pure POPG vesicles could cause structural changes in lysozyme in 20 min, but very little structural changes could be observed for lysozyme incubated with POPC/POPG (9:1) for an entire month [183]. If the conformation of lysozyme did change with pure DPPS, it did not cause protein insertion; however, results from DPPS and POPG lipids are not necessarily comparable as it has been shown that antimicrobial peptides interact differently with anionic lipids depending on the headgroup and acyl chain properties [196].

Lactoferrin could not insert into any of the lipids. Investigations of lactoferrin insertion with these polar lipids are less common than lysozyme. Only one experiment

was found investigating the ability of human milk lactoferrin to insert into DPPC, whereby the protein was unable to do so when the monolayer was at 35 mN/m, but it inserted below 15 mN/m [197]. Like lysozyme, lactoferrin is positively charged at pH 7.4 [119], but it is also larger at ~80 kDa [118], compared to lysozyme which is ~15 kDa [100]. The larger molecular weight would limit the ability to insert into monolayers at tear film surface pressures in the time scale observed for these experiments.

Lastly, tear lipocalin also did not insert into the monolayers, but with DPPE and DPPS, it appeared to destabilize the films by lowering their surface pressure. This was significant compared to the buffer control in DPPE, but not DPPS. Tear lipocalin has been shown to bind phospholipids using a colorimetric assay and mass spectrometry, but PE and PS lipids were not identified [60,136]. Despite being overall negatively charged at pH 7.4, tear lipocalin is amphipathic and has been shown by Saaren-Seppälä *et al.* to bind lipid monolayers regardless of charge, whether positive, negative, or neutral [138]. Tear lipocalin has been reported by Gasymov *et al.* to change conformation upon lipid binding [198], and Saaren-Seppälä *et al.* suggest this may occur when binding to lipid membranes, but the exact structural changes are unknown [138].

Lipocalin may have been able to bind lipids and remove them from the monolayer whereby the smaller headgroup of DPPE may have facilitated this process. In the case of DPPS, the negatively charged lipid may have been able to interact with a patch of positively charged amino acids on the protein [135]. One might think that the headgroups of both DPPE and DPPS could be more easily solubilized than the other lipids, provided

the tails could be accommodated in the hydrophobic pocket of tear lipocalin. Unfortunately, the lipids are in the opposite orientation required for this arrangement, with the acyl chains pointed toward the air, away from the aqueous subphase and the cavity of lipocalin. The lipids would have to flip in order to be captured by lipocalin, or lipocalin would have to undergo conformation changes to achieve the proper orientation within lipid/water interface, or a combination of both events. Additionally, lipocalin may temporarily insert into the monolayer, which results in closer proximity of the hydrophobic cavity to the nonpolar acyl chains. DPPE and DPPS have more hydrophilic headgroups than DPPC or PSM and this may allow lipocalin to better remove them from the monolayer, but this was not the case with PGC despite its hydrophilic glucosyl moiety [169,170]. PGC may have experienced tighter packing, preventing lipocalin from inserting into the monolayer. Saaren-Seppälä *et al.* studied the insertion of human tear lipocalin into neutral (POPC), anionic (POPC/POPG (8:2)), and cationic lipid monolayers (POPC/sphingosine (8:2)) [138]. Lipocalin was able to insert into the films if the initial surface pressure of the films was below 25 mN/m, over 45 minutes [138], but the differences in headgroups and the unsaturated acyl tails make these films more fluid than those investigated here.

4.3.2.2 Lipid Mixtures with Low Protein Concentrations

Low concentrations of lysozyme and lactoferrin did not insert any of the lipid mixtures. Roberts *et al.* measured the interactions between monolayers with HEWL and

DPPC:DPPG (7:3) monolayers with surfaces pressures of 41 mN/m and 39 mN/m respectively, and no changes in surface pressure were observed [105]. Tear lipocalin appears to destabilize the DPPS (-) and PGC (-) mixtures, much like the pure DPPE and DPPS. DPPE was present in all three mixtures, yet the quinary mixture was not destabilized. The number of lipids in the quinary mixture with relatively small molecular areas allowed for better packing, making it more difficult for tear lipocalin to remove lipids from the monolayer (figure 4.19).

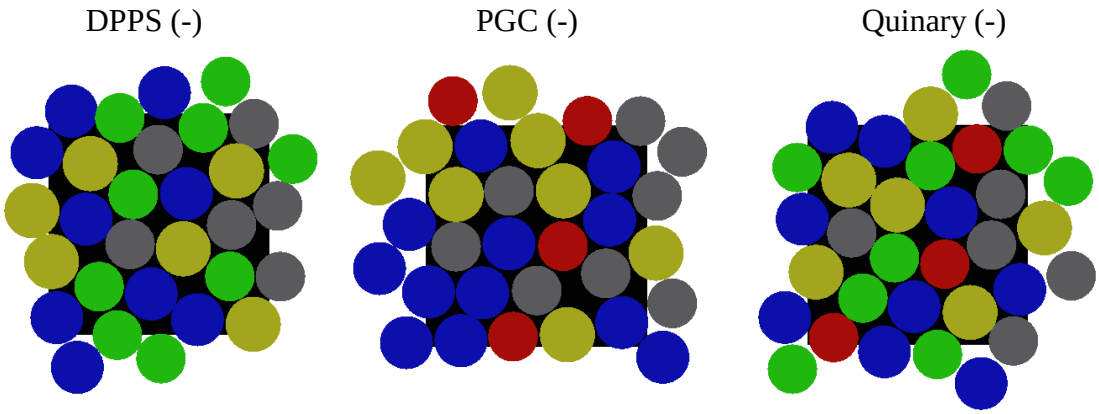

Figure 4.19. Schematic highlighting differences between the packing of the lipid mixtures. For demonstration purposes, the differences between each mixture were enhanced by using average molecular area of each pure lipid at 26 mN/m as the diameter of each disk. The pure lipids were DPPC (blue), DPPE (grey), PGC (green), PSM (yellow), and DPPS (red). Pixel analysis for the amount of the black square exposed was 13519 for DPPS (-), 13374 for PGC (-), and 12316 for the quinary mixture.

4.3.2.3 Quinary Lipid Mixture with Varied Protein Concentrations

Biologically relevant concentrations of lysozyme or lactoferrin do not insert into the quinary lipid mixture. No matter the concentration, surface pressures decreased and were not significantly different from the buffer control. No definitive trends were seen as protein concentrations were increased.

4.3.3 Isocycle Stage – Reversibility

It appears that none of the proteins at 0.01 mg/mL affect the reversibility of pure polar layer lipids found in the tear film, in the range of surface pressures found in whole tear samples. Even with tear lipocalin possibly destabilizing DPPE and DPPS during the constant area stage, reversibility was not affected. This indicates that each pure lipid is capable of stable film cycling within the surface pressure range studied here, and that low concentrations of proteins do not alter this behavior. The reversibility of the lipid mixtures was also not affected by any of the proteins. Lysozyme and lactoferrin at biologically relevant concentrations were also unable to affect the reversibility of the quinary lipid mixture.

4.3.4 Isocycle Stage – Compression/Expansion Moduli

4.3.4.1 Pure Lipids with Low Protein Concentrations

For DPPC, the PBS control became more fluid beginning with expansion in cycle 3. All three proteins appeared to rigidify DPPC during expansion, but not significantly so

for compression. A similar effect was seen for PSM, but it began with the compression during cycle 2. Lysozyme and lactoferrin generally rigidified the films. These variations are subtle, and due to their inconsistency are not compelling enough to suggest the proteins are having an effect at such low concentrations. Experiments using tear film lipids and proteins with a similar protocol are difficult to find because they often use meibomian secretions [87,197], or use low surface pressures during cycling, allowing protein insertion into the films [85,150,199]. Once proteins insert into the film, which was not observed here, substantial changes to the hysteresis of lipid monolayers have been observed. Roberts *et al.* injected HEWL into the subphase of a DPPC monolayer at 41 mN/m and took interfacial sheer rheology measurements, but found that the lysozyme had no effect [105]. The final concentration of HEWL was not provided, but the authors did say they injected 0.1 mL of 100 mg/mL protein solution, and so the final subphase concentration was likely similar to what was used in the current work.

The proteins did not seem to interact with DPPE, PGC, or DPPS in a way that affected the elastic nature of the films. For DPPE and PGC this seems understandable as DPPE is zwitterionic and PGC is neutral. It is unexpected that DPPS does not appear to interact with lysozyme or lactoferrin, as both proteins are positively charged at pH 7.4, given that electrostatic interactions are very important for initial adsorption [105,183,185–189].

One final point is that compression and expansion moduli have a similar magnitude for each lipid mixture regardless of protein. This symmetry explains why

reversibility was generally around 1, as the change in surface pressure was similar for both compression and expansion isotherms. Overall, protein concentrations at 0.01 mg/mL do not appear to affect the elastic nature of the films, even if electrostatic attraction is present.

4.3.4.2 Lipid Mixtures with Low Protein Concentrations

For the DPPS (-), tear lipocalin seemed to fluidize the monolayer more than lysozyme, but not the PBS control, so this only suggests that lipocalin may destabilize the DPPS (-) mixture. The results for lipocalin do seem to align with the destabilization seen in the constant area stage. No clear trends emerged for the PGC (-) mixture or the quinary mixture. In the same study mentioned earlier, Roberts et al. found no changes in rheology for DPPC:DPPG (7:3) monolayers for the interactions with HEWL [105]. But again, the 0.01 mg/mL concentration may have been too low to detect a change.

4.3.4.3 Quinary Lipid Mixture with Varied Protein Concentrations

The quinary lipid mixture became more relaxed with lysozyme and lactoferrin at 1 mg/mL, the lower range of concentration in the tear film [108,109,115,116]. This was especially pronounced for lactoferrin, which reduced the compression and expansion moduli to values consistent with the LE phase [158]. The study of less complex lipid mixtures is required to narrow down the changes in lipid organization to specific lipid classes responsible for this effect. A study by Svitova and Lin used whole tear lipids at 48

mN/m, with a biological relevant concentration (2 mg/mL) of HEWL injected into the aqueous phase and found that it did not change the surface pressure significantly, but it did increase its relaxation time, suggesting it adsorbed to the film and fluidized it [43,182]. This effect persisted even after the aqueous phase with free lysozyme had been exchanged, indicating the retention of bound lysozyme [43,182]. This demonstrates that changing rheological properties of lipid films at high surface pressure is possible and that HEWL can bind to lipids found in whole tears. Their lipid films were again whole tear extracts, and ~90 nm thick [43], compared to quinary monolayer which is likely around 3 nm thick [200]. The quinary model may be an accurate mimic to study protein effects on the polar lipid layer of the tear film. Lysozyme and lactoferrin fluidizing the monolayer may indicate an additional role of proteins in the tear film. A rigid stable monolayer is preferable to act as a barrier to environmental contaminants, but if it is too rigid it may be unable to spread quickly after a blink. Proteins may help to reduce the rigidity of the monolayer, providing an appropriate barrier that can spread quickly enough to shield and reduce the surface tension the aqueous layer.

Over many cycles, the relaxing effect of the proteins is reduced, and they appear to reach a state of equilibrium. The 1 mg/mL concentration retains lower compression and expansion moduli than the control, but not much lower than the other protein concentrations. Perhaps this is due to the shear stress on the monolayer mechanically disrupting the interactions with the proteins.

How this would compare to *in vivo* conditions is difficult to ascertain. The blink is much faster, but there are also inter-blink periods where the lipid layer would not experience continuous compression and expansion as in this experiment. Also, the nonpolar lipids appear to insert amongst the hydrophobic chains of the polar lipids, and fluidize the lipid layer [179,180]. This may disrupt the steric hindrance of the lipid headgroups and allow for hydrophobic residues to insert. We appeared to see peripheral binding this experiment, but we could potentially see insertion with presence of nonpolar lipids.

4.4 Conclusions

It appears that the time scale for these experiments may not have been long enough to observe insertion of the proteins into the monolayer films. It is possible that tear lipocalin may destabilize pure DPPS and PGC films. It may also destabilize the quaternary mixtures lacking DPPS and PGC, but the quinary mixture was unaffected. This destabilization did not affect the reversibility or the elastic nature of the films. Low concentrations of proteins do not appear to change the reversibility of the films, or the compression and expansion moduli, for any pure lipid or lipid mixture. Biologically relevant concentrations of lysozyme and lactoferrin do not change the reversibility of the quinary mixture, but did fluidize it despite the lack of insertion. This effect was reduced over many blink cycles.

Chapter Five: Brewster Angle Microscopy

5.1 General Chapter Overview

To see how proteins affect the lateral organization of the lipid films at surface pressures found in tear film samples, the experiments described in chapters three and four were repeated so they could be imaged using Brewster Angle Microscopy (BAM). This chapter is again divided into results and discussion sections regarding the three stages of the experiments, the constant pressure stage, the constant area stage, and the isocycle stage. The main purpose of these experiments was to see how proteins interact with the lipid monolayers during blinking, which was mimicked during the isocycle stage. To prepare the film for isocycles, constant pressure and area stages were necessary and they will be discussed briefly. The effects of subphase protein concentrations of 0.01 mg/mL on the five pure lipids will be presented first, followed by the three lipid mixtures. An additional experiment was performed with varied concentrations of lysozyme and lactoferrin with the quinary lipid mixture, so that the effect of higher protein concentrations on lateral organization could be observed.

All images presented in this chapter are of an area with the dimensions 218 x 271 μm, and have been scaled down from their original sizes produced by EP3 View, the software used to run the BAM. All images are 21% of their original size with the exception of the images in figure 5.1, which are 16% of their original size. Many of the images were quite dark, a problem caused by changes in the height of the subphase during the experiments. To help with this, the brightness and contrast of most images

have been adjusted so that structural comparisons can be made. The brightness was not adjusted for DPPC, DPPE, PSM, and PGC for the lowest surface pressures shown in figure 5.1 as no domains were visible. Also, a section of each image has been magnified to 2x of the scaled down image, and this is shown in the bottom right corner of each image. All changes to the images were done using the GNU Image Manipulation Program (GIMP).

5.2 Results

5.2.1 Constant Pressure Stage

5.2.1.1 Pure Lipids

During the constant pressure stage, all films were compressed to a surface pressure of 26 mN/m, the resting surface pressure of tear film samples [41], whereby the LC phase predominated (figure 5.1). DPPC at 6.9 mN/m was in LE phase, by 7.8 mN/m it had entered a phase coexistence plateau and small LC domains had begun to form, by 9.9 mN/m the majority of the film was in the LC phase, and by 25.9 mN/m very little LE phase could be seen. Generally domains were asymmetrical multi-lobed structures. The lobes appeared less numerous for the small domains at 7.8 mN/m, but grew in complexity by 9.9 mN/m. At 25.9 mN/m, the LC domains were almost touching each other but not merging, a morphology that resembles a marbled texture.

Below 0.7 mN/m, DPPE appeared to be predominantly in LE phase, but the LC phase formed in the narrow surface pressure range between 0.7 mN/m and 1.2 mN/m

(figure 5.1). Small LC domains and domain growth as seen with DPPC were not observed with DPPE. Since DPPE formed an amorphous LC phase at low surface pressures, changes in lateral organization were not observed up to 26 mN/m.

PGC behaved similarly to DPPE, except higher surface pressures were required for the formation of the LC phase, as gaps of LE phase were still observed at 3.5 mN/m and 15.2 mN/m (figure 5.1). By 26 mN/m it established a continuous amorphous phase. Both DPPE and PGC near tear film surface pressure have an amorphous morphology. Small contaminant particles can be seen as bright points on the two images, DPPE at 1.2 mN/m and PGC at 3.5 mN/m.

The LC domains of PSM did not grow nearly as large as any of the other lipids (figure 5.1). LC domains can be seen to form by 12.6 mN/m, these domains grew to a size much smaller than DPPC and appeared to lack a lobed morphology. By 16.2 mN/m, many of these domains were visible and they continued to be compressed closer together until they densely blanked the image at 24.3 mN/m. Near 26 mN/m, the film had a sand-like texture.

DPPS was similar to DPPC in domain formation, except LC domains were seen at lower surface pressures, as indicated at 0.9 mN/m (figure 5.1). The lobes of larger LC domains were more pronounced for DPPS than DPPC . Between 0.9 and 4.5 mN/m, LC domains had grown and become quite close, some domains looked like they may have fused, but upon close inspection it can be seen that the borders of the LC domains were still intact. By 23.7 mN/m, the film almost had a more amorphous quality, some LE

borders were still visible, but they were faint. Like DPPC, DPPS had a marbled texture near 26 mN/m, but with a less distinct LE phase.

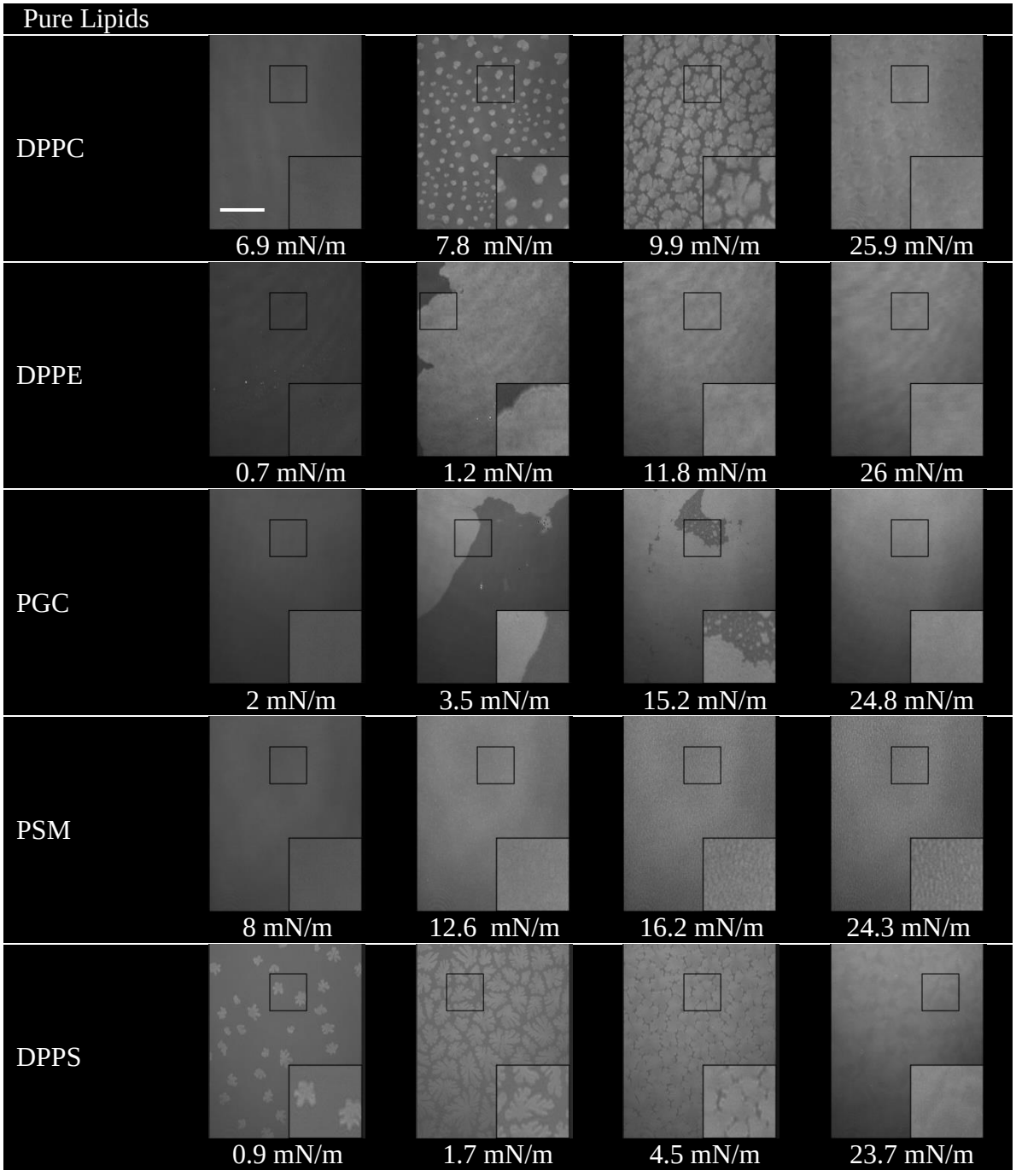

Figure 5.1. BAM images of pure lipids during initial compression to 26 mN/m. Select images highlight formation and growth of LC domains. The inset is magnified 2x.

5.2.1.2 Lipid Mixtures

Two quaternary lipid mixtures and one quinary mixture were investigated. The quaternary mixtures each lacked a lipid found in the quinary mixture. DPPS (-) had a molar ratio of 3 PC : 2 PE : 3 GC : 2 SM, which resembles earlier compositions published by Shine and McCulley with meibomian secretions [153–156]. PGC (-) had a molar ratio of 3 PC : 2 PE : 2 SM : 1 PS and resembles more recent publications of whole tear polar lipid profiles [5,60,73]. The quinary mixture had a molar ratio of 3 PC : 2 PE : 3 GC : 2 SM : 1 PS, a combination of all polar lipid classes identified from the literature, with the exception of OAHFAs. For lipid mixtures, images from similar surface pressures were chosen to highlight differences in LC domain growth (figure 5.2). The lobed structures of the domains appear similar. The sizes of the domains for the PGC (-) and quinary mixtures appear similar, but some larger domains were observed in the DPPS (-) mixture. Domain growth appears similar for the DPPS (-) and PGC (-) mixtures, but larger LC domains were seen at lower pressures for the quinary mixture. Near 26 mN/m, all films had the appearance of complex lobed LC domains compressed closely together but not merged entirely. The LE boundaries appear to be more pronounced in the DPPS (-) mixture than the other two mixtures. All three films had a marbled morphology similar to pure DPPC and DPPS near 26 mN/m.

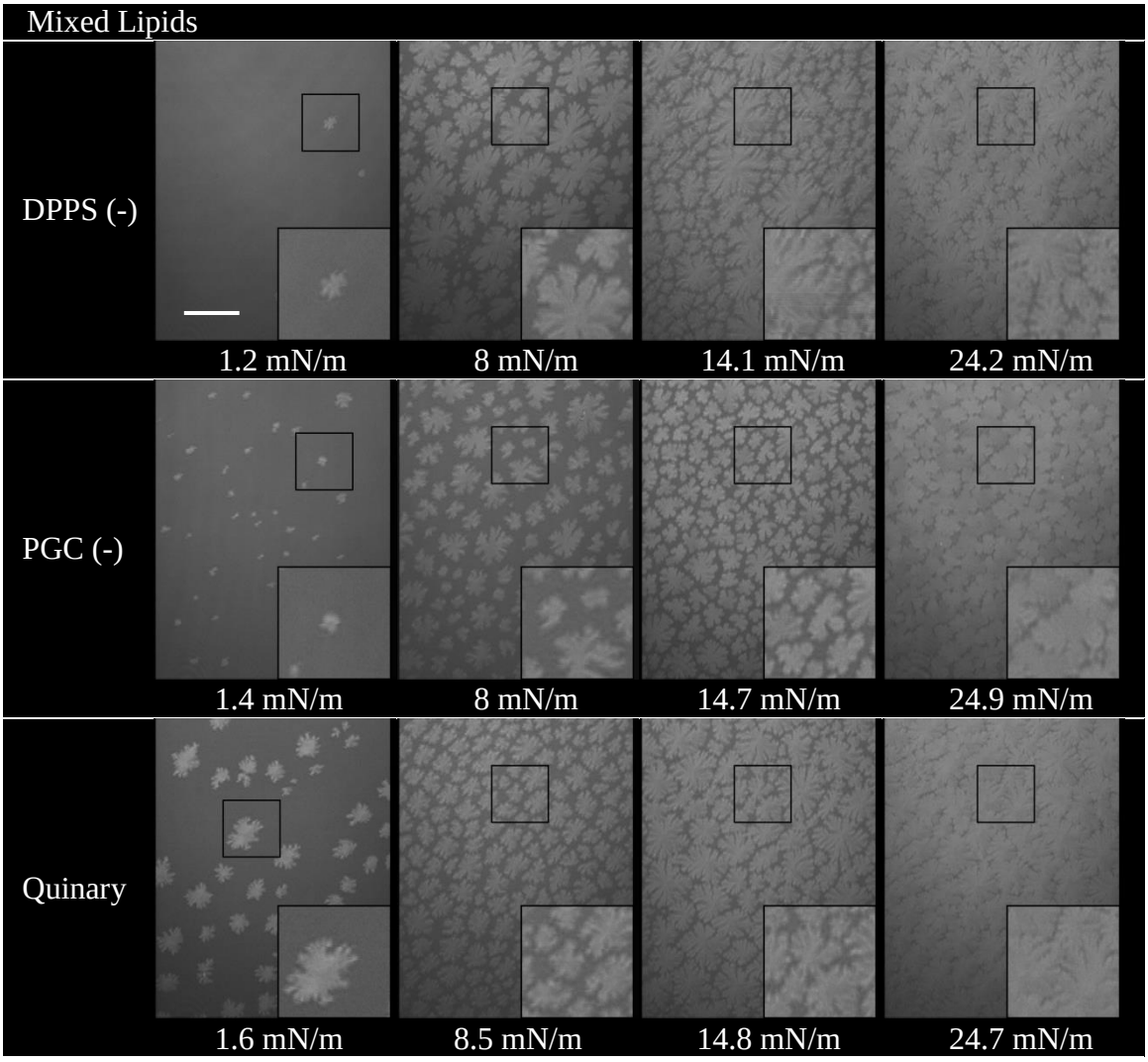

Figure 5.2. BAM images of lipid mixtures during initial compression to 26 mN/m. Select images shown to highlight formation and growth of LC domains. The quinary mixture had a molar ratio of 3 PC : 2 PE : 3 GC : 2 SM : 1 PS, the other two quaternary mixtures each lacked one lipid found in the quinary mixture. DPPS (-) lacked DPPS, and PGC (-) lacked PGC. The inset is magnified 2x.

5.2.2 Constant Area Stage

5.2.2.1 Pure Lipids with Low Protein Concentrations

With few exceptions, most of the images taken during the area control stage for each pure lipid were similar over the course of the stage (figures 5.3 to 5.7). During this stage, the barrier position was fixed after maintaining a surface pressure of 26 mN/m for the pressure control stage. Injection of either a 1 x PBS buffer control or protein solvated in 1 x PBS buffer occurred after a minute of incubation, and the final subphase protein concentration was 0.01 mg/mL. Images were taken before injection, immediately after injection, and 30 minutes after injection. For each lipid, differences in brightness and clarity can be seen for the starting state before injection. These differences were caused by subtle changes in focus, subphase height, and air flow. An example of this is DPPC, the starting states for PBS and tear lipocalin appear different from the starting states of lysozyme and lactoferrin before injection had occurred (figure 5.3). So to determine if a protein is having an effect on domain morphology, comparisons were made between the images after injection to the starting state before injection for a particular trial. Sometimes bright spots occurred that were likely contaminants or dust, as they were observed both before and after injection. These spots tended to move in a specific direction over time.

DPPC, DPPE, PGC, and DPPS showed no changes in lateral organization immediately after injection of any protein (figures 5.3 to 5.5, and 5.7). For DPPC and DPPS, the boundaries of LC phases appeared to blur after 30 minutes of incubation

(figures 5.3 and 5.7). For DPPC with injected lysozyme or lactoferrin, LC domain structure could be seen before and immediately after injection, but appeared less distinct after 30 minutes (figure 5.3). Domain structure of DPPC with PBS and tear lipocalin were not visualized clearly before injection, and so it is unclear if the same trend occurred. For DPPS with the PBS control and lactoferrin, LC domain structure was visible before and immediately after injection, and still appeared distinct after 30 minutes of incubation (figure 5.7). For DPPS with lysozyme and tear lipocalin, domain structure was again visible before and immediately after injection, but appeared to blur after 30 minutes. DPPE and PGC had amorphous structures near 26 mN/m, and so changes could not be observed over the 30 minute incubation (figures 5.4 and 5.5). There were some defects in the PGC film with tear lipocalin, but they were present before protein injection (figure 5.5).

For PSM, no differences were observed for PBS and lactoferrin, (figure 5.6). Domain structure differed before injection for the lysozyme, and this carried through until the end of the constant area stage. PSM with tear lipocalin was initially similar to PBS and lactoferrin, but differed by the end of the stage. This alternate morphology contained regularly distributed dark patches, and they were larger than the LC domains normally seen with PSM. Difficulty was encountered during imaging of PSM where surface pressure would drop rapidly. More trials were run for PSM, but for lysozyme and lipocalin trials, surface pressures still declined as low as 10 and 10.5 mN/m respectively.

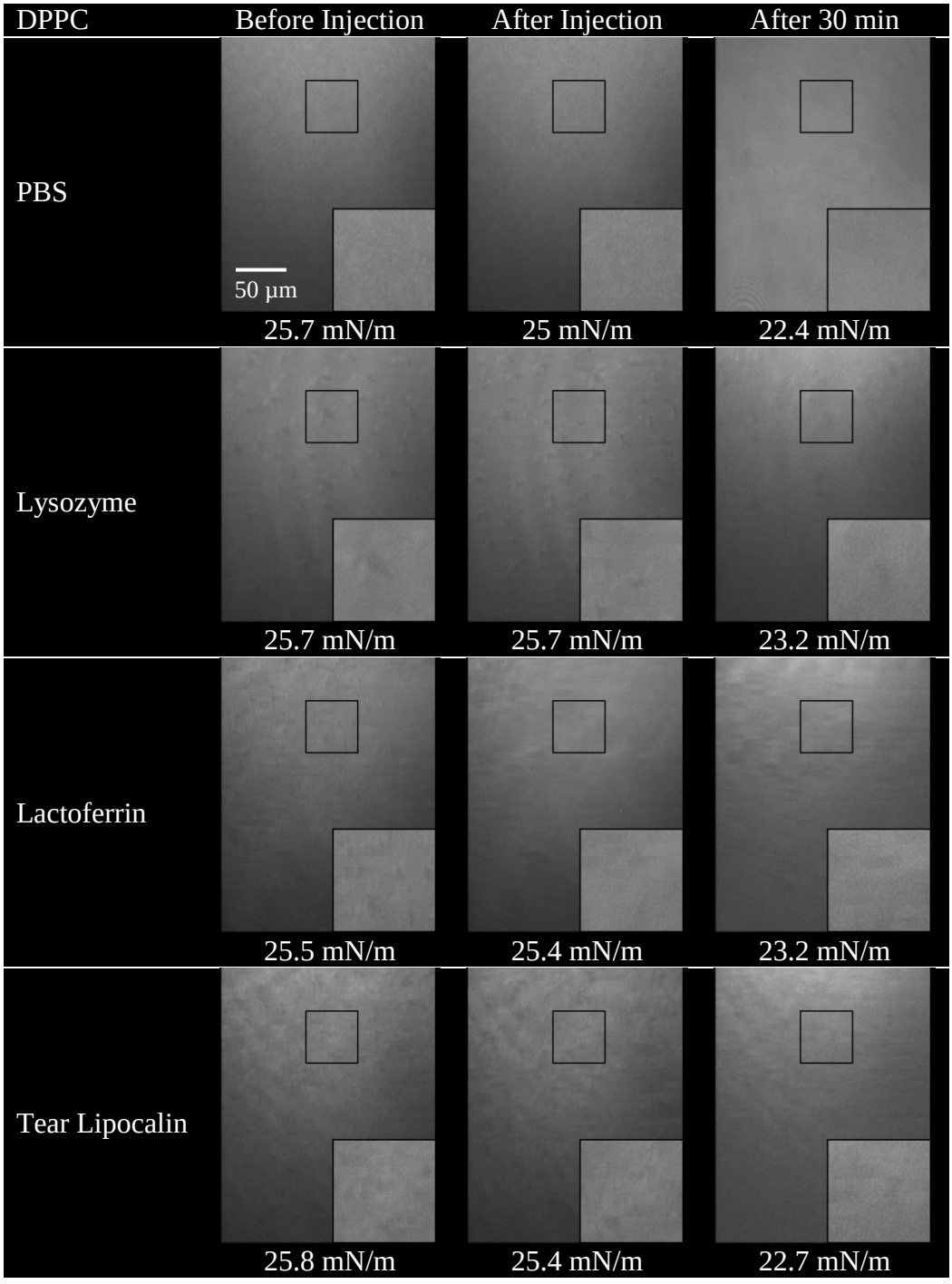

Figure 5.3. BAM images of DPPC where protein was injected into the subphase during the area control stage. See general overview for experimental conditions (page 131).

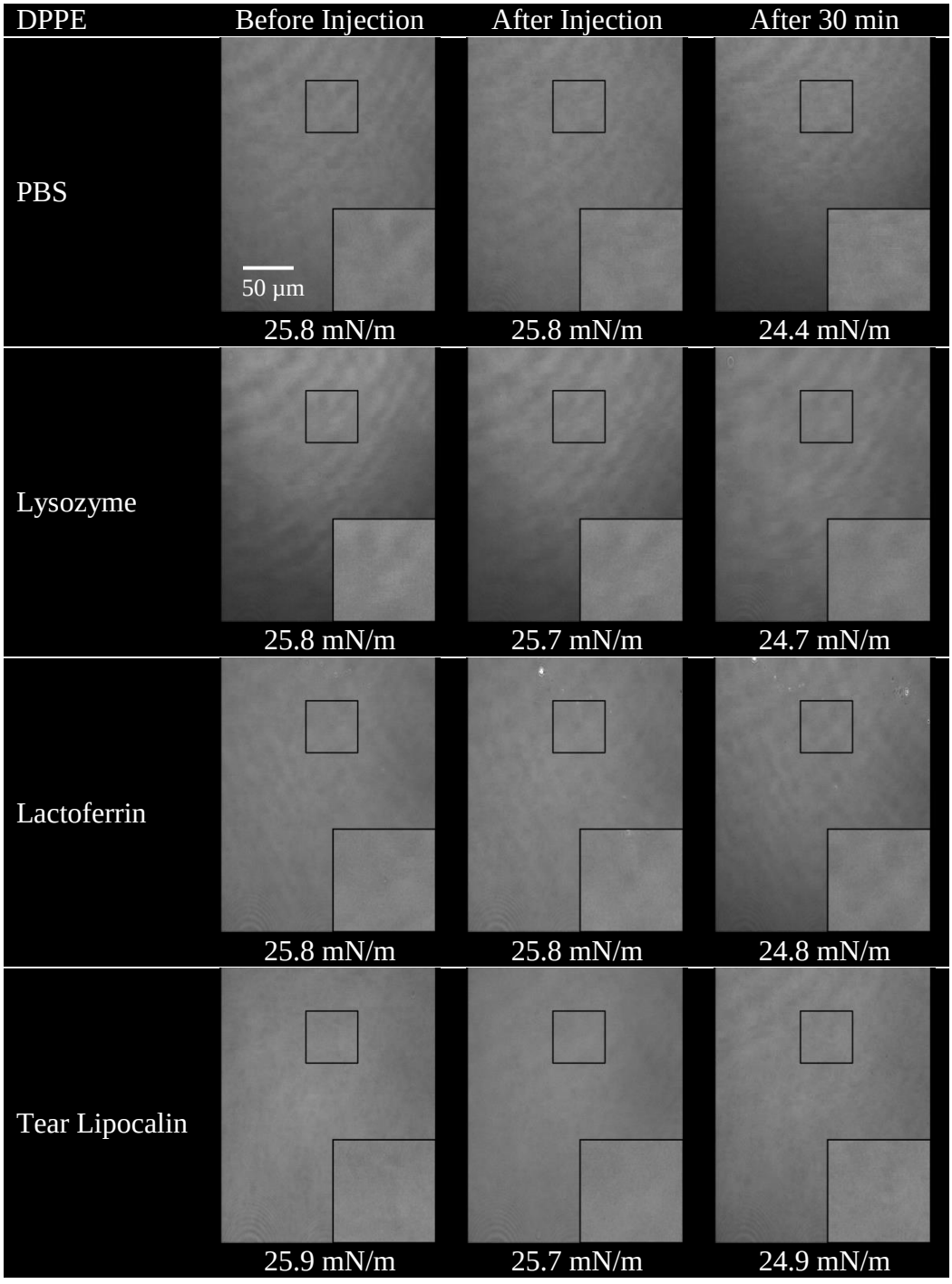

Figure 5.4. BAM images of DPPE where protein was injected into the subphase during the area control stage. See general overview for experimental conditions (page 131).

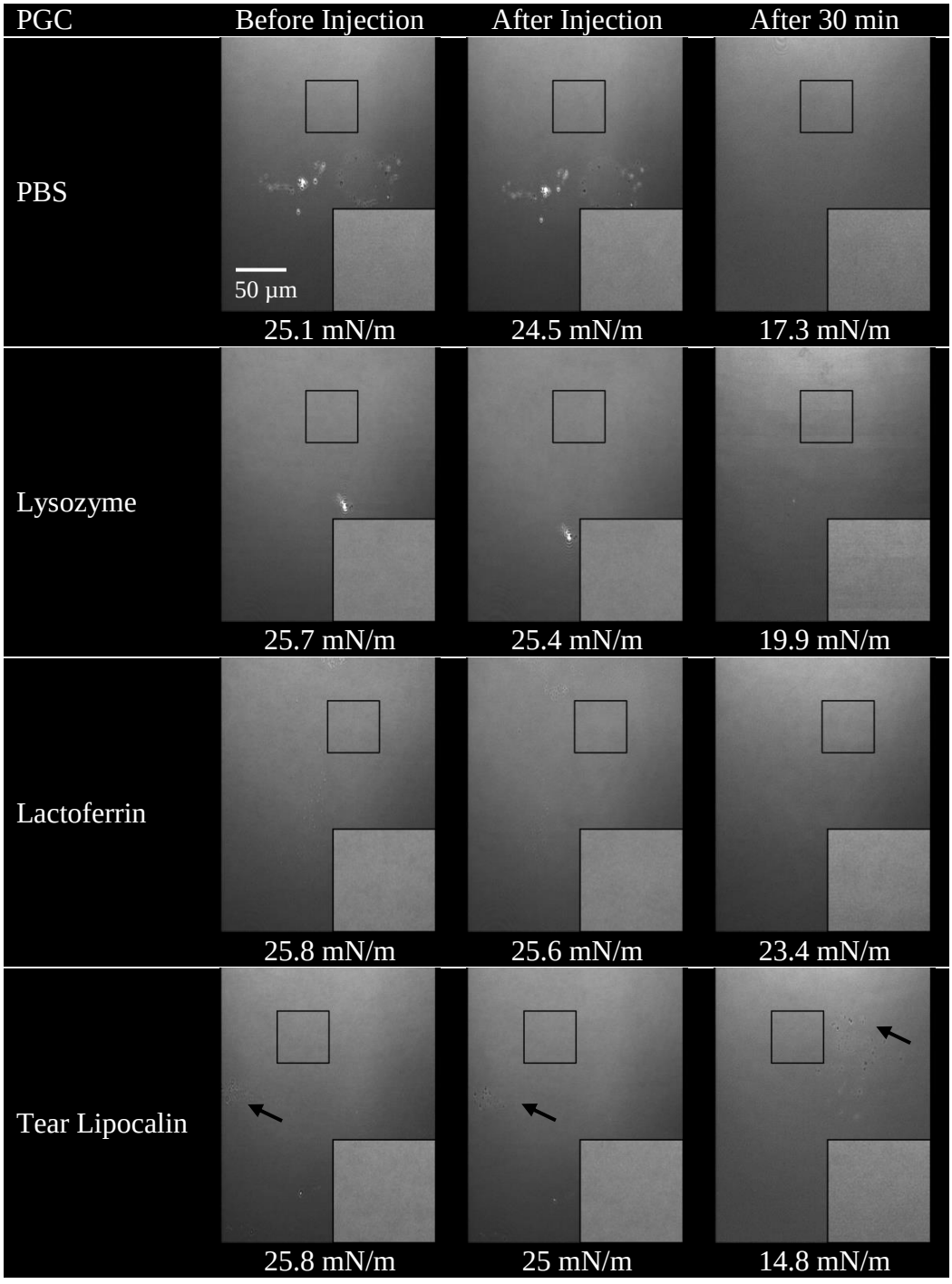

Figure 5.5. BAM images of PGC where protein was injected into the subphase during the area control stage. See general overview for experimental conditions (page 131).

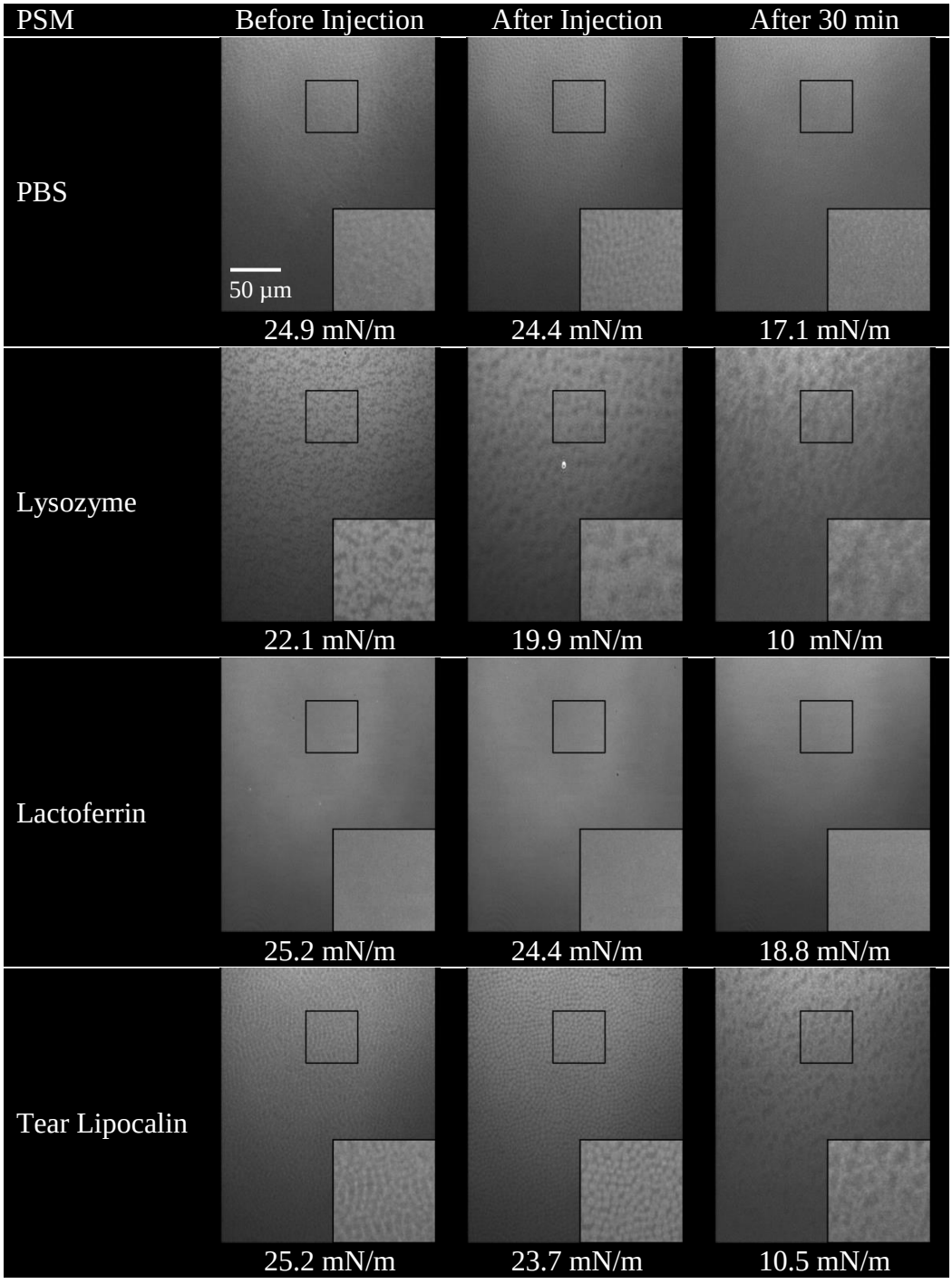

Figure 5.6. BAM images of PSM where protein was injected into the subphase during the area control stage. See general overview for experimental conditions (page 131).

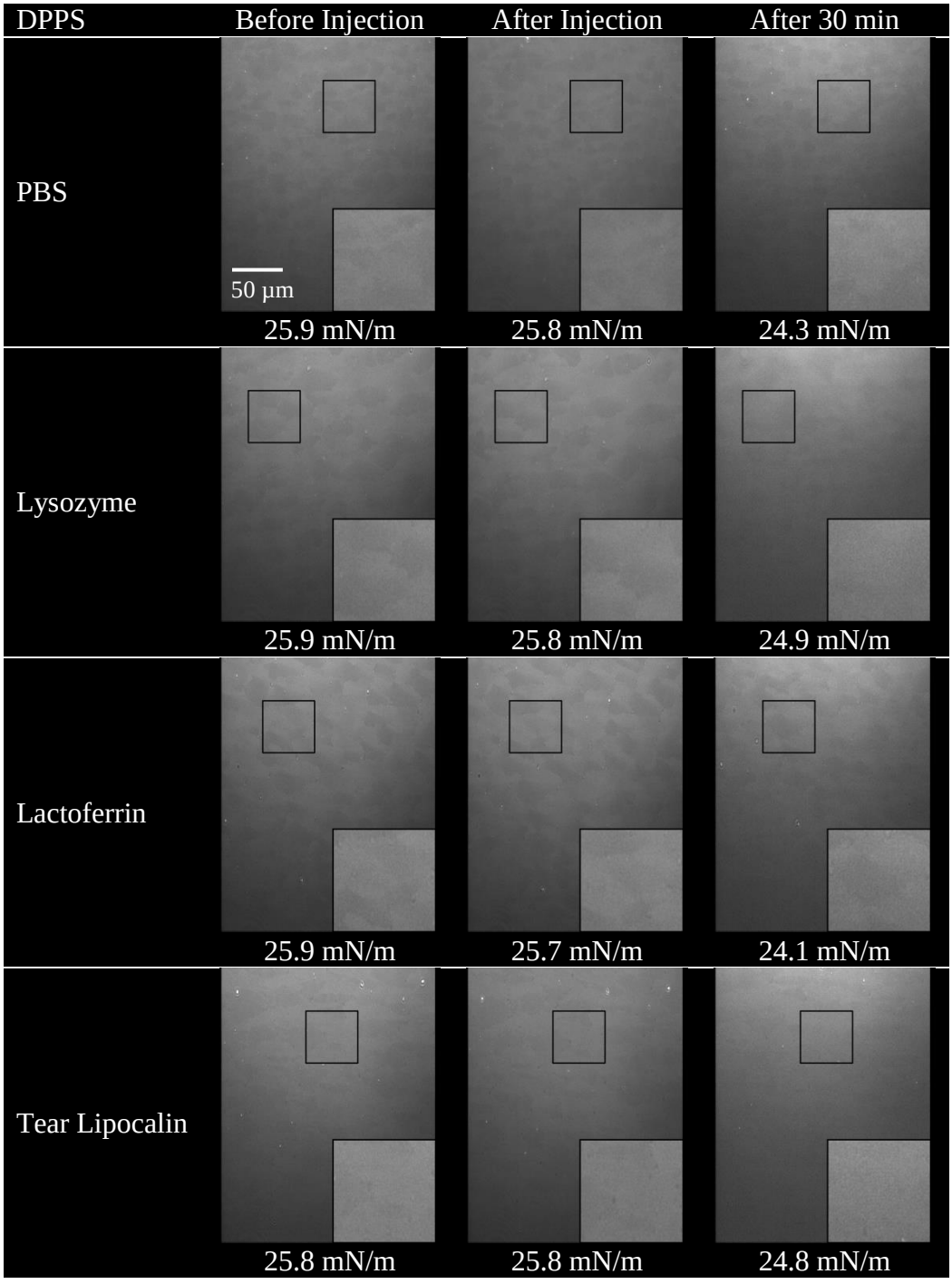

Figure 5.7. BAM images of DPPS where protein was injected into the subphase during the area control stage. See general overview for experimental conditions (page 131).

5.2.2.2 Lipid Mixtures with Low Protein Concentrations

The lipid mixtures initially appeared to be similar to the pure lipids, with a marbled morphology similar to DPPC and DPPS (figures 5.8 to 5.10). The domain organization does not appear to change immediately after buffer or protein injection for any lipid mixture. For the DPPS(-) (3 PC : 2 PE : 3 GC : 2 SM molar ratio) mixture, LC domain structure generally became less distinct after 30 minutes of incubation, especially so for tear lipocalin (figure 5.8). The PGC(-) (3 PC : 2 PE : 2 SM : 1 PS molar ratio) and quinary (3 PC : 2 PE : 2 : 3 GC : SM : 1 PS molar ratio) mixtures appeared to retain their structure more for the buffer control and lysozyme over the 30 minute incubation, but lost structure for lactoferrin and tear lipocalin (figures 5.9 and 5.10). Again, the loss of structure appears more pronounced for tear lipocalin.

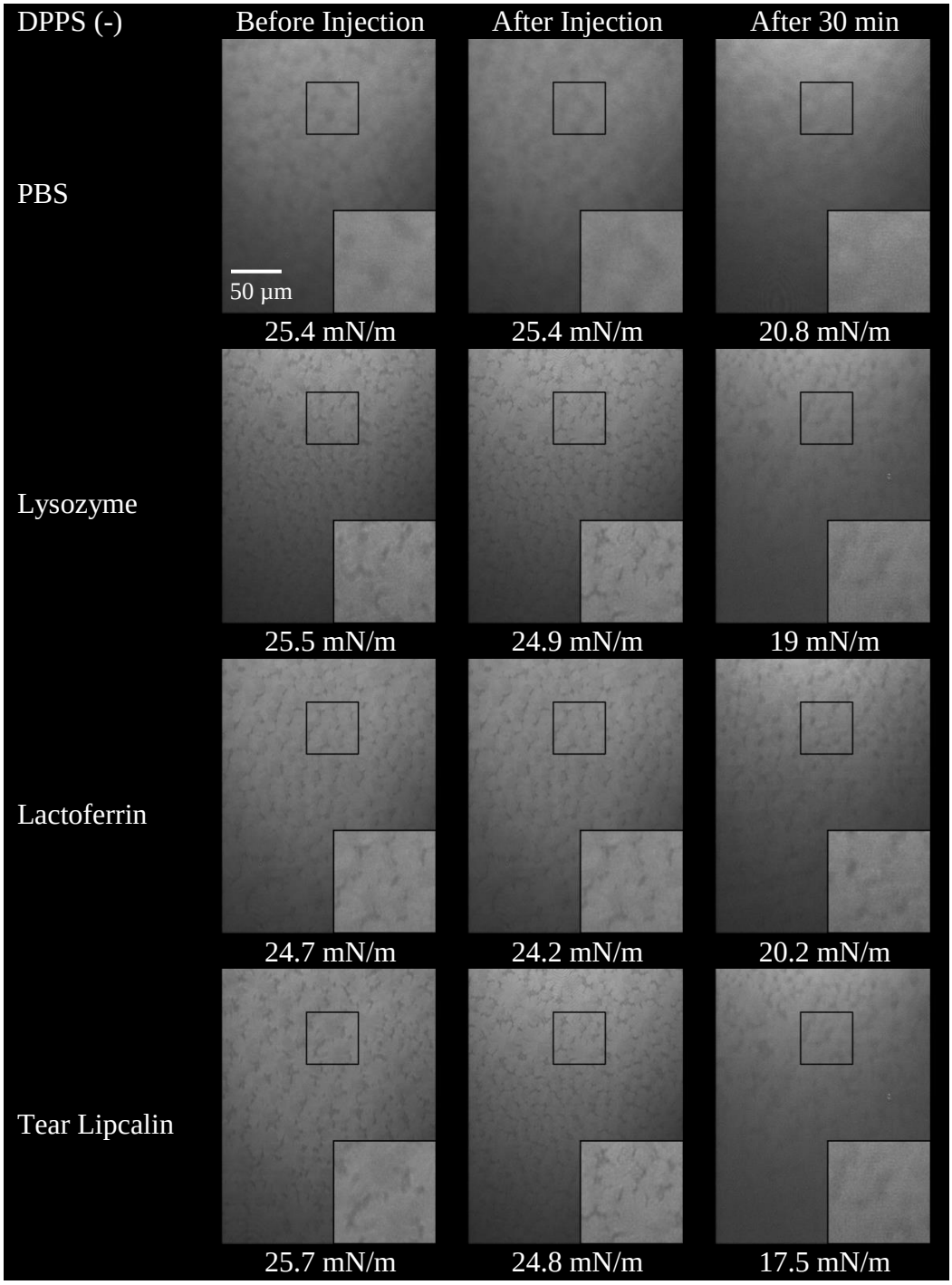

Figure 5.8. BAM images of the DPPS (-) mixture where protein was injected into the subphase during the area control stage. See for experimental conditions (page 131).

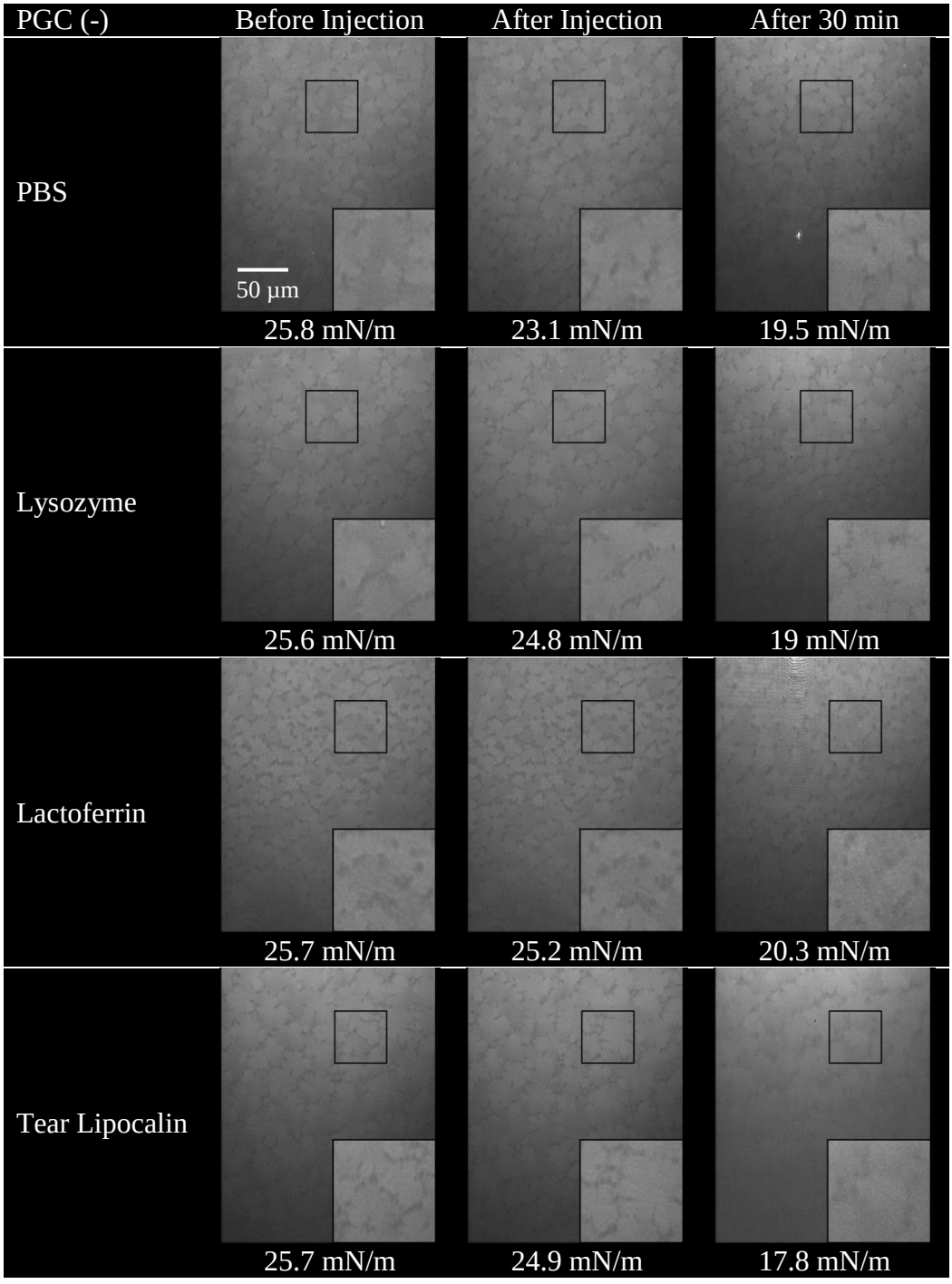

Figure 5.9. BAM images of the PGC (-) mixture where protein was injected into the subphase during the area control stage. See for experimental conditions (page 131).

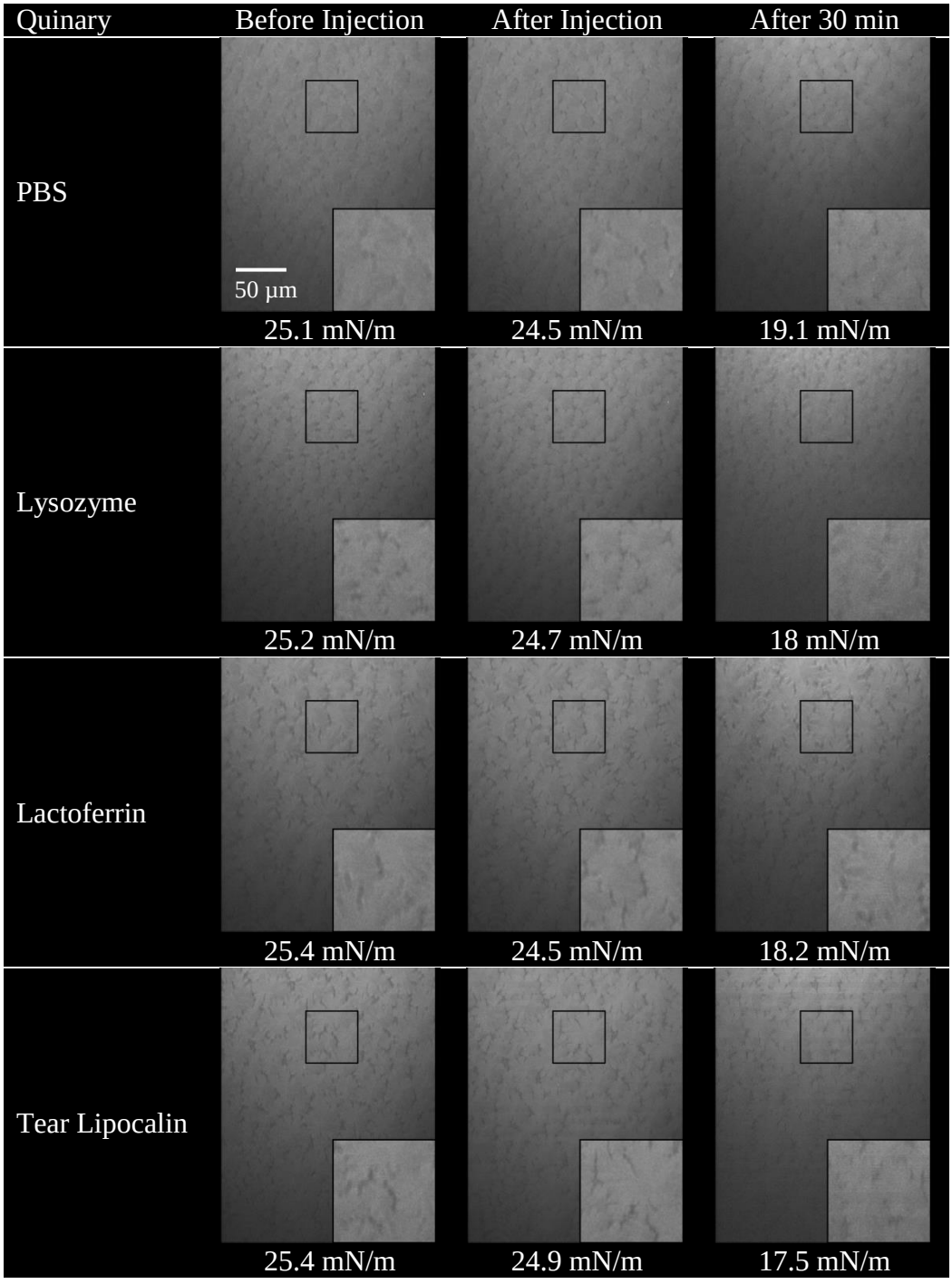

Figure 5.10. BAM images of the quinary mixture where protein was injected into the subphase during the area control stage. See for experimental conditions (page 131).

5.2.2.3 Quinary Lipid Mixture with Varied Protein Concentrations

To assess the ability of higher concentrations of protein to change the lateral organization of the monolayers, an experiment was run with the quinary lipid mixture that varied the protein concentrations of lysozyme and lactoferrin. Tear lipocalin was not used in this experiment because of the time required to express and purify the protein. The final subphase protein concentrations were 0.05, 0.2, and 1 mg/mL. For lysozyme, there did not seem to be any changes in lateral domain structure, even at 1 mg/mL, over the 30 minute incubation (figure 5.11). The LC phase for the 1 mg/mL lysozyme appeared to have smaller domains, still tightly packed together, but this same texture persisted through the injection and incubation period. The quinary mixture was able to retain its structure with the buffer control and 0.5 mg/mL lactoferrin, but the LC domains appear to have reduced in size for the 0.05 mg/mL lactoferrin (Figure 5.12). For 0.2 and 1 mg/mL lactoferrin, a blurring of the LC phase boundaries was visible after the incubation period.

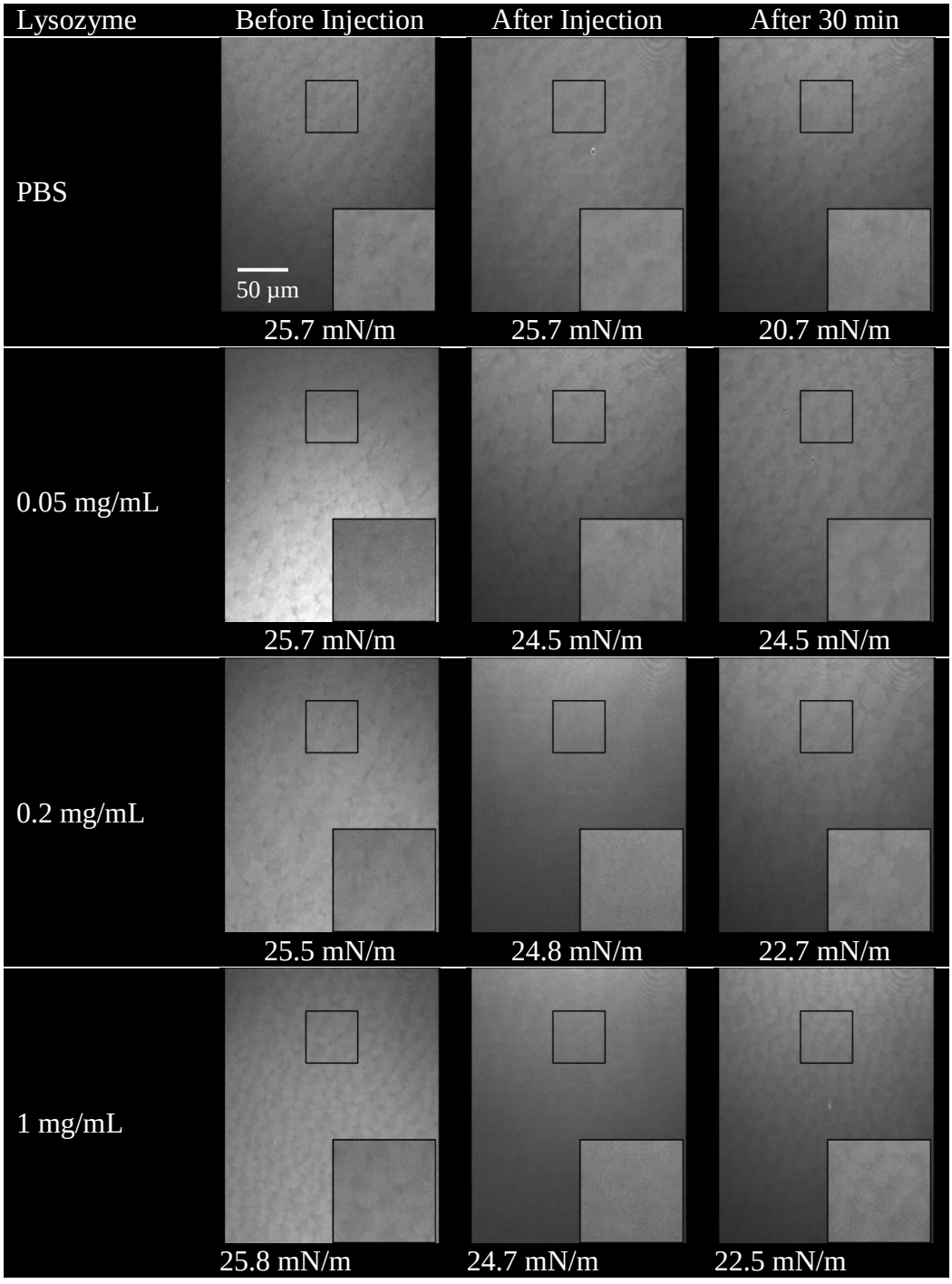

Figure 5.11. BAM images of the quinary mixture during the constant area stage with varying concentrations of lysozyme. See fore experiment conditions (page 142).

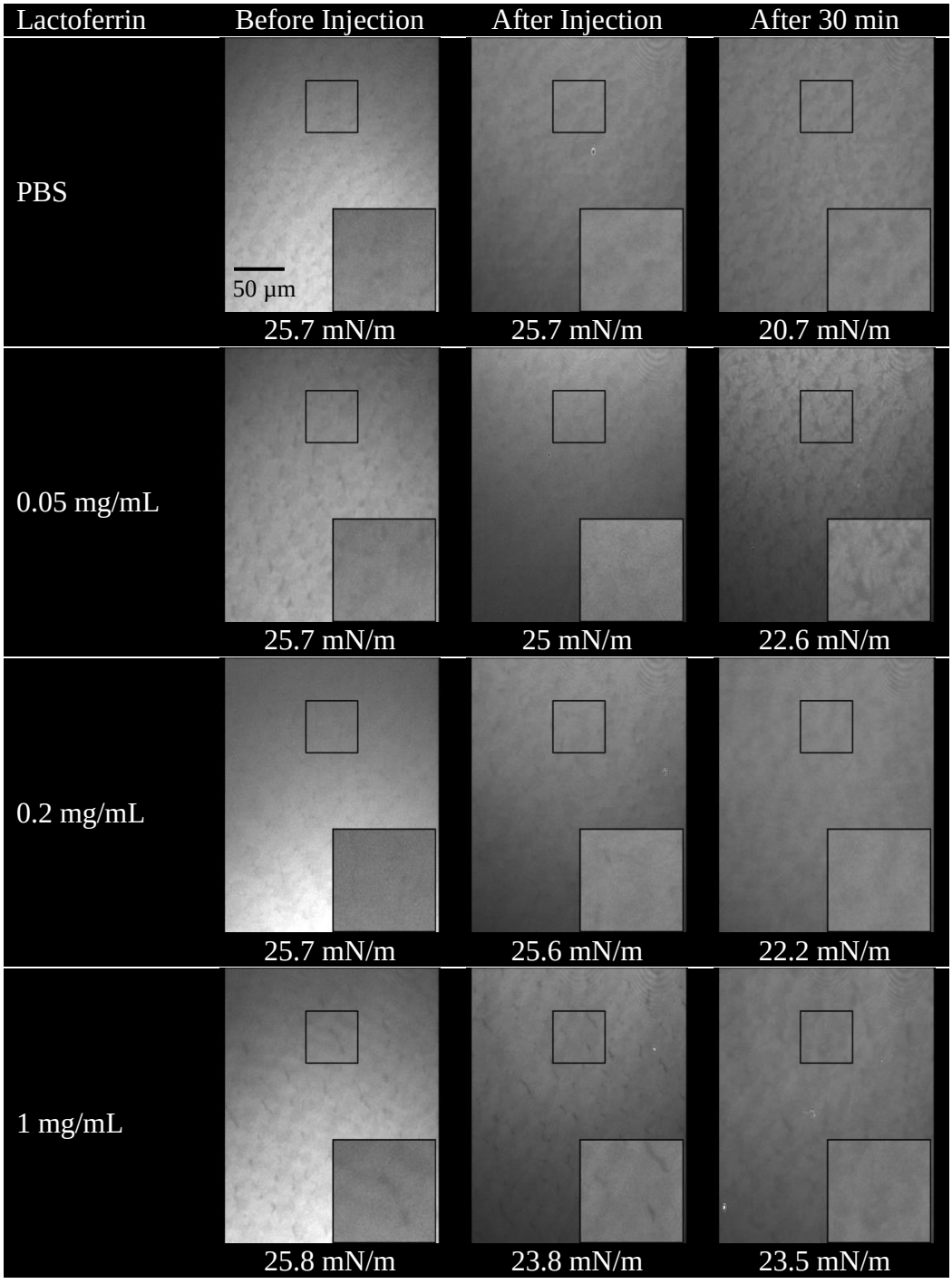

Figure 5.12. BAM images of the quinary mixture during the constant area stage with varying concentrations of lactoferrin. See fore experiment conditions (page 142).

5.2.3 Isocycle Stage

5.2.3.1 Pure Lipids with Low Protein Concentrations

For trials with low protein concentrations, the lipid films were cycled five times between 20 mN/m and 35 mN/m after incubation, this is thought to be the normal tear film surface pressure range [41,42]. Images were taken near both those surface pressures for the first and fifth cycles. Five cycles were chosen because the morphology of the lipid film is stable over five blinks, as observed *in viv*o with interference microscopy [157]. By the end of the area control stage, some of the images were quite dark due to changes in subphase level, and remained dark during the isocycles. To avoid disturbing the surface films, the trough was not re-leveled to brighten the image.

The lateral organization of the pure lipid films generally does not appear to change with lysozyme, lactoferrin, and tear lipocalin at a subphase concentration of 0.01 mg/mL after five cycles (figures 5.13 to 5.17). No differences were observed when images of the first and fifth cycles near 35 mN/m were compared for all pure lipids, with all proteins. The same lack of change is seen when the first and fifth cycles near 20 mN/m are compared. The dark patches observed for the area control stage for PSM (figure 5.6), for both lysozyme and tear lipocalin where present for the first cycle, and persisted until the fifth cycle during isocycles (figure 5.16). For tear lipocalin, the dark patches were not visible at 33.8 mN/m for the fifth cycle, but returned when expanded to 20.3 mN/m.

Occasionally, differences were observed between images taken near 20 mN/m versus those at 35mN/m. This is the case for the DPPC/PBS trial, the images at 20 mN/m were quite dark and interference patterns could be seen whereas the images near 35 mN/m were brighter and more uniform (figure 5.13). Also with DPPS/PBS, the images near 20 mN/m had sharper LC/LE boundaries compared with images taken near 35 mN/m (figure 5.17).

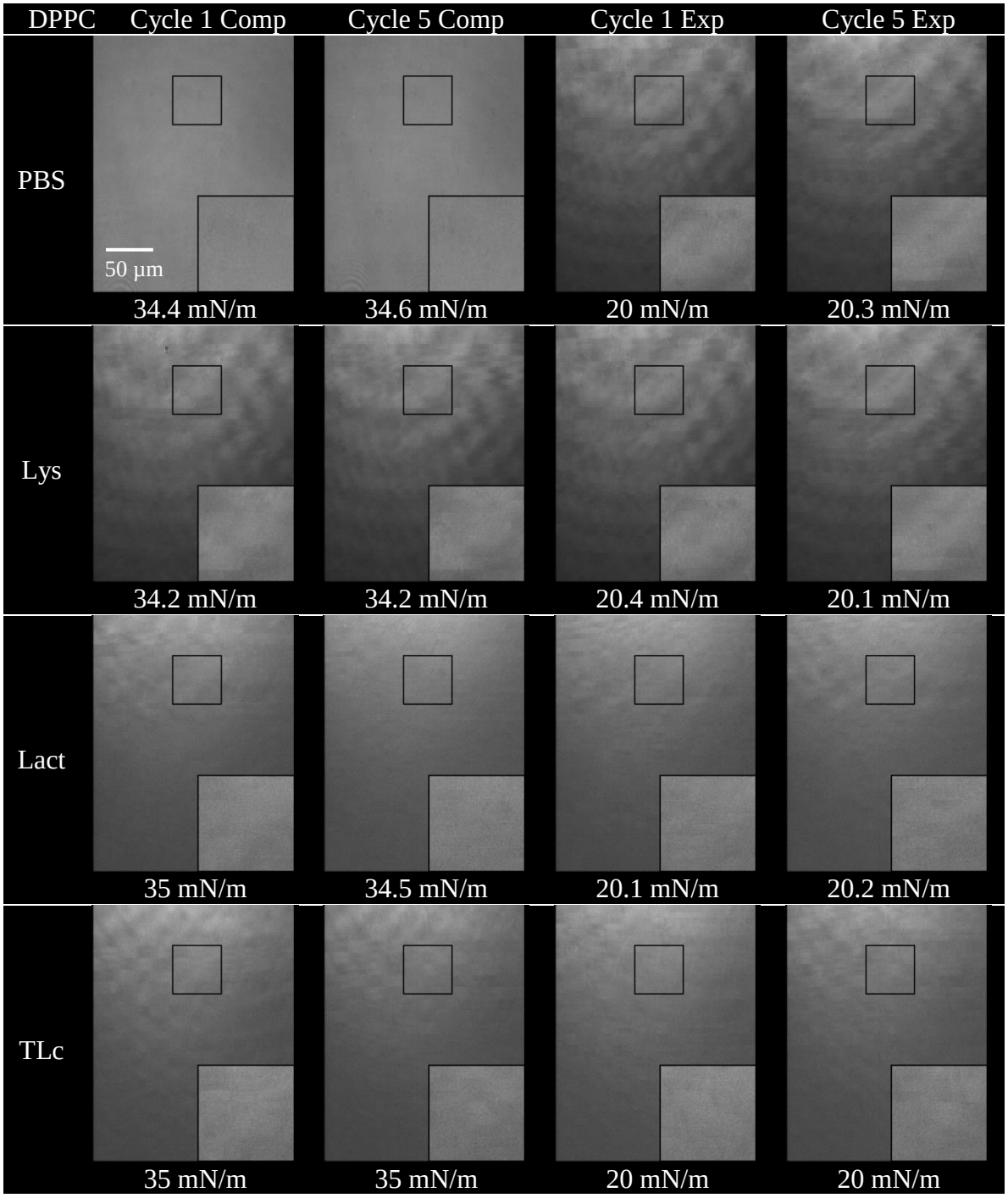

Figure 5.13. BAM images of DPPC during isocycles with no protein (PBS), lysozyme (Lys), lactoferrin (Lact), or tear lipocalin (TLc). For experimental conditions (page 145).

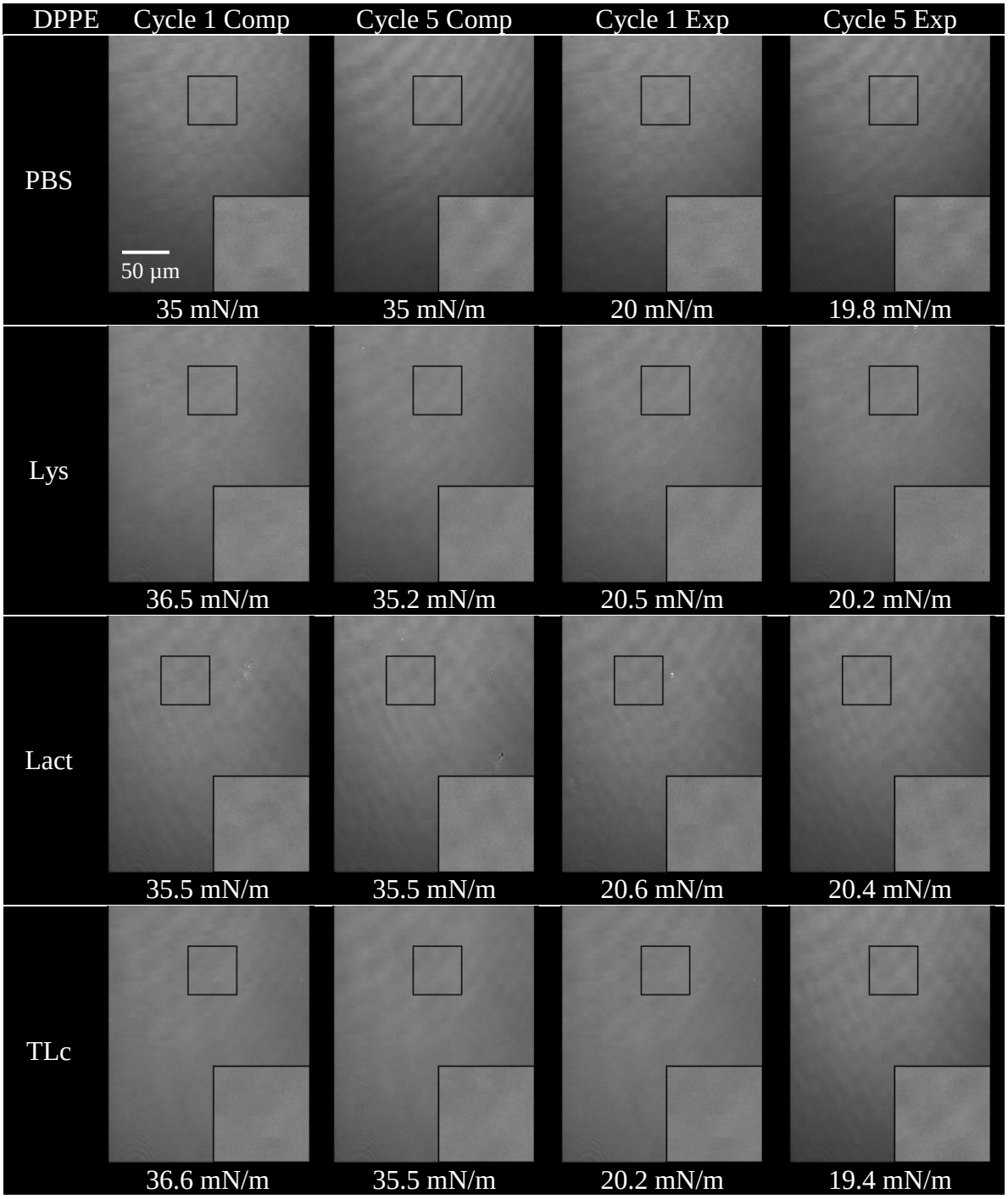

Figure 5.14. BAM images of DPPE during isocycles with no protein (PBS), lysozyme (Lys), lactoferrin (Lact), or tear lipocalin (TLc). For experimental conditions (page 145).

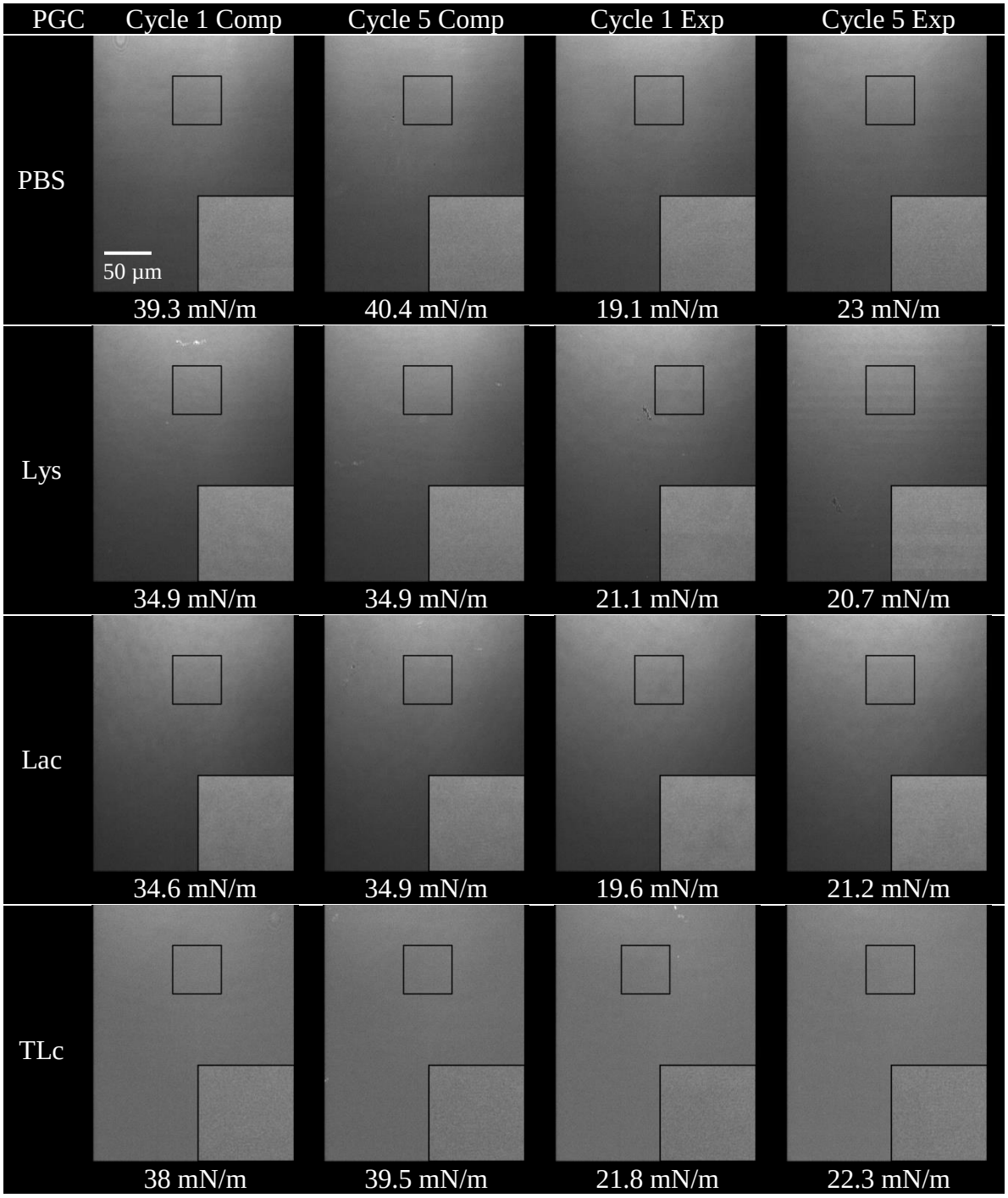

Figure 5.15. BAM images of PGC during isocycles with no protein (PBS), lysozyme (Lys), lactoferrin (Lact), or tear lipocalin (TLc). For experimental conditions (page 145).

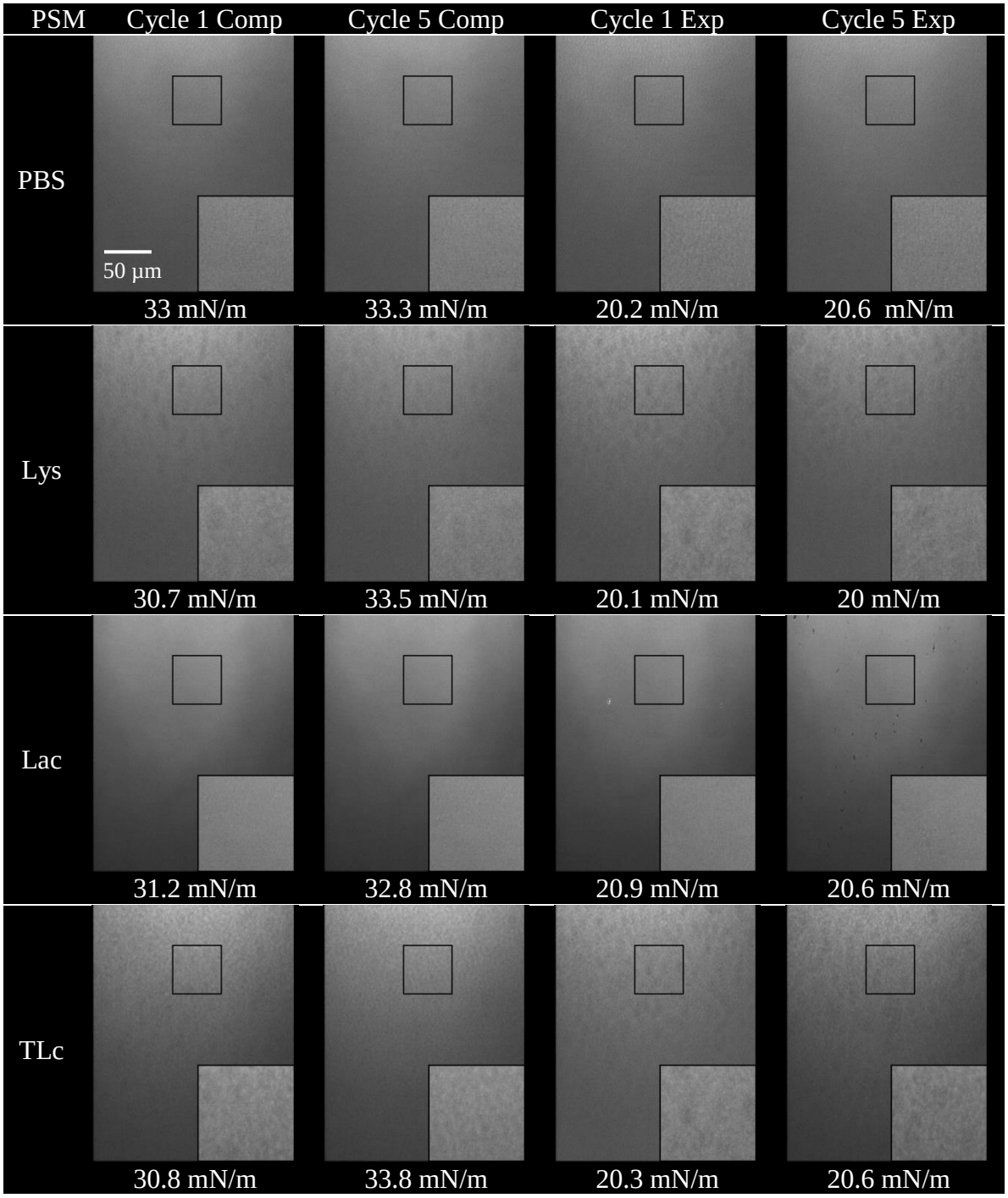

Figure 5.16. BAM images of PSM during isocycles with no protein (PBS), lysozyme (Lys), lactoferrin (Lact), or tear lipocalin (TLc). For experimental conditions (page 145).

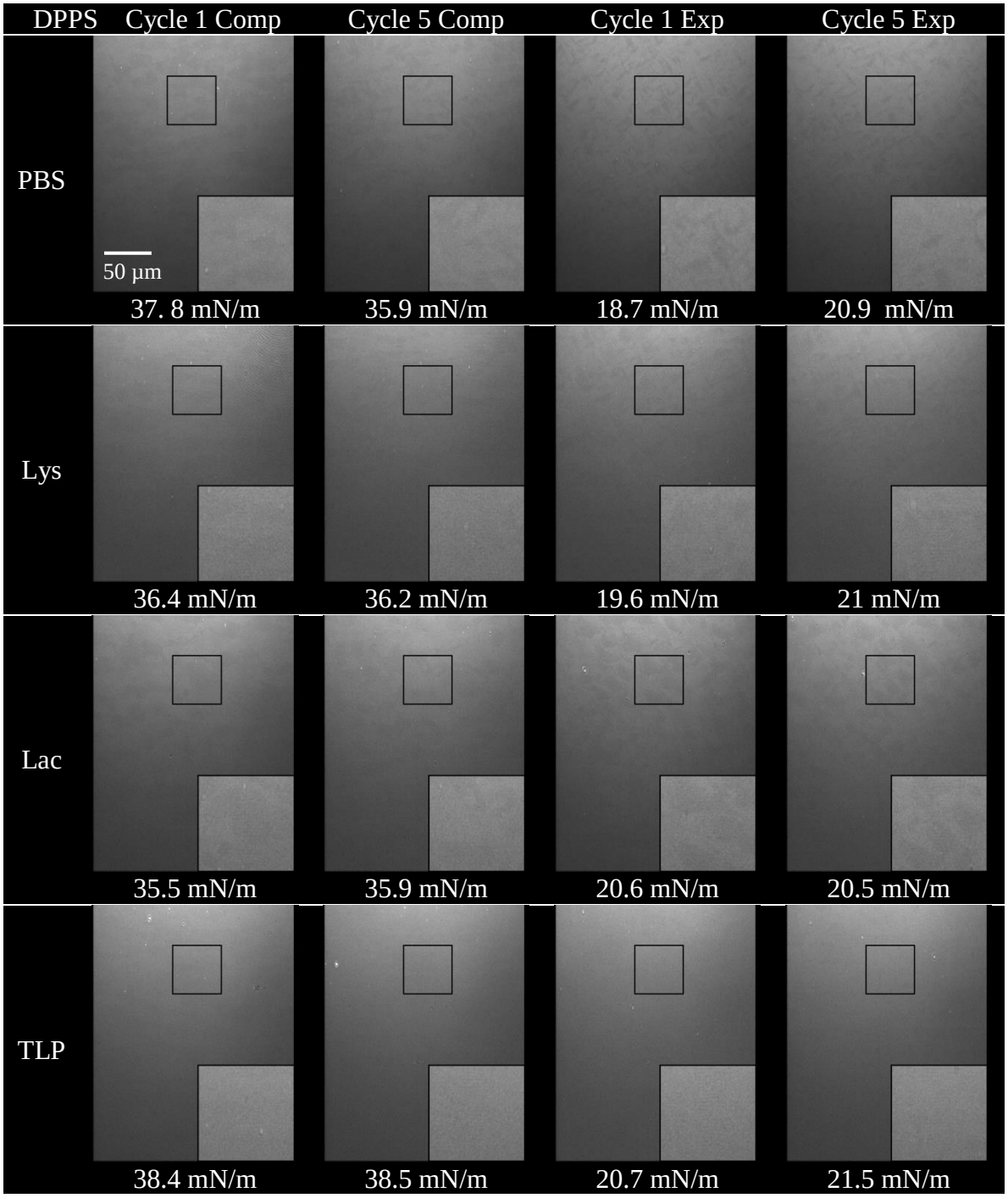

Figure 5.17. BAM images of DPPS during isocycles with no protein (PBS), lysozyme (Lys), lactoferrin (Lact), or tear lipocalin (TLc). For experimental conditions (page 145).

5.2.3.2 Lipid Mixtures with Low Protein Concentrations

As with the pure lipids, the proteins did not appear to affect the lateral organization of the lipid mixtures during cycling (figures 5.18 to 5.20). Again, when comparing images for the first and fifth cycles, near either 35 mN/m or 20 mN/m, no change in domain morphology is seen. Unlike the pure lipids, the LE boundaries are generally much more distinct at 20 mN/m then at 35 mN/m. Some large contaminates were visible for the DPPS (-) mixture (figure 5.18).

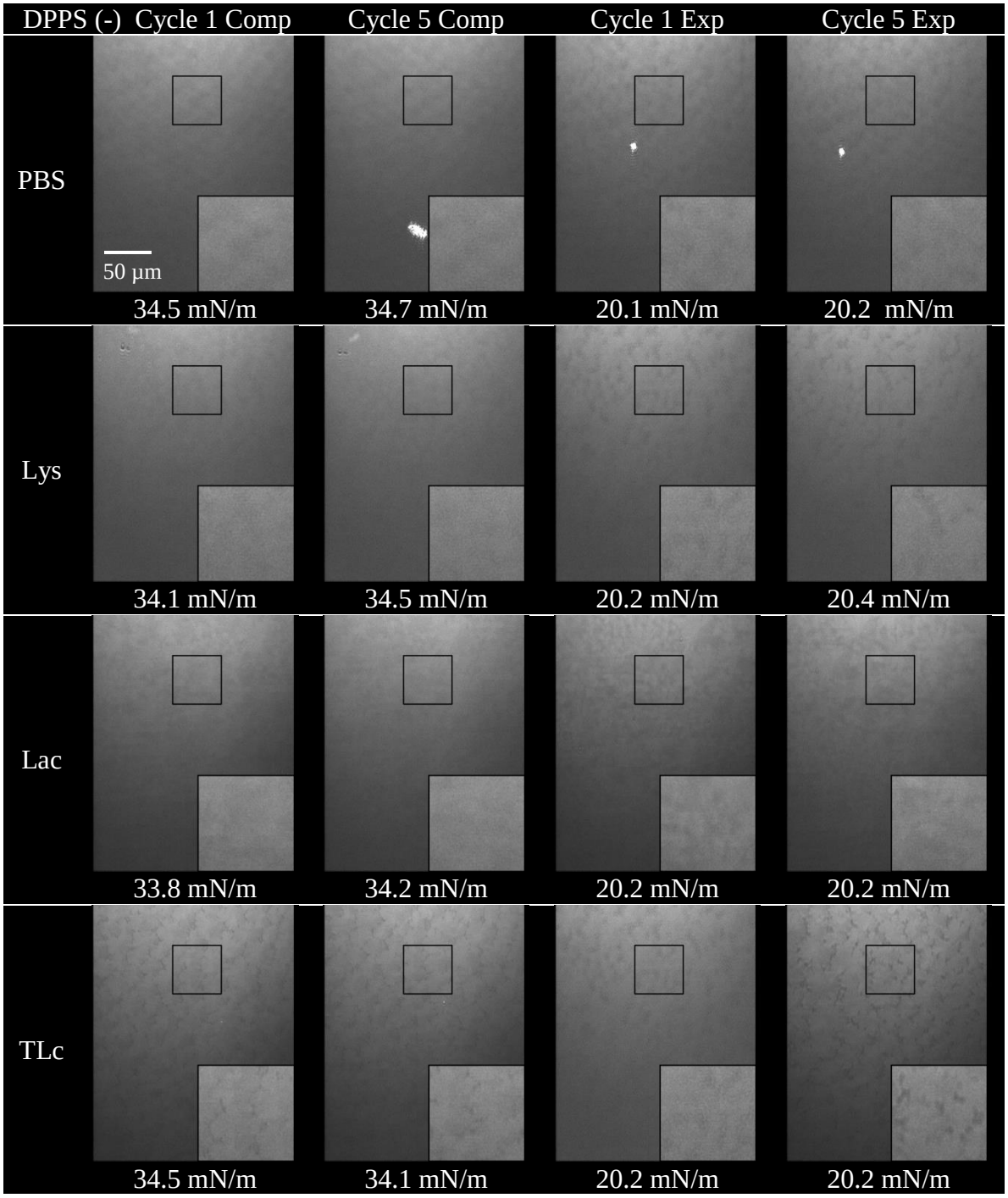

Figure 5.18. BAM images of DPPS (-) during isocycles with no protein (PBS), lysozyme (Lys), lactoferrin (Lact), or tear lipocalin (TLc). For experimental conditions (page 145).

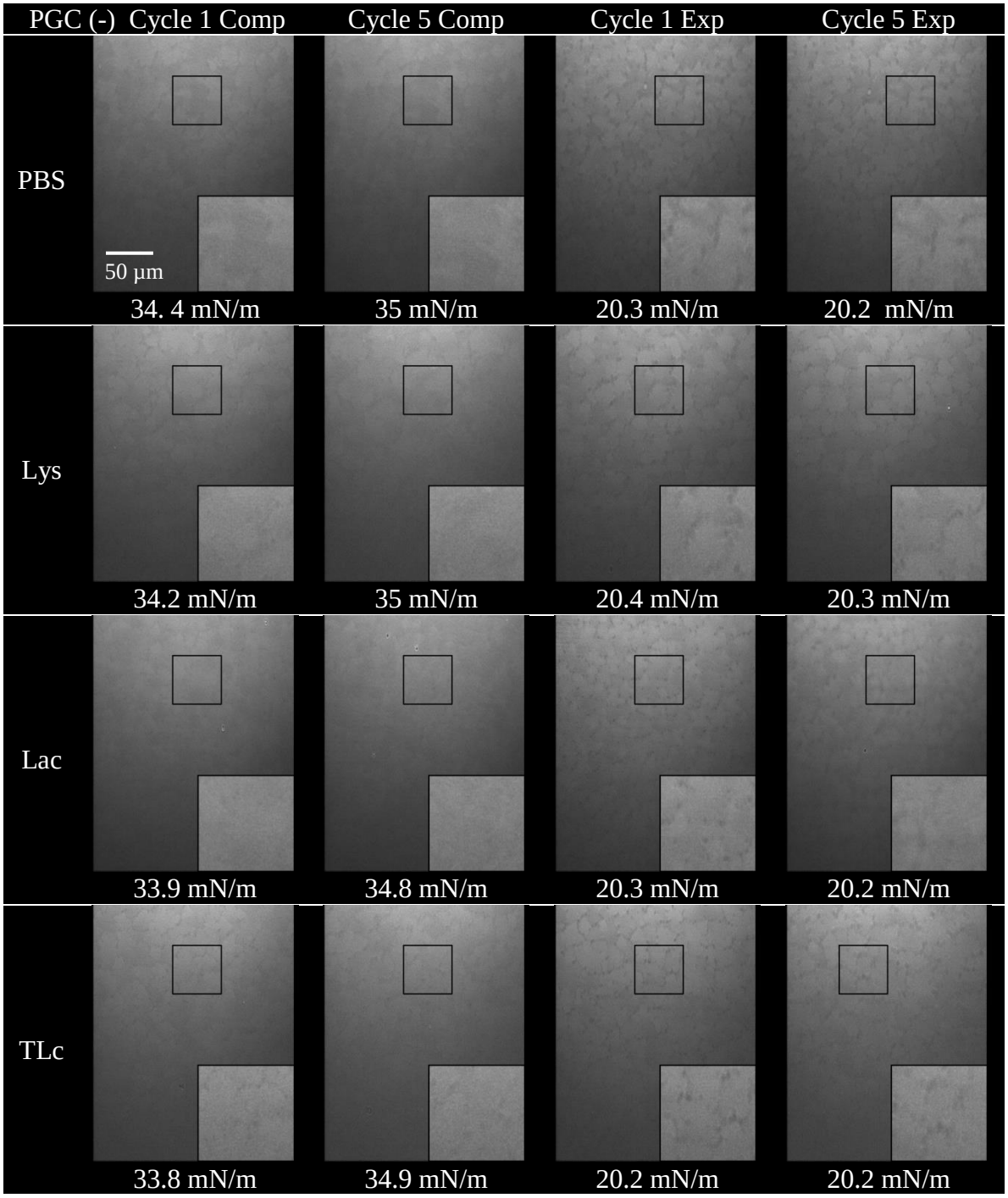

Figure 5.19. BAM images of PGC (-) during isocycles with no protein (PBS), lysozyme (Lys), lactoferrin (Lact), or tear lipocalin (TLc). For experimental conditions (page 145).

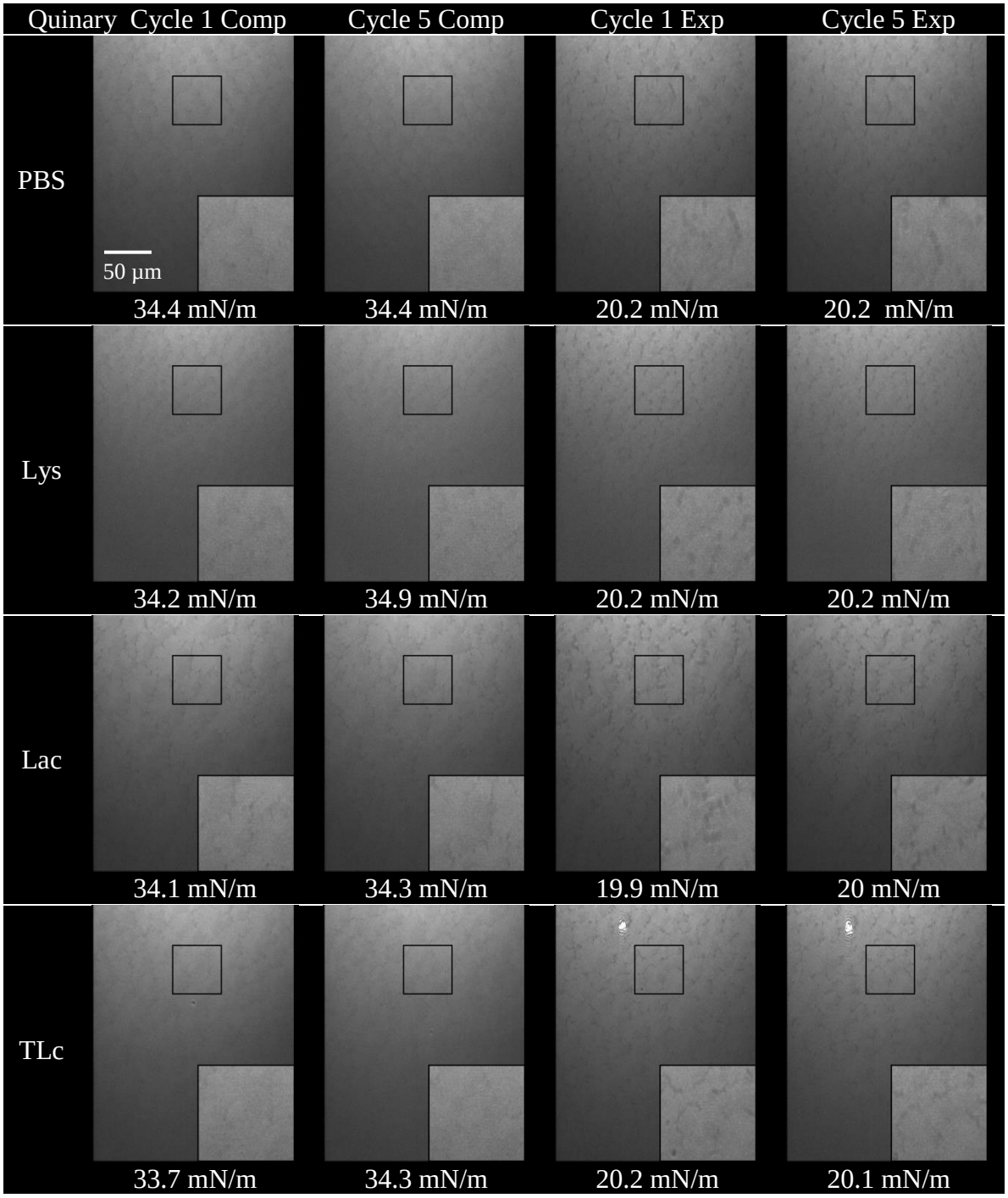

Figure 5.20. BAM images of quinary during isocycles with no protein (PBS), lysozyme (Lys), lactoferrin (Lact), or tear lipocalin (TLc). For experimental conditions (page 145).

5.2.3.3 Quinary Lipid Mixture with Varied Protein Concentrations

Since no changes in lateral organization were observed for the pure lipids or lipid mixtures with low protein concentrations over five cycles, it was decided to continue cycling to see if that would change the lateral organization of the system when the varied protein concentration experiments were run. Injecting 10 mL of buffer or protein solution raised the level of the subphase and made the images brighter, compared to darker images of the 0.5 mL injection for the low protein concentrations. Even over 20 cycles, with concentrations as high as 1 mg/mL, no changes in lateral organization were seen for any system (figures 5.21 and 5.22). Again, this is comparing images for the first and fifth cycles at either 20 mN/m or 35 mN/m. Like the lipid mixtures with low protein concentration, the LE phase became more distinct for all systems near 20 mN/m, and appeared to blur near 35 mN/m.

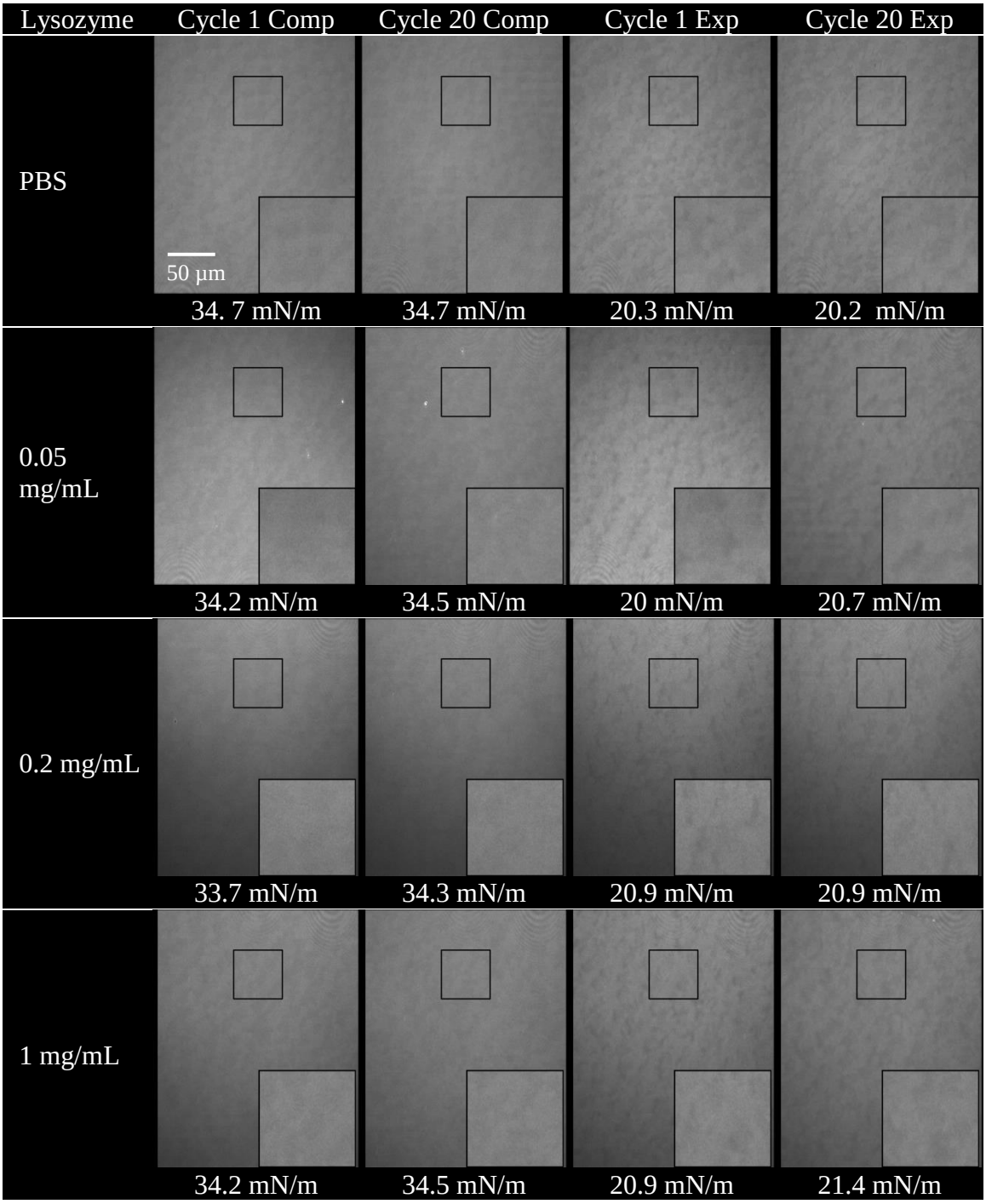

Figure 5.21. BAM images of quinary mixture during isocycles with various lysozyme concentrations. For experimental conditions (page 145).

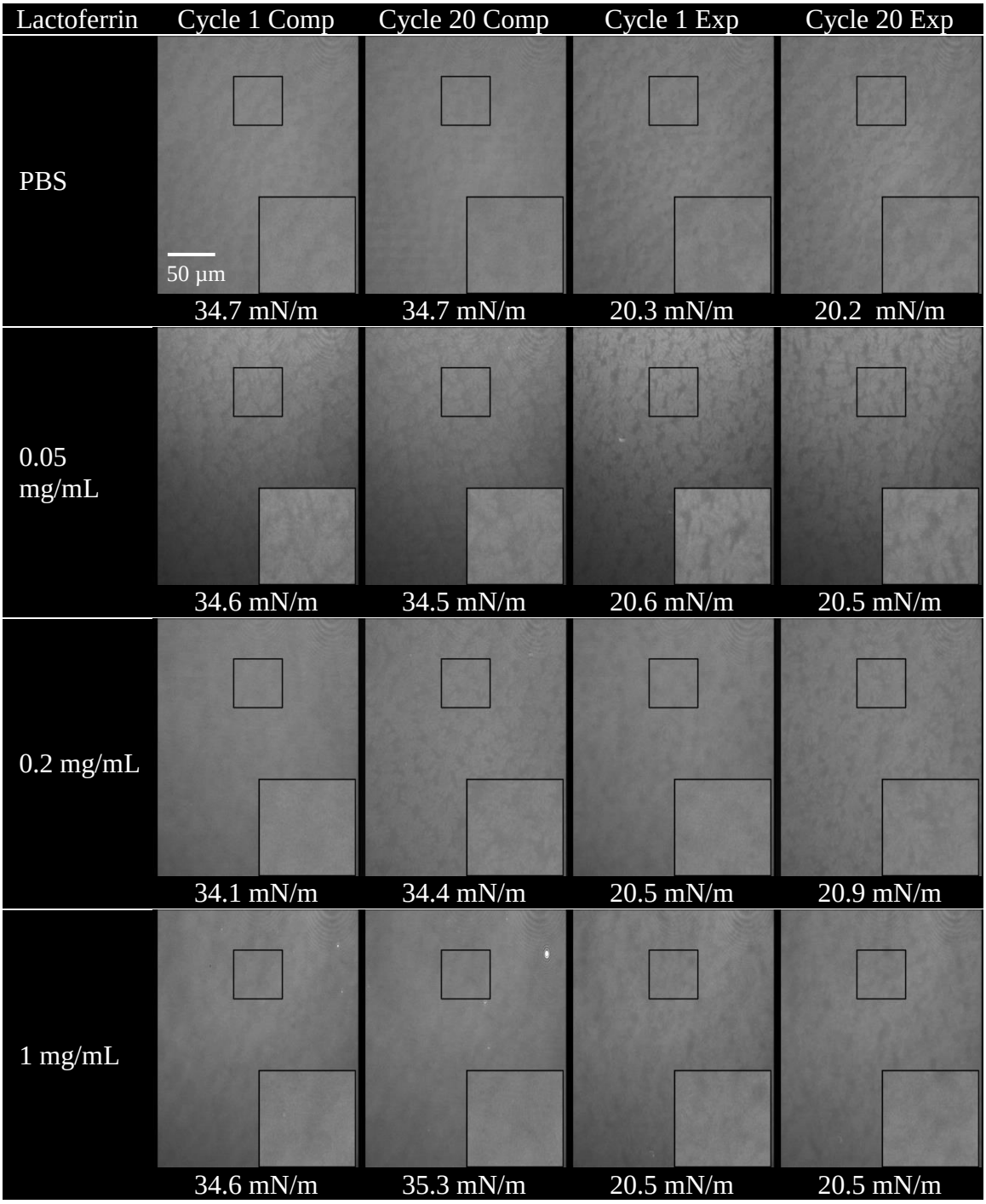

Figure 5.22. BAM images of quinary mixture during isocycles with various lysozyme concentrations. For experimental conditions (page 145).

5.3 Discussion

5.3.1 Constant Pressure Stage

5.3.1.1 Pure Lipids

BAM was used to visualize changes in the lateral organization of lipid monolayers due to the presence of proteins initially injected into the subphase. The bright domains visualized in the images are LC domains [145]. During the pressure control stage, the morphology and growth of LC domains was observed and compared to the literature. DPPC, DPPE, PGC, and PSM have been part of work previously published by Patterson *et al.*, and the domain morphology and growth for all these lipids is identical [154]. DPPC formed multi-lobed structures under common experimental conditions, consistent with Patterson *et al.* and Tae *et al.* [154,159]. Patterson *et al.* showed slightly larger domains with more multi-lobed structures at lower pressures, but ultimately similar shapes emerge in both experiments [154]. The slower compression speed (70 vs 96 cm^2/min for Patterson *et al.*) probably accounts for the difference in the growth rate [178,201,202]. The LC domains had the non-equilibrium fractal-like growth patterns discussed in a review by Nandi and Vollhardt [178]. LC domains formed under quasi-static compression rates are thought to be circular, though this does not appear to have been validated experimentally [201]. Increasing the speed of compression yields bean-like shapes, and the faster compression rate in this experiment yielded the multi-lobed structures observed here [201]. Bean-like domains have been observed to relax to form circular domains over 12 hours [201], but this relaxation was not observed here due to the

short duration of the experiment. Nandi and Vollhardt proposed that when the lipids are compressed quickly, they do not have time to explore enough conformations to reach the lowest energy state [178]. Their initial conformation affected the structures formed during nucleation of LC domains, and continued to have an effect during domain growth [178].

DPPE and PGC formed a homogenous LC phase at low surface pressures, but the growth of the PGC domains happens over a larger range of surface pressures. Regions of LE phase were not observed above 2 mN/m in DPPE, whereas LE phase gaps could still be overserved at 15.2 mN/m for PGC. DPPE has not been imaged with BAM using similar conditions by researchers other than Patterson *et al.*, but low pressure growth of a homogenous LC phase has been observed over a water subphase by Chen et al. [203]. PGC is rarely studied, so no other literature images were available for reference.

Few experiments have been performed with PSM, and so BAM images could not be found beyond results from Patterson *et al.*, which do exhibit the sand-like texture seen here [154]. Kuikka *et al.* and Sakamoto *et al.* did publish epifluorescence images of PSM on a Tris buffered subphase, visualized with fluorescent dyes [160,171]. Those domains appeared to be large, multi-lobed domains, but this is probably the result of different experimental conditions.

DPPS was also consistent with the literature at higher pressures, the same marbled look is present [159,163]. Tae *et al.* was the only study showing images of DPPS at lower

surface pressures, they did have the marbled texture, but there appears to be large LE gaps in the film [159].

5.3.1.2 Mixed Lipids

The DPPS (-) mixture was the only film that had been previously viewed using BAM. The multi-lobed domains are similar to those imaged by Patterson [154], but they were smaller, probably a result of compression speed [178,201,202]. The LC domains for all lipid mixtures formed at low pressures, but the quinary mixture appeared to form at lower pressures than the two quaternary mixtures. The texture of the compressed film near 26 mN/m was similar for all three films.

5.3.2 Constant Area Stage

5.3.2.1 Pure Lipids with Low Protein Concentrations

None of the proteins at subphase concentrations at 0.01 mg/mL seemed to affect DPPC, DPPE, PGC, or DPPS immediately after injection. DPPE and PGC had an amorphous morphology where LC domains are not distinct and so changes could not be observed. DPPC and DPPS initially had a marbled morphology from 20 to 35 mN/m. For DPPC, the LC domains appeared to be less stable with lysozyme and lactoferrin after 30 minutes of incubation, and domains lost some boundary structure. The domain structure for the PBS control and tear lipocalin was not apparent before injection and immediately after injection, so the same effect could not be observed over the incubation. DPPS

appeared to retain its structure for the 30 minute incubation for PBS and lactoferrin, but lost structure with lysozyme and tear lipocalin. This is only partly consistent with the surface pressure decreases observed in chapter four, where a significant surface pressure decrease could only be seen for tear lipocalin, not lysozyme. The trends of surface pressure decreases seen in chapter four hint that tear lipocalin can destabilize all pure lipids, and this was partially confirmed with BAM visualization.

A few bright spots appeared on some images, DPPS for example before and after lipocalin injection. These were contaminants and not protein/lipid clusters formed due to the injection of protein because of their presence before and after injection. The duration of the experiment was long enough to allow environmental contaminants such as dust to settle on the films. These contaminants appeared to move in a continuous direction over the incubation period, indicating that the monolayers experienced a very slow flow despite their rigidity.

The small sand-like LC domains of PSM also remained consistent with PBS and lactoferrin, despite the pressure dropping as low as 13.4 mN/m. Dark patches were visible for PSM before the injection of lysozyme and persisted until the end of the incubation. The same dark patches appeared with PSM 30 minutes after tear lipocalin was injected. These patches seem to be correlated with the extreme surface pressure decline experienced for both systems during BAM imaging. This is likely due to pausing compression to take images during the pressure control stage, changing the rate of compression which is important for domain growth [178,201,202]. Due to the low

pressure drop, lysozyme or lipocalin may have been able to insert. It does not seem that these patches are gaps of LE phase, they are visible and remain roughly the same size even to high surface pressures during cycling. During the course of the varied protein concentration experiments, it was observed that improperly cleaned lysozyme will create large light grey domains, or bright ridges (images not shown). This is different than the dark patches seen here, but this may be due to lysozyme denaturation during cleaning, or that the protein was already present on the surface during lipid deposition. Ultimately, the nature of these patches is unknown.

Unfortunately, few experiments exist that observe the insertion of lysozyme, lactoferrin, or tear lipocalin into pure lipid films using BAM. Most experiments used epifluorescence microscopy, with meibomian lipids at low surface pressures [87,139,193]. Even when insertion of lysozyme has been observed with DPPC, the initial surface pressure for protein injection was 0 mN/m [193]. These differences negate any useful comparison to the present work. Trusova *et al.* examined the effect of HEWL on solid-supported lipid bilayers (SLBs) of egg yolk phosphatidylcholine using total internal reflection fluorescence (TIRF) microscopy [186]. Though this experiment had vast differences with the current work, they did not observe any morphological changes in response to HEWL over 60 minutes of incubation [186].

5.3.2.2 Lipid Mixtures with Proteins

As with the pure lipids, low concentrations of protein did not appear to affect any of the lipid mixtures immediately after injection. The DPPS(-) mixture appeared to generally lose structure for the buffer control and three proteins, suggesting it was a less stable film. The PGC(-) and quinary mixtures appeared more stable for the buffer control and lysozyme, but less so for lactoferrin and tear lipocalin. All three lipid mixtures appeared to be more susceptible to tear lipocalin. This can be correlated with the surface pressure decline in chapter four (page 88) for all three mixtures, but less so for the quinary mixture.

Biologically relevant concentrations of lysozyme, as high as 1 mg/mL, do not appear to change the morphology of the quinary mixture within the 30 minute incubation. The LC boundaries did appear to become less distinct for the lactoferrin system at 0.2 and 1 mg/mL. This would be consistent with the large reduction in compression and expansion moduli observed with 1 mg/mL concentrations of lactoferrin. The loss of morphology varies at concentrations of lactoferrin below 0.05 mg/mL.

In the experiment discussed earlier from Trusova *et al.* regarding SLBs, the clustering of cardiolipin – an anionic lipid – mixed with egg yolk PC (19:1 PC/CL molar ratio) could be seen within minutes of exposure to low levels of HEWL (1.5 ug/mL) [186]. But as stated earlier, this experiment provides little comparison with the current work. Egg yolk PC has a lot of oleic fatty acyl chains so the film is very different from

DPPC [204]. Clustering of cardiolipin was visible because a fluorescent dye was used, and the image resolution was fifteen times that of the BAM images presented here.

5.3.3 Isocycle Stage

5.3.3.1 Pure Lipids with Low Protein Concentrations

With the exception of PSM, none of the pure lipids were affected by low concentrations of protein during cycling. Patterson *et al.* observed that gaps would appear in DPPE monolayers by the fifth compression [155]. Those experiments were different in that they expanded the film to the gas phase during each cycle, and the surface pressure where the instability was observed was 9.8 mN/m, much lower than the tear film surface pressure range [41,42,155]. The dark patches observed in the PSM film with lysozyme and tear lipocalin were retained during cycling. Interestingly, the patches are not as visible for lipocalin near 35 mN/m for the fifth cycle, but they reappear when expanded to 20 mN/m. Over multiple compressions, the film may have been recovering its original lateral organization seen before the pressure drop. It appears that all pure lipids are capable of stable film cycling within the surface pressure range of the tear film, and that this is unaffected by low levels of lysozyme, lactoferrin, and tear lipocalin.

5.3.3.2 Lipid Mixtures with Proteins

Again, none of the proteins at low subphase concentrations appeared to alter the ability for any lipid mixture to undergo repeated compression and expansion, the domain

morphologies remained consistent for 5 cycles. Only DPPS (-) had been previously studied by Patterson *et al.* [155], where the domains grew in size over the 5 cycles, but this was visible only at lower surface pressures.

Due to the ability of all of the lipids to stably cycle during 5 cycles, it was decided to extend the number of cycles to 20 for the varied protein trials. Even with the increased number of cycles, the quinary mixture appeared to lack any defects. The morphology did not change, even with biologically relevant concentrations of lysozyme. In chapter four, it was seen that lactoferrin at 1 mg/mL initially severely decreased the compression and expansion moduli, but these moduli increased after several cycles (page 109) After the constant area stage, the boundaries of the condensed phase were blurred for 0.2 and 1 mg/mL lactoferrin, consistent with lowering of the compression and expansion moduli. The LC phase boundaries did not become more distinct after cycling. So the relaxation of the film could be correlated with condensed phase boundaries becoming less distinct, but the subsequent rigidification of the film after 20 cycles did not appear to reverse this process.

5.4 Conclusions

Condensed phase growth and morphologies of all pure lipids and the DPPS (-) lipid mixture are consistent with literature. The lateral organization of DPPE and PGC was amorphous and variation could not be seen with low concentrations of lysozyme, lactoferrin, or tear lipocalin. For DPPC there was some loss of domain structure after the

30 minute incubation period with 0.01 mg/mL lysozyme and lactoferrin. For DPPS, a similar loss of structure was observed with lysozyme and tear lipocalin. PSM appears to have been destabilized during BAM imaging, preventing a useful conclusion.

The DPPS (-) mixture appeared to be less stable than the PGC (-) or quinary mixtures. All three mixtures were destabilized by low concentrations of lactoferrin and tear lipocalin, especially tear lipocalin. The quinary mixture did not show variation with high lysozyme concentrations. The condensed phase boundaries of the quinary mixture did appear to become blurred with the initial relaxation caused by 0.2 and 1 mg/mL lactoferrin concentrations, but did not regain the distinct boundaries with the rigidification observed over 20 cycles in chapter four.

All films appeared to retain their morphology and stability after film cycling, despite changes observed before cycling began.

Chapter Six: Conclusions and Future Directions

6.1 Summary

The precorneal tear film protects the corneal epithelium from numerous sources of stress and damage, and is essential for high visual acuity as it provides a smooth surface for light entering the eye. This film is primarily water, including ions, but has a wide range of different kinds of lipids and proteins. The lipids appear to self-assemble into a multilayered structure to shield aqueous layer from the external environment. A polar lipid layer provides an interface between the aqueous layer and a thick nonpolar lipid layer. The lipids are thought to increase the surface pressure (lower the surface tension) of the aqueous layer and allow it to spread across the surface of the eye, and also slow evaporation. These characteristics depend on the ability of the lipid film to maintain coverage and stability during repeated blinking. Stability in this case refers to the lipid layer's ability to maintain high surface pressures, so it does not collapse and form dry patches exposing epithelial cells to the air. Experiments regarding the polar lipids identified in the tear film were carried out *in vitro*. DPPC, DPPE, PSM, PGC, and DPPS represent these lipid classes, and are thought to form a monolayer interfacing the aqueous layer with the nonpolar lipids. The exact composition of the polar layer is still not known, so in addition to studying pure lipid monolayers, two quaternary mixtures with biologically relevant ratios were investigated, as well as one quinary mixture combining all lipid classes. Lysozyme, lactoferrin, and tear lipocalin are three major proteins found

in the tear film and have been shown to interact with these some of these lipids and are thought to insert into the lipid layer.

The objective of this study was to assess how the major tear film proteins affect the dynamics of the polar lipid films, and so they were injected into the subphase beneath lipid monolayers in a Langmuir trough. According to the literature, the resting tear film surface pressure appears to be 26 to 29 mN/m [41], but it has been shown that it may reach as high as 37 mN/m when compressed during a blink [42]. These surface pressures were used in these experiments. First, lipid-only films were initially held at 26 mN/m where buffer was injected into the subphase, to provide a baseline for comparison with protein interactions later on. These showed that all lipid films experienced a decrease in surface pressure after the injection of buffer and a 30 minute incubation period. DPPE was the most stable during incubation, while PGC was the least. Lipid mixtures all exhibited similar stability to PGC, the quinary mixture appeared to be slightly more stable, but not significantly so. To mimic blinking, the lipid films were cycled between 20 and 35 mN/m five times. All lipid films were highly reversible as the compression and expansion isotherms nearly overlapped. All pure lipids had large compression and expansion moduli during cycling compared to literature values, indicating this experiment greatly rigidified the films. This may be indicative of *in vivo* rigidity, where the polar lipid film is continually in use.

Low concentrations of lysozyme, lactoferrin, and tear lipocalin were injected into the subphase of the pure lipid and mixed lipid monolayers. No insertion was seen for any

lipid/protein combination as surface pressures continued to decrease. Results suggested that low concentrations of tear lipocalin may destabilize monolayers of pure lipids and quaternary lipid mixtures during the 30 minute incubation period, but the quinary lipid mixture seemed to be somewhat protected. The destabilization effect needs to be validated as it was only significant for pure DPPE and the quaternary mixture lacking DPPS, and was only indicative with most other films. Low levels of lactoferrin or lysozyme did not destabilize the lipid films. High levels of lysozyme and lactoferrin were tested with the quinary lipid mixture, and no destabilization was seen. None of the proteins changed the highly reversible nature of any film, even biologically relevant concentrations of lysozyme and lactoferrin tested with the quinary mixture. Low concentrations of any protein did not appear to change the compression or expansion moduli of the films during cycling. High levels of lysozyme and lactoferrin were tested with the quinary lipid mixture, and fluidization of the quinary mixture was seen, especially with lactoferrin.

Brewster Angle Microscopy (BAM) was used to validate these results. For DPPE and PGC, the films were amorphous in the tear film surface pressure range, and so changes could not be detected. DPPC, PSM, and DPPS did have enough structure where changes were sometimes observed. Proteins did not drastically alter the morphology of liquid condensed domains at low concentrations, or with biologically relevant concentrations of lactoferrin and lysozyme with the quinary lipid mixture. Some loss of domain structure could be observed with DPPC with lysozyme or lactoferrin, and DPPS

with lysozyme or tear lipocalin. This was seen as a blurring of LC boundaries. The loss of structure for DPPS and tear lipocalin did correlate with the earlier trend in surface pressure decrease, which itself was not significant. The quaternary mixture lacking DPPS generally appeared to lose structure regardless of the absence or presence of proteins, while the quaternary mixture lacking PGC and the quinary mixture only lost structure with lysozyme and lactoferrin. This was especially apparent with subphase concentrations above 0.2 mg/mL. This correlated with the decreased rigidity of the quinary film seen earlier with biologically relevant concentrations of lysozyme and lactoferrin. No defects were seen during film cycling, suggesting all films could maintain stability regardless of the presence or absence of the proteins.

6.2 Conclusions

Differences between the rigidity of pure lipids were evident, but lipid mixtures had similar characteristics. Various lipid mixtures may have similar if not equal stability, but they are equally capable of maintaining stability during blinking within the normal tear film surface pressure range. This may indicate that different lipid mixtures could serve a similar function. Overall, it does seem that lysozyme and lactoferrin may increase the elasticity of polar lipid films, even before insertion. This may indicate that proteins help the polar layer to spread by reducing the rigidity of the film, and perhaps work to create an appropriate balance between a highly rigid film capable providing a solid barrier, and a more fluid film capable of spreading.

6.3 Future Directions

Little is known about the dynamics of polar lipids and proteins experienced in the tear film *in vivo*, and there are no experimental methodologies yet available to address this. For the foreseeable future, we will have to rely on further *in vitro* experiments to help investigate these interactions. There are many avenues available for continued research. Most published studies of these lipids and proteins often allow protein insertion in the gas phase, which greatly changes the surface pressure isotherms compared to the more biologically relevant surface pressure range used here. Continued studies of these interactions at relevant surface pressures may provide additional insight.

Changes in rigidity or long term stability during cycling could be used to see if the loss of a particular polar lipid class could be correlated with dry eye syndrome. More investigations of relevant pure lipids and lipid mixtures, including simpler mixtures, are required. These experiments could also include extended cycling to see how long these films could maintain their stability. All of the pure lipids and mixtures displayed no defects while being cycled for five blinks, and the quinary mixture displayed no defects when cycled twenty times. It would be interesting to increase the number of cycles for the other lipid films to see if they have the same long term stability as the quinary mixture, and if this would correlate with polar lipid abnormalities in dry eye. Also, the lipid mixtures had similar expansion and compression moduli, while pure lipids had variable

rigidity, some more or less rigid than the mixtures. If specific lipid classes are removed from these mixtures, their rigidity may change.

As stated in a recent review by Georgiev, Eftimov, and Yokoi, one of the primary challenges with tear film research is assessing how the results of *in vitro* biophysical experiments relate to the lipid layer *in vivo* [205] . So it is difficult to assess the biological relevance of the experiments presented here. To bridge the gap, the authors propose combining *in vitro* studies and *in vivo* studies [205]. We have seen here and that pure lipids perform differently, and previous experiments by Patterson *et al.* have shown that different lipids can alter the behavior of lipid mixtures [154,155]. This may be assessed *in vivo* by spiking the tear film of volunteers with a specific lipid class, to see if tear breakup time, or interferometry images can be altered. Proteins present more of a challenge because lysozyme, lactoferrin, and tear lipocalin are highly abundant. There have been knock-out mice that cannot express lysozyme or lactoferrin, which are used to assess the impact on immune function [206,207] , but no tear lipocalin knock-out model has been reported. It may be possible to test tear breakup time and look at interferometry images with these mice to test effect on the lipid layer *in vivo*.

The composition of polar lipid layer in the tear film is still unknown. As new information becomes available, the experiments presented here can be repeated to study the performance of newly discovered lipid mixtures. This should also include the addition of (O-acyl)-ω-hydroxy fatty acids (OAHFAs) as they have been found to be a major polar lipid class in meibomian secretions, but comparable to the concentration of PC lipids in

whole tear samples [5,47,72,84]. The ability of OAHFAs to maintain stability in the range of surface pressures found in the tear film has not yet been examined. As more data is gathered about the characteristics of the polar lipid layer in the tear film, the lipid mixtures presented in this thesis can be evaluated for their potential as biomimetics. The quinary mixture has already behaved similarly to whole tear lipids in the presence of biologically relevant concentrations of lysozyme. If further validation could be carried out, these lipid mixtures could be used to assess the impact of airborne contaminants and new drug delivery systems, and possibly prevent the unnecessary use of animal models if severe disruption is evident.

Biologically relevant concentrations of lysozyme and lactoferrin displayed the most notable effects on the quinary mixture in this study. It is of interest to know if these concentrations would have similar effects on pure lipids and other lipid mixtures, and to identify specific lipid classes responsible for the interactions. Also, the effects on the polar lipid layer by protein concentrations higher than those found naturally could be assessed. This data may be used to decide whether high concentrations of proteins should be investigated as a potential therapy for eye infections. Recombinant human lysozyme is fairly inexpensive, but recombinant lactoferrin is costly, so new methods would be necessary to conserve protein. This may be accomplished by using low protein concentrations and extending the duration of the experiments to see if protein insertion was possible at larger time scales.

Longer duration experiments could be used with low concentrations of human recombinant tear lipocalin. The role of tear lipocalin remains unknown. It may have the ability to destabilize lipid films, but this needs validation. A longer duration of incubation may allow for statistically significant results regarding the loss of surface pressure. This destabilization would be undesirable, so perhaps specific lipid mixtures, like the quinary mixture, are necessary for intrinsic protection. Moreover, what would the effects on the film integrity be if significant destabilization occurs before cycling.

To determine the biological significance of these *in vitro* experiments, more understanding of the polar lipid layer is necessary. Little is known about the effects of polar lipid composition on dry eye syndrome. Shine and McCully reported that deficiencies in PE and SM may be involved with Keratoconjunctivitis Sicca (KCS) [56]. This work was published in 1998 with meibomian secretions, and the current understanding regarding the origin of polar lipids in the tear film has changed. Researchers are still trying to work out the composition of the polar layer in healthy individuals, let alone what the differences in patients with dry eye. As more of this information becomes available, these proposed biophysical studies can be used as an additional line of evidence to validate polar lipid abnormalities if they are present in disease states.

Regarding lipid-protein interactions, the recently published TFOS DEWS II Tear Film Report, which is a review of the role of the tear film in dry eye disease (DED), called for additional studies to uncover the role of proteins within the lipid layer [208]. It

proposes current literature about the interactions is confusing, that lipid-protein interactions may be necessary to reduce evaporation of the aqueous layer, but that proteins can also disruptive to the function of meibomian secretions [208]. The studies cited involve meibomian films, so understanding the role of polar lipids regarding proteins may provide clarity regarding this problem.

References

[1] E. King-Smith, B. Fink, R. Hill, K. Koelling, J. Tiffany, The thickness of the tear film, Curr. Eye Res., 29 (2004) 357–368.

[2] L. Zhou, R.W. Beuerman, Tear analysis in ocular surface diseases, Prog. Retin. Eye Res., 31 (2012) 527–550.

[3] R.J. Braun, Dynamics of the Tear Film, Annu. Rev. Fluid Mech., 44 (2012) 267–297.

[4] F. Paulsen, G. Langer, W. Hoffmann, M. Berry, Human lacrimal gland mucins, Cell Tissue Res., 316 (2004) 167–177.

[5] S.H.J. Brown, C.M.E. Kunnen, E. Duchoslav, N.K. Dolla, M.J. Kelso, E.B. Papas, P. Lazon de la Jara, M.D.P. Willcox, S.J. Blanksby, T.W. Mitchell, A comparison of patient matched meibum and tear lipidomes, Invest. Ophthalmol. Vis. Sci., 54 (2013) 7417–7424.

[6] J.V. Jester, N. Nicolaides, R.E. Smith, Meibomian gland studies: histologic and ultrastructural investigations, Invest. Ophthalmol. Vis. Sci., 20 (1981) 537–547.

[7] E. Wolff, The muco-cutaneous junction of the lidmargin and the distribution of the tear fluid, Trans Am Ophthalmol Soc, 66 (1946) 291–308.

[8] J. Tiffany, Physiological functions of the meibomian glands, Prog. Retin. Eye Res., 14 (1995) 47–74.

[9] N. Ehlers, CHAPTER I: Introduction, Acta Ophthalmol. (Copenh.), 43 (1965) 11–18.

[10] S.C. Pflugfelder, Z. Liu, D. Monroy, D.Q. Li, M.E. Carvajal, S.A. Price-Schiavi, N. Idris, A. Solomon, A. Perez, K.L. Carraway, Detection of sialomucin complex (MUC4) in human ocular surface epithelium and tear fluid, Invest. Ophthalmol. Vis. Sci., 41 (2000) 1316–1326.

[11] I.K. Gipson, P. Argüeso, Role of mucins in the function of the corneal and conjunctival epithelia, Int. Rev. Cytol., 231 (2003) 1–49.

[12] F. Mantelli, P. Argüeso, Functions of ocular surface mucins in health and disease, Curr. Opin. Allergy Clin. Immunol., 8 (2008) 477–483.

[13] I.K. Gipson, Distribution of mucins at the ocular surface, Exp. Eye Res., 78 (2004) 379–388.

[14] F. Mantelli, J. Mauris, P. Argüeso, The ocular surface epithelial barrier and other mechanisms of mucosal protection: from allergy to infectious diseases, Curr. Opin. Allergy Clin. Immunol., 13 (2013) 563–568.

[15] B. Walcott, The Lacrimal Gland and Its Veil of Tears, News Physiol. Sci. Int. J. Physiol. Prod. Jointly Int. Union Physiol. Sci. Am. Physiol. Soc., 13 (1998) 97–103.

[16] K. Tsubota, Tear dynamics and dry eye, Prog. Retin. Eye Res., 17 (1998) 565–596.

[17] D.K. Sen, G.S. Sarin, Tear glucose levels in normal people and in diabetic patients, Br. J. Ophthalmol., 64 (1980) 693–695.

[18] G.A. de Souza, L.M.F. Godoy, M. Mann, Identification of 491 proteins in the tear fluid proteome reveals a large number of proteases and protease inhibitors, Genome Biol., 7 (2006) R72.
[19] L. Zhou, S.Z. Zhao, S.K. Koh, L. Chen, C. Vaz, V. Tanavde, X.R. Li, R.W. Beuerman, In-depth analysis of the human tear proteome, J. Proteomics, 75 (2012) 3877–3885.
[20] B. Glasgow, Tissue expression of lipocalins in human lacrimal and von Ebner's glands: colocalization with lysozyme, Graefes Arch. Clin. Exp. Ophthalmol., 233 (1995) 513–522.
[21] U. Stahl, M. Willcox, F. Stapleton, Osmolality and tear film dynamics: Osmolality and tear film dynamics, Clin. Exp. Optom., 95 (2012) 3–11.
[22] J.P. Gilbard, Human Tear Film Electrolyte Concentrations in Health and Dry-Eye Disease:, Int. Ophthalmol. Clin., 34 (1994) 27–36.
[23] N.J. Van Haeringen, Clinical biochemistry of tears, Surv. Ophthalmol., 26 (1981) 84–96.
[24] L.G. Carney, Human Tear pH: Diurnal Variations, Arch. Ophthalmol., 94 (1976) 821.
[25] K.B. Green-Church, I. Butovich, M. Willcox, D. Borchman, F. Paulsen, S. Barabino, B.J. Glasgow, The International Workshop on Meibomian Gland Dysfunction: Report of the Subcommittee on Tear Film Lipids and Lipid-Protein Interactions in Health and Disease, Invest. Ophthalmol. Vis. Sci., 52 (2011) 1979–1993.
[26] G. van Meer, D.R. Voelker, G.W. Feigenson, Membrane lipids: where they are and how they behave, Nat. Rev. Mol. Cell Biol., 9 (2008) 112–124.
[27] J.P. McCulley, W. Shine, A compositional based model for the tear film lipid layer, Trans. Am. Ophthalmol. Soc., 95 (1997).
[28] L.L.M. van Deenen, Some Structural and Dynamic Aspects of Lipids in Biological Membranes, Ann. N. Y. Acad. Sci., 137 (1966) 717–730.
[29] J.M. Boggs, Intermolecular hydrogen bonding between lipids: influence on organization and function of lipids in membranes, Can. J. Biochem., 58 (1980) 755–770.
[30] H. Möhwald, Phospholipid monolayers, in: R. Lipowsky, E. Sackmann (Eds.), Struct. Dyn. Membr. Cells Vesicles, Elsevier B.V., Amsterdam, 1995: pp. 161–211.
[31] M.C. Phillips, D. Chapman, Monolayer characteristics of saturated 1,2-diacyl phosphatidylcholines (lecithins) and phosphatidylethanolamines at the air-water interface, Biochim. Biophys. Acta Biomembr., 163 (1968) 301–313.
[32] L. Salem, The Role of Long-Range Forces in the Cohesion of Lipoproteins, Can. J. Biochem. Physiol., 40 (1962) 1287–1298.
[33] R.A. Demel, W.S.M. Geurts van Kessel, L.L.M. van Deenen, The properties of polyunsaturated lecithins in monolayers and liposomes and the interactions of

these lecithins with cholesterol, Biochim. Biophys. Acta Biomembr., 266 (1972) 26–40.
[34] A. Seelig, J. Seelig, Effect of a single cis double bond on the structure of a phospholipid bilayer, Biochemistry (Mosc.), 16 (1977) 45–50.
[35] F. Miano, X. Zhao, J.R. Lu, J. Penfold, Coadsorption of Human Milk Lactoferrin into the Dipalmitoylglycerolphosphatidylcholine Phospholipid Monolayer Spread at the Air/Water Interface, Biophys. J., 92 (2007) 1254–1262.
[36] N. Efron, G. Young, N.A. Brennan, Ocular surface temperature, Curr. Eye Res., 8 (1989) 901–906.
[37] R.G. Linton, D.H. Curnow, W.J. Riley, The Meibomian Glands: An Investigation into the Secretion and Some Aspects of the Physiology, Br. J. Ophthalmol., 45 (1961) 718–723.
[38] N. Nicolaides, Skin lipids II Lipid class composition of samples from various species and anatomical sites, J. Am. Oil Chem. Soc., 42 (1965) 691–702.
[39] S.I. Brown, D.G. Dervichian, The oils of the meibomian glands Physical and surface characteristics, Arch. Ophthalmol. Chic. Ill 1960, 82 (1969) 537–540.
[40] B.L. Ong, J.R. Larke, Meibomian gland dysfunction: some clinical, biochemical and physical observations, Ophthalmic Physiol. Opt. J. Br. Coll. Ophthalmic Opt. Optom., 10 (1990) 144–148.
[41] B. Nagyova, J.M. Tiffany, Components responsible for the surface tension of human tears, Curr. Eye Res., 19 (1999) 4–11.
[42] B. Yañez-Soto, M.J. Mannis, I.R. Schwab, J.Y. Li, B.C. Leonard, N.L. Abbott, C.J. Murphy, Interfacial phenomena and the ocular surface, Ocul. Surf., 12 (2014) 178–201.
[43] T.F. Svitova, M.C. Lin, Dynamic interfacial properties of human tear-lipid films and their interactions with model-tear proteins in vitro, Adv. Colloid Interface Sci., 233 (2016) 4–24.
[44] F.J. Holly, Formation and rupture of the tear film, Exp. Eye Res., 15 (1973) 515–525.
[45] N. Ehlers, Chapter V: On the Lid Margin, the Meibomian Glands and Their Secretion, Acta Ophthalmol. (Copenh.), 43 (1965) 67–75.
[46] N. Nicolaides, J.K. Kaitaranta, T.N. Rawdah, J.I. Macy, F.M. Boswell, R.E. Smith, Meibomian gland studies: comparison of steer and human lipids, Invest. Ophthalmol. Vis. Sci., 20 (1981) 522–536.
[47] S.M. Lam, L. Tong, X. Duan, A. Petznick, M.R. Wenk, G. Shui, Extensive characterization of human tear fluid collected using different techniques unravels the presence of novel lipid amphiphiles, J. Lipid Res., 55 (2014) 289–298.
[48] D.A. Dartt, Formation and Function of the Tear Film, in: L.A. Levin, P.L. Kaufman (Eds.), Adlers Physiol. Eye Clin. Appl., 11th ed, Saunders/Elsevier, Edinburgh ; New York, 2011: pp. 350–362.
[49] A.J. Bron, J.M. Tiffany, S.M. Gouveia, N. Yokoi, L.W. Voon, Functional aspects of the tear film lipid layer, Exp. Eye Res., 78 (2004) 347–360.

[50] T.J. Millar, B.S. Schuett, The real reason for having a meibomian lipid layer covering the outer surface of the tear film – A review, Exp. Eye Res., 137 (2015) 125–138.
[51] J.T. Saville, Z. Zhao, M.D.P. Willcox, S.J. Blanksby, T.W. Mitchell, Detection and Quantification of Tear Phospholipids and Cholesterol in Contact Lens Deposits: The Effect of Contact Lens Material and Lens Care Solution, Invest. Ophthalmol. Vis. Sci., 51 (2010) 2843–2851.
[52] J.S. Andrews, Human tear film lipids I Composition of the principal non-polar component, Exp. Eye Res., 10 (1970) 223–227.
[53] C.C. Cory, W. Hinks, J.L. Burton, S. Shuster, Meibomian gland secretion in the red eyes of rosacea, Br. J. Dermatol., 89 (1973) 25–27.
[54] J.M. Tiffany, Individual variations in human meibomian lipid composition, Exp. Eye Res., 27 (1978) 289–300.
[55] N. Nicolaides, E.C. Ruth, Unusual fatty acids in the lipids of steer and human meibomian gland excreta, Curr. Eye Res., 2 (1982) 93–98.
[56] W.E. Shine, J.P. McCulley, Keratoconjunctivitis sicca associated with meibomian secretion polar lipid abnormality, Arch. Ophthalmol. Chic. Ill 1960, 116 (1998) 849–852.
[57] A. Rohit, F. Stapleton, S.H.J. Brown, T.W. Mitchell, M.D.P. Willcox, Comparison of Tear Lipid Profile among Basal, Reflex, and Flush Tear Samples:, Optom. Vis. Sci., 91 (2014) 1391–1395.
[58] A. Robciuc, A.H. Rantamäki, M. Jauhiainen, J.M. Holopainen, Lipid-modifying enzymes in human tear fluid and corneal epithelial stress response, Invest. Ophthalmol. Vis. Sci., 55 (2014) 16–24.
[59] N.J. van Haeringen, E. Glasius, Cholesterol in human tear fluid, Exp. Eye Res., 20 (1975) 271–274.
[60] A.W. Dean, B.J. Glasgow, Mass Spectrometric Identification of Phospholipids in Human Tears and Tear Lipocalin, Investig. Opthalmology Vis. Sci., 53 (2012) 1773.
[61] J.C. Wright, G.E. Meger, A review of the schirmer test for tear production, Arch. Ophthalmol., 67 (1962) 564–565.
[62] L. Cwiklik, Tear film lipid layer: A molecular level view, Biochim. Biophys. Acta Biomembr., 1858 (2016) 2421–2430.
[63] S. Mishima, D.M. Maurice, The oily layer of the tear film and evaporation from the corneal surface, Exp. Eye Res., 1 (1961) 39–45.
[64] W. Mathers, Evaporation from the ocular surface, Exp. Eye Res., 78 (2004) 389–394.
[65] A.H. Rantamaki, M. Javanainen, I. Vattulainen, J.M. Holopainen, Do lipids retard the evaporation of the tear fluid?, Invest. Ophthalmol. Vis. Sci., 53 (2012) 6442–6447.

[66] P. Kulovesi, J. Telenius, A. Koivuniemi, G. Brezesinski, I. Vattulainen, J.M. Holopainen, The impact of lipid composition on the stability of the tear fluid lipid layer, Soft Matter, 8 (2012) 5826–5834.
[67] A.D. Pucker, K.M. Haworth, The presence and significance of polar meibum and tear lipids, Ocul. Surf., 13 (2015).
[68] A.D. Pucker, K.M. Haworth, Authors' Response, Ocul. Surf., 13 (2015) 179–180.
[69] G.A. Georgiev, Controversies Regarding the Role of Polar Lipids in Human and Animal Tear Film Lipid Layer, Ocul. Surf., 13 (2015) 176–178.
[70] A.D. Pucker, J.J. Nichols, Analysis of meibum and tear lipids, Ocul. Surf., 10 (2012) 230–250.
[71] J.P. McCulley, W.E. Shine, Eyelid disorders: the meibomian gland, blepharitis, and contact lenses, Eye Contact Lens, 29 (2003) S93-5; discussion S115-8, S192-4.
[72] S.M. Lam, L. Tong, S.S. Yong, B. Li, S.S. Chaurasia, G. Shui, M.R. Wenk, Meibum Lipid Composition in Asians with Dry Eye Disease, PLoS ONE, 6 (2011) e24339.
[73] A.H. Rantamäki, T. Seppänen-Laakso, M. Oresic, M. Jauhiainen, J.M. Holopainen, Human Tear Fluid Lipidome: From Composition to Function, PLoS ONE, 6 (2011) e19553.
[74] I.A. Butovich, E. Uchiyama, M.A.D. Pascuale, J.P. McCulley, Liquid Chromatography–Mass Spectrometric Analysis of Lipids Present in Human Meibomian Gland Secretions, Lipids, 42 (2007) 765–776.
[75] I.A. Butovich, E. Uchiyama, J.P. McCulley, Lipids of human meibum: mass-spectrometric analysis and structural elucidation, J. Lipid Res., 48 (2007) 2220–2235.
[76] K.M. Saari, V. Aho, V. Paavilainen, T.J. Nevalainen, Group II PLA(2) content of tears in normal subjects, Invest. Ophthalmol. Vis. Sci., 42 (2001) 318–320.
[77] B.D. Sullivan, J.E. Evans, M.R. Dana, D.A. Sullivan, Influence of aging on the polar and neutral lipid profiles in human meibomian gland secretions, Arch. Ophthalmol. Chic. Ill 1960, 124 (2006) 1286–1292.
[78] D. Borchman, G.N. Foulks, M.C. Yappert, Confirmation of Changes in Human Meibum Lipid Infrared Spectra with Age Using Principal Component Analysis, Curr. Eye Res., 35 (2010) 778–786.
[79] S.H.J. Brown, C.M.E. Kunnen, E.B. Papas, P. Lazon de la Jara, M.D.P. Willcox, S.J. Blanksby, T.W. Mitchell, Intersubject and Interday Variability in Human Tear and Meibum Lipidomes: A Pilot Study, Ocul. Surf., 14 (2016) 43–48.
[80] K.-C. Yoon, B.-Y. Song, M.-S. Seo, Effects of Smoking on Tear Film and Ocular Surface, Korean J. Ophthalmol., 19 (2005) 18.
[81] B. Maggio, M.L. Fanani, C.M. Rosetti, N. Wilke, Biophysics of sphingolipids II Glycosphingolipids: An assortment of multiple structural information transducers at the membrane surface, Biochim. Biophys. Acta Biomembr., 1758 (2006) 1922–1944.

[82] R. Skarjune, E. Oldfield, Physical studies of cell surface and cell membrane structure Deuterium nuclear magnetic resonance studies of N-palmitoylglucosylceramide (cerebroside) head group structure, Biochemistry (Mosc.), 21 (1982) 3154–3160.
[83] C. Luna, K.M. Stroka, H. Bermudez, H. Aranda-Espinoza, Thermodynamics of monolayers formed by mixtures of phosphatidylcholine/phosphatidylserine, Colloids Surf. B Biointerfaces, 85 (2011) 293–300.
[84] I.A. Butovich, J.C. Wojtowicz, M. Molai, Human tear film and meibum Very long chain wax esters and (O-acyl)-omega-hydroxy fatty acids of meibum, J. Lipid Res., 50 (2009) 2471–2485.
[85] S.T. Tragoulias, P.J. Anderton, G.R. Dennis, F. Miano, T.J. Millar, Surface pressure measurements of human tears and individual tear film components indicate that proteins are major contributors to the surface pressure, Cornea, 24 (2005) 189–200.
[86] P.T. Janssen, O.P. van Bijsterveld, The relations between tear fluid concentrations of lysozyme, tear-specific prealbumin and lactoferrin, Exp. Eye Res., 36 (1983) 773–779.
[87] T.J. Millar, P. Mudgil, I.A. Butovich, C.K. Palaniappan, Adsorption of human tear lipocalin to human meibomian lipid films, Invest. Ophthalmol. Vis. Sci., 50 (2009) 140–151.
[88] A.M. McDermott, Antimicrobial compounds in tears, Exp. Eye Res., 117 (2013) 53–61.
[89] D.C. Phillips, The three-dimensional structure of an enzyme molecule, Sci. Am., 215 (1966) 78–90.
[90] M. Derde, V. Lechevalier, C. Guérin-Dubiard, M.-F. Cochet, S. Jan, F. Baron, M. Gautier, V. Vié, F. Nau, Hen Egg White Lysozyme Permeabilizes *Escherichia coli* Outer and Inner Membranes, J. Agric. Food Chem., 61 (2013) 9922–9929.
[91] A. Fleming, On a Remarkable Bacteriolytic Element Found in Tissues and Secretions, Proc. R. Soc. B Biol. Sci., 93 (1922) 306–317.
[92] P. Jollès, J. Jollès, What's new in lysozyme research? Always a model system, today as yesterday, Mol. Cell. Biochem., 63 (1984).
[93] C.C.F. Blake, D.F. Koenig, G.A. Mair, A.C.T. North, D.C. Phillips, V.R. Sarma, Structure of Hen Egg-White Lysozyme: A Three-dimensional Fourier Synthesis at 2 Å Resolution, Nature, 206 (1965) 757–761.
[94] M. Muraki, K. Harata, N. Sugita, K. Sato, Origin of Carbohydrate Recognition Specificity of Human Lysozyme Revealed by Affinity Labeling †, ‡, Biochemistry (Mosc.), 35 (1996) 13562–13567.
[95] W. Humphrey, A. Dalke, K. Schulten, VMD – Visual Molecular Dynamics, J. Mol. Graph., 14 (1996) 33–38.
[96] J. Stone, An Efficient Library for Parallel Ray Tracing and Animation, Computer Science Department, University of Missouri-Rolla, 1998.

[97] T.J. Dolinsky, J.E. Nielsen, J.A. McCammon, N.A. Baker, PDB2PQR: an automated pipeline for the setup of Poisson-Boltzmann electrostatics calculations, Nucleic Acids Res., 32 (2004) W665–W667.
[98] D.A. Case, D.S. Cerutti, T.E. Cheatham, III, T.A. Darden, R.E. Duke, T.J. Giese, H. Gohlke, A.W. Goetz, D. Greene, N. Homeyer, S. Izadi, A. Kovalenko, T.S. Lee, S. LeGrand, P. Li, C. Lin, J. Liu, R. Luchko, D. Luo, D. Mermelstein, et al., AMBER 2017, University of California, San Francisco, 2017.
[99] H. Li, A.D. Robertson, J.H. Jensen, Very fast empirical prediction and rationalization of protein pKa values, Proteins Struct. Funct. Bioinforma., 61 (2005) 704–721.
[100] L. Callewaert, C.W. Michiels, Lysozymes in the animal kingdom, J. Biosci., 35 (2010) 127–160.
[101] D.M. Irwin, Z.M. Gong, Molecular Evolution of Vertebrate Goose-Type Lysozyme Genes, J. Mol. Evol., 56 (2003) 234–242.
[102] P. Huang, W. Li, J. Xie, X. Yang, D. Jiang, S. Jiang, L. Yu, Characterization and expression of HLysG2, a basic goose-type lysozyme from the human eye and testis, Mol. Immunol., 48 (2011) 524–531.
[103] J. Jollès, P. Jollès, Comparison between human and bird lysozymes: Note concerning the previously observed deletion, FEBS Lett., 22 (1972) 31–33.
[104] Y. Taniyama, Y. Yamamoto, M. Nakao, M. Kikuchi, M. Ikehara, Role of disulfide bonds in folding and secretion of human lysozyme in saccharomycescerevisiae, Biochem. Biophys. Res. Commun., 152 (1988) 962–967.
[105] S.A. Roberts, I.W. Kellaway, K.M.G. Taylor, B. Warburton, K. Peters, Combined surface pressure-interfacial shear rheology studies of the interaction of proteins with spread phospholipid monolayers at the air–water interface, Int. J. Pharm., 300 (2005) 48–55.
[106] Z. Liu, B. García-Díaz, B. Catacchio, E. Chiancone, H.J. Vogel, Protecting Gram-negative bacterial cell envelopes from human lysozyme: Interactions with Ivy inhibitor proteins from Escherichia coli and Pseudomonas aeruginosa, Biochim. Biophys. Acta Biomembr., (2015).
[107] J. Huang, L. Wu, D. Yalda, Y. Adkins, S.L. Kelleher, M. Crane, B. Lonnerdal, R.L. Rodriguez, N. Huang, Expression of functional recombinant human lysozyme in transgenic rice cell culture, Transgenic Res., 11 (2002) 229–239.
[108] D.K. Sen, G.S. Sarin, Biological variations of lysozyme concentration in the tear fluids of healthy persons, Br. J. Ophthalmol., 70 (1986) 246–248.
[109] R.J. Fullard, C. Snyder, Protein levels in nonstimulated and stimulated tears of normal human subjects, Invest. Ophthalmol. Vis. Sci., 31 (1990) 1119–1126.
[110] H.J. Vogel, Lactoferrin, a bird's eye view, Biochem. Cell Biol., 90 (2012) 233–244.
[111] M.L. Groves, The Isolation of a Red Protein from Milk, J. Am. Chem. Soc., 82 (1960) 3345–3350.

[112] B. Johansson, Chromatographic Separation of Lactalbumin from Human Milk Whey on Calcium Phosphate Columns, Nature, 181 (1958) 996–997.
[113] P.L. Masson, J.F. Heremans, E. Schonne, Lactoferrin, an iron-binbng protein ni neutrophilic leukocytes, J. Exp. Med., 130 (1969) 643–658.
[114] R.M. Bennett, T. Kokocinski, Lactoferrin content of peripheral blood cells, Br. J. Haematol., 39 (1978) 509–521.
[115] J. Flanagan, M. Willcox, Role of lactoferrin in the tear film, Biochimie, 91 (2009) 35–43.
[116] V. Ng, P. Cho, S. Mak, A. Lee, Variability of tear protein levels in normal young adults: between-day variation, Graefes Arch. Clin. Exp. Ophthalmol. Albrecht Von Graefes Arch. Für Klin. Exp. Ophthalmol., 238 (2000) 892–899.
[117] M. Haridas, B.F. Anderson, E.N. Baker, Structure of human diferric lactoferrin refined at 22 A resolution, Acta Crystallogr. D Biol. Crystallogr., 51 (1995) 629–646.
[118] B.F. Anderson, H.M. Baker, E.J. Dodson, G.E. Norris, S.V. Rumball, J.M. Waters, E.N. Baker, Structure of human lactoferrin at 32-A resolution, Proc. Natl. Acad. Sci. U. S. A., 84 (1987) 1769–1773.
[119] Lactoferrin Structure Function and Genetics, in: Lact. Its Role Wound Heal., Springer Netherlands, Dordrecht, 2012: pp. 43–66.
[120] J.M. Aramini, H.J. Vogel, Quadrupolar metal ion NMR studies of metalloproteins, Biochem. Cell Biol., 76 (1998) 210–222.
[121] B.F. Anderson, H.M. Baker, G.E. Norris, D.W. Rice, E.N. Baker, Structure of human lactoferrin: crystallographic structure analysis and refinement at 28 A resolution, J. Mol. Biol., 209 (1989) 711–734.
[122] H.M. Baker, E.N. Baker, A structural perspective on lactoferrin function, Biochem. Cell Biol., 90 (2012) 320–328.
[123] S.A. González-Chávez, S. Arévalo-Gallegos, Q. Rascón-Cruz, Lactoferrin: structure, function and applications, Int. J. Antimicrob. Agents, 33 (2009) 301.e1-301.e8.
[124] J.J. Bullen, H.J. Rogers, L. Leigh, Iron-binding proteins in milk and resistance to Escherichia coli infection in infants, Br. Med. J., 1 (1972) 69–75.
[125] J. He, P. Furmanski, Sequence specificity and transcriptional activation in the binding of lactoferrin to DNA, Nature, 373 (1995) 721–724.
[126] D.I. Chan, E.J. Prenner, H.J. Vogel, Tryptophan- and arginine-rich antimicrobial peptides: Structures and mechanisms of action, Biochim. Biophys. Acta Biomembr., 1758 (2006) 1184–1202.
[127] W. Bellamy, M. Takase, K. Yamauchi, H. Wakabayashi, K. Kawase, M. Tomita, Identification of the bactericidal domain of lactoferrin, Biochim. Biophys. Acta Protein Struct. Mol. Enzymol., 1121 (1992) 130–136.
[128] H.N. Hunter, A.R. Demcoe, H. Jenssen, T.J. Gutteberg, H.J. Vogel, Human Lactoferricin Is Partially Folded in Aqueous Solution and Is Better Stabilized in a

Membrane Mimetic Solvent, Antimicrob. Agents Chemother., 49 (2005) 3387–3395.
[129] G. Iannella, G. Di Nardo, R. Plateroti, P. Rossi, A.M. Plateroti, P. Mariani, G. Magliulo, Investigation of pepsin in tears of children with laryngopharyngeal reflux disease, Int. J. Pediatr. Otorhinolaryngol., 79 (2015) 2312–2315.
[130] R.J. Fullard, D.M. Kissner, Purification of the isoforms of tear specific prealbumin, Curr. Eye Res., 10 (1991) 613–628.
[131] B. Bonavida, A.T. Sapse, E.E. Sercarz, Specific Tear Prealbumin: a Unique Lachrymal Protein absent from Serum and other Secretions, Nature, 221 (1969) 375–376.
[132] D.A. Dartt, Tear lipocalin: structure and function, Ocul. Surf., 9 (2011) 126–138.
[133] D.A. Breustedt, I.P. Korndörfer, B. Redl, A. Skerra, The 18-A crystal structure of human tear lipocalin reveals an extended branched cavity with capacity for multiple ligands, J. Biol. Chem., 280 (2005) 484–493.
[134] D.R. Flower, A.C.T. North, T.K. Attwood, Structure and sequence relationships in the lipocalins and related proteins, Protein Sci., 2 (1993) 753–761.
[135] B.J. Glasgow, O.K. Gasymov, Focus on Molecules: Tear lipocalin, Exp. Eye Res., 92 (2011) 242–243.
[136] B.J. Glasgow, A.R. Abduragimov, Z.T. Farahbakhsh, K.F. Faull, W.L. Hubbell, Tear lipocalins bind a broad array of lipid ligands, Curr. Eye Res., 14 (1995) 363–372.
[137] M. Fluckinger, H. Haas, P. Merschak, B.J. Glasgow, B. Redl, Human tear lipocalin exhibits antimicrobial activity by scavenging microbial siderophores, Antimicrob. Agents Chemother., 48 (2004) 3367–3372.
[138] H. Saaren-Seppälä, M. Jauhiainen, T.M.T. Tervo, B. Redl, P.K.J. Kinnunen, J.M. Holopainen, Interaction of purified tear lipocalin with lipid membranes, Invest. Ophthalmol. Vis. Sci., 46 (2005) 3649–3656.
[139] P. Mudgil, T.J. Millar, Adsorption of apo- and holo-tear lipocalin to a bovine Meibomian lipid film, Exp. Eye Res., 86 (2008) 622–628.
[140] The definition and classification of dry eye disease: report of the Definition and Classification Subcommittee of the International Dry Eye WorkShop (2007), Ocul. Surf., 5 (2007) 75–92.
[141] S.M. Lam, L. Tong, B. Reux, X. Duan, A. Petznick, S.S. Yong, C.B.S. Khee, M.J. Lear, M.R. Wenk, G. Shui, Lipidomic analysis of human tear fluid reveals structure-specific lipid alterations in dry eye syndrome, J. Lipid Res., 55 (2014) 299–306.
[142] P. Dynarowicz-Łątka, A. Dhanabalan, O.N. Oliveira, Modern physicochemical research on Langmuir monolayers, Adv. Colloid Interface Sci., 91 (2001) 221–293.
[143] R.E. Brown, H.L. Brockman, Using Monomolecular Films to Characterize Lipid Lateral Interactions, in: T.J. McIntosh (Ed.), Lipid Rafts, Humana Press, Totowa, NJ, 2007: pp. 41–58.

[144] M. Sophocleous, Understanding and explaining surface tension and capillarity: an introduction to fundamental physics for water professionals, Hydrogeol. J., 18 (2010) 811–821.
[145] D. Hoenig, D. Moebius, Direct visualization of monolayers at the air-water interface by Brewster angle microscopy, J. Phys. Chem., 95 (1991) 4590–4592.
[146] M.W. Hawco, P.J. Davis, K.M. Keough, Lipid fluidity in lung surfactant: monolayers of saturated and unsaturated lecithins, J. Appl. Physiol., 51 (1981) 509–515.
[147] S.A. Tabak, R.H. Notter, J.S. Ultman, S.M. Dinh, Relaxation effects in the surface pressure behavior of dipalmitoyl lecithin, J. Colloid Interface Sci., 60 (1977) 117–125.
[148] L.J. Peltonen, J. Yliruusi, Surface Pressure, Hysteresis, Interfacial Tension, and CMC of Four Sorbitan Monoesters at Water–Air, Water–Hexane, and Hexane–Air Interfaces, J. Colloid Interface Sci., 227 (2000) 1–6.
[149] C. Alonso, T. Alig, J. Yoon, F. Bringezu, H. Warriner, J.A. Zasadzinski, More Than a Monolayer: Relating Lung Surfactant Structure and Mechanics to Composition, Biophys. J., 87 (2004) 4188–4202.
[150] S.Y. Nishimura, G.M. Magana, H.A. Ketelson, G.G. Fuller, Effect of lysozyme adsorption on the interfacial rheology of DPPC and cholesteryl myristate films, Langmuir ACS J. Surf. Colloids, 24 (2008) 11728–11733.
[151] X. Lu, R. Shi, C. Hao, H. Chen, L. Zhang, J. Li, G. Xu, R. Sun, Behavior of lysozyme adsorbed onto biological liquid crystal lipid monolayer at the air/water interface, Chin. Phys. B, 25 (2016) 090506.
[152] M. Patterson, Biophysical Characterization of a Biomimetic from the Tear Film Lipid Layer, University of Calgary, 2014.
[153] M. Patterson, H.J. Vogel, E.J. Prenner, Interactions of lysozyme with a tear film polar lipid layer biomimetic, Biochem. Cell Biol.-Biochim. Biol. Cell., 92 (2014) 587–587.
[154] M. Patterson, H.J. Vogel, E.J. Prenner, Biophysical characterization of monofilm model systems composed of selected tear film phospholipids, Biochim. Biophys. Acta Biomembr., 1858 (2016) 403–414.
[155] M. Patterson, H.J. Vogel, E.J. Prenner, The effect of repeated lateral compression and expansions mimicking blinking on selected tear film polar lipid monofilms, Biochim. Biophys. Acta Biomembr., 1859 (2017) 319–330.
[156] W.E. Shine, J.P. McCulley, Ocular sicca signs associated with meibomian gland secretion polar lipids, Iovs, 39 (1998) S533–S533.
[157] A.J. Bron, J.M. Tiffany, S.M. Gouveia, N. Yokoi, L.W. Voon, Functional aspects of the tear film lipid layer, Exp. Eye Res., 78 (2004) 347–360.
[158] M. Broniatowski, M. Flasiński, P. Dynarowicz-Łątka, J. Majewski, Grazing Incidence Diffraction and X-ray Reflectivity Studies of the Interactions of Inorganic Mercury Salts with Membrane Lipids in Langmuir Monolayers at the Air/Water Interface, J. Phys. Chem. B, 114 (2010) 9474–9484.

[159] G. Tae, H. Yang, K. Shin, S.K. Satija, N. Torikai, X-ray reflectivity study of a transcription-activating factor-derived peptide penetration into the model phospholipid monolayers, J. Pept. Sci., 14 (2008) 461–468.
[160] S. Sakamoto, H. Nakahara, O. Shibata, Miscibility behavior of sphingomyelin with phytosterol derivatives by a Langmuir monolayer approach, J. Oleo Sci., 62 (2013) 809–824.
[161] E. Guzmán, L. Liggieri, E. Santini, M. Ferrari, F. Ravera, Effect of Hydrophilic and Hydrophobic Nanoparticles on the Surface Pressure Response of DPPC Monolayers, J. Phys. Chem. C, 115 (2011) 21715–21722.
[162] A.R.P. Varela, A.M.P.S. Gonçalves da Silva, A. Fedorov, A.H. Futerman, M. Prieto, L.C. Silva, Effect of glucosylceramide on the biophysical properties of fluid membranes, Biochim. Biophys. Acta Biomembr., 1828 (2013) 1122–1130.
[163] B. Sandrino, E.C. Wrobel, T.M. Nobre, L. Caseli, S.R. Lazaro, A.C. Júnior, J.R. Garcia, O.N. Oliveira, K. Wohnrath, Interaction between active ruthenium complex [RuCl 3 (dppb)(VPy)] and phospholipid Langmuir monolayers: Effects on membrane electrical properties, Chem. Phys. Lett., 649 (2016) 29–36.
[164] K.A. Suresh, J. Nittmann, F. Rondelez, Pattern growth during the liquid expanded-liquid condensed phase transition in langmuir monolayers of myristic acid, in: P. Bothorel, E.J. Dufourc (Eds.), Trends Colloid Interface Sci. III, Steinkopff, Darmstadt, 1989: pp. 184–193.
[165] D. Gidalevitz, Y. Ishitsuka, A.S. Muresan, O. Konovalov, A.J. Waring, R.I. Lehrer, K.Y.C. Lee, Interaction of antimicrobial peptide protegrin with biomembranes, Proc. Natl. Acad. Sci., 100 (2003) 6302–6307.
[166] S. Leekumjorn, A.K. Sum, Molecular Simulation Study of Structural and Dynamic Properties of Mixed DPPC/DPPE Bilayers, Biophys. J., 90 (2006) 3951–3965.
[167] V.M. Kaganer, H. Möhwald, P. Dutta, Structure and phase transitions in Langmuir monolayers, Rev. Mod. Phys., 71 (1999) 779.
[168] F. Wei, W. Xiong, W. Li, W. Lu, H.C. Allen, W. Zheng, Assembly and relaxation behaviours of phosphatidylethanolamine monolayers investigated by polarization and frequency resolved SFG-VS, Phys Chem Chem Phys, 17 (2015) 25114–25122.
[169] S. Sonnino, A. Prinetti, L. Mauri, V. Chigorno, G. Tettamanti, Dynamic and Structural Properties of Sphingolipids as Driving Forces for the Formation of Membrane Domains, Chem. Rev., 106 (2006) 2111–2125.
[170] P.B. Hitchcock, R. Mason, K.M. Thomas, G.G. Shipley, Structural chemistry of 1,2 dilauroyl-DL-phosphatidylethanolamine: molecular conformation and intermolecular packing of phospholipids, Proc. Natl. Acad. Sci. U. S. A., 71 (1974) 3036–3040.
[171] M. Kuikka, B. Ramstedt, H. Ohvo-Rekilä, J. Tuuf, J.P. Slotte, Membrane Properties of D-erythro-N-acyl Sphingomyelins and Their Corresponding Dihydro Species, Biophys. J., 80 (2001) 2327–2337.
[172] E.N. Baker, H.M. Baker, Molecular structure, binding properties and dynamics of lactoferrin, Cell. Mol. Life Sci. CMLS, 62 (2005) 2531–2539.

[173] D. Vaknin, M.S. Kelley, B.M. Ocko, Sphingomyelin at the air–water interface, J. Chem. Phys., 115 (2001) 7697–7704.
[174] J. Miñones, J.. Rodríguez Patino, O. Conde, C. Carrera, R. Seoane, The effect of polar groups on structural characteristics of phospholipid monolayers spread at the air–water interface, Colloids Surf. Physicochem. Eng. Asp., 203 (2002) 273–286.
[175] G.E.G. Gonçalves, F.S. de Souza, J.H.G. Lago, L. Caseli, The interaction of eugenol with cell membrane models at the air–water interface is modulated by the lipid monolayer composition, Biophys. Chem., 207 (2015) 7–12.
[176] J.M. Crane, G. Putz, S.B. Hall, Persistence of Phase Coexistence in Disaturated Phosphatidylcholine Monolayers at High Surface Pressures, Biophys. J., 77 (1999) 3134–3143.
[177] E.C. Smith, J.M. Crane, T.G. Laderas, S.B. Hall, Metastability of a Supercompressed Fluid Monolayer, Biophys. J., 85 (2003) 3048–3057.
[178] N. Nandi, D. Vollhardt, Effect of Molecular Chirality on the Morphology of Biomimetic Langmuir Monolayers, Chem. Rev., 103 (2003) 4033–4076.
[179] P. Kulovesi, J. Telenius, A. Koivuniemi, G. Brezesinski, A. Rantamäki, T. Viitala, E. Puukilainen, M. Ritala, S.K. Wiedmer, I. Vattulainen, J.M. Holopainen, Molecular Organization of the Tear Fluid Lipid Layer, Biophys. J., 99 (2010) 2559–2567.
[180] J. Telenius, A. Koivuniemi, P. Kulovesi, J.M. Holopainen, I. Vattulainen, Role of Neutral Lipids in Tear Fluid Lipid Layer: Coarse-Grained Simulation Study, Langmuir, 28 (2012) 17092–17100.
[181] A. Wizert, D.R. Iskander, L. Cwiklik, Organization of Lipids in the Tear Film: A Molecular-Level View, PLoS ONE, 9 (2014) e92461.
[182] T.F. Svitova, M.C. Lin, Thick Human Tear Lipid Films: Effect of Lipids Interaction with Model Tear Proteins on Interfacial Properties, Invest. Ophthalmol. Vis. Sci., 55 (2014) 41–41.
[183] T. Al Kayal, S. Nappini, E. Russo, D. Berti, M. Bucciantini, M. Stefani, P. Baglioni, Lysozyme interaction with negatively charged lipid bilayers: protein aggregation and membrane fusion, Soft Matter, 8 (2012) 4524.
[184] A.M. Melo, J.C. Ricardo, A. Fedorov, M. Prieto, A. Coutinho, Fluorescence Detection of Lipid-Induced Oligomeric Intermediates Involved in Lysozyme "Amyloid-Like" Fiber Formation Driven by Anionic Membranes, J. Phys. Chem. B, 117 (2013) 2906–2917.
[185] M. Ohno, T. Toyota, T. Nomoto, M. Fujinami, Interfacial tension in adsorption of lysozyme onto a lipid monolayer formed at a water/chloroform interface, Colloids Surf. Physicochem. Eng. Asp., 480 (2015) 85–90.
[186] V.M. Trusova, G.P. Gorbenko, I. Akopova, J.G. Molotkovsky, I. Gryczynski, J. Borejdo, Z. Gryczynski, Morphological changes of supported lipid bilayers induced by lysozyme: Planar domain formation vs multilayer stacking, Colloids Surf. B Biointerfaces, 80 (2010) 219–226.

[187] T. Al Kayal, E. Russo, L. Pieri, G. Caminati, D. Berti, M. Bucciantini, M. Stefani, P. Baglioni, Interactions of lysozyme with phospholipid vesicles: effects of vesicle biophysical features on protein misfolding and aggregation, Soft Matter, 8 (2012) 9115.
[188] M. Derde, F. Nau, C. Guérin-Dubiard, V. Lechevalier, G. Paboeuf, S. Jan, F. Baron, M. Gautier, V. Vié, Native and dry-heated lysozyme interactions with membrane lipid monolayers: Lipid packing modifications of a phospholipid mixture, model of the Escherichia coli cytoplasmic membrane, Biochim. Biophys. Acta Biomembr., 1848 (2015) 1065–1073.
[189] G.P. Gorbenko, V.M. Ioffe, P.K.J. Kinnunen, Binding of Lysozyme to Phospholipid Bilayers: Evidence for Protein Aggregation upon Membrane Association, Biophys. J., 93 (2007) 140–153.
[190] J.-J. Luo, F.-G. Wu, S.-S. Qin, Z.-W. Yu, In Situ Unfolded Lysozyme Induces the Lipid Lateral Redistribution of a Mixed Lipid Model Membrane, J. Phys. Chem. B, 116 (2012) 12381–12388.
[191] M. Arias, A.L. Hilchie, E.F. Haney, J.G.M. Bolscher, M.E. Hyndman, R.E.W. Hancock, H.J. Vogel, Anticancer activities of bovine and human lactoferricin-derived peptides [1], Biochem. Cell Biol., 95 (2017) 91–98.
[192] M. Arias, L.J. McDonald, E.F. Haney, K. Nazmi, J.G.M. Bolscher, H.J. Vogel, Bovine and human lactoferricin peptides: chimeras and new cyclic analogs, BioMetals, 27 (2014) 935–948.
[193] P. Mudgil, M. Torres, T.J. Millar, Adsorption of lysozyme to phospholipid and meibomian lipid monolayer films, Colloids Surf. B Biointerfaces, 48 (2006) 128–137.
[194] K. Arnold, D. Hoekstra, S. Ohki, Association of lysozyme to phospholipid surfaces and vesicle fusion, Biochim. Biophys. Acta Lipids Lipid Metab., 1124 (1992) 88–94.
[195] D. Marsh, Lateral pressure in membranes, Biochim. Biophys. Acta Rev. Biomembr., 1286 (1996) 183–223.
[196] W. Jing, E.J. Prenner, H.J. Vogel, A.J. Waring, R.I. Lehrer, K. Lohner, Headgroup structure and fatty acid chain length of the acidic phospholipids modulate the interaction of membrane mimetic vesicles with the antimicrobial peptide protegrin-1, J. Pept. Sci., 11 (2005) 735–743.
[197] F. Miano, M. Calcara, T.J. Millar, V. Enea, Insertion of tear proteins into a meibomian lipids film, Colloids Surf. B Biointerfaces, 44 (2005) 49–55.
[198] O.K. Gasymov, A.R. Abduragimov, T.N. Yusifov, B.J. Glasgow, Structural changes in human tear lipocalins associated with lipid binding, Biochim. Biophys. Acta BBA - Protein Struct. Mol. Enzymol., 1386 (1998) 145–156.
[199] A. Tsanova, G.A. Georgiev, Z. Lalchev, In Vitro Application of Langmuir Monolayer Model to Study In Vivo Biological Systems, Biotechnol. Biotechnol. Equip., 26 (2012) 185–190.

[200] D.F. Kienle, J.V. de Souza, E.B. Watkins, T.L. Kuhl, Thickness and refractive index of DPPC and DPPE monolayers by multiple-beam interferometry, Anal. Bioanal. Chem., 406 (2014) 4725–4733.
[201] K.J. Klopfer, T.K. Vanderlick, Isotherms of Dipalmitoylphosphatidylcholine (DPPC) Monolayers: Features Revealed and Features Obscured, J. Colloid Interface Sci., 182 (1996) 220–229.
[202] C.W. McConlogue, T.K. Vanderlick, A Close Look at Domain Formation in DPPC Monolayers, Langmuir, 13 (1997) 7158–7164.
[203] X. Chen, Z. Huang, W. Hua, H. Castada, H.C. Allen, Reorganization and Caging of DPPC, DPPE, DPPG, and DPPS Monolayers Caused by Dimethylsulfoxide Observed Using Brewster Angle Microscopy, Langmuir, 26 (2010) 18902–18908.
[204] C. Blesso, Egg Phospholipids and Cardiovascular Health, Nutrients, 7 (2015) 2731–2747.
[205] G.A. Georgiev, P. Eftimov, N. Yokoi, Structure-function relationship of tear film lipid layer: A contemporary perspective, Exp. Eye Res., 163 (2017) 17–28.
[206] T. Ganz, Increased inflammation in lysozyme M-deficient mice in response to Micrococcus luteus and its peptidoglycan, Blood, 101 (2003) 2388–2392.
[207] P.P. Ward, M. Mendoza-Meneses, P.W. Park, O.M. Conneely, Stimulus-Dependent Impairment of the Neutrophil Oxidative Burst Response in Lactoferrin-Deficient Mice, Am. J. Pathol., 172 (2008) 1019–1029.
[208] M.D.P. Willcox, P. Argüeso, G.A. Georgiev, J.M. Holopainen, G.W. Laurie, T.J. Millar, E.B. Papas, J.P. Rolland, T.A. Schmidt, U. Stahl, T. Suarez, L.N. Subbaraman, O.Ö. Uçakhan, L. Jones, TFOS DEWS II Tear Film Report, Ocul. Surf., 15 (2017) 366–403.

Appendix

Permission for figure 3.11 (page 81) from Wizert *et al.* © **Wizert et al.** Wizert A, Iskander DR, Cwiklik L. Organization of Lipids in the Tear Film: A Molecular-Level View. Roccatano D, editor. PLoS ONE. 2014 Mar 20;9(3):e92461. Image url: https://doi:10.1371/journal.pone.0092461.g008, licensed under CC BY 4.0.

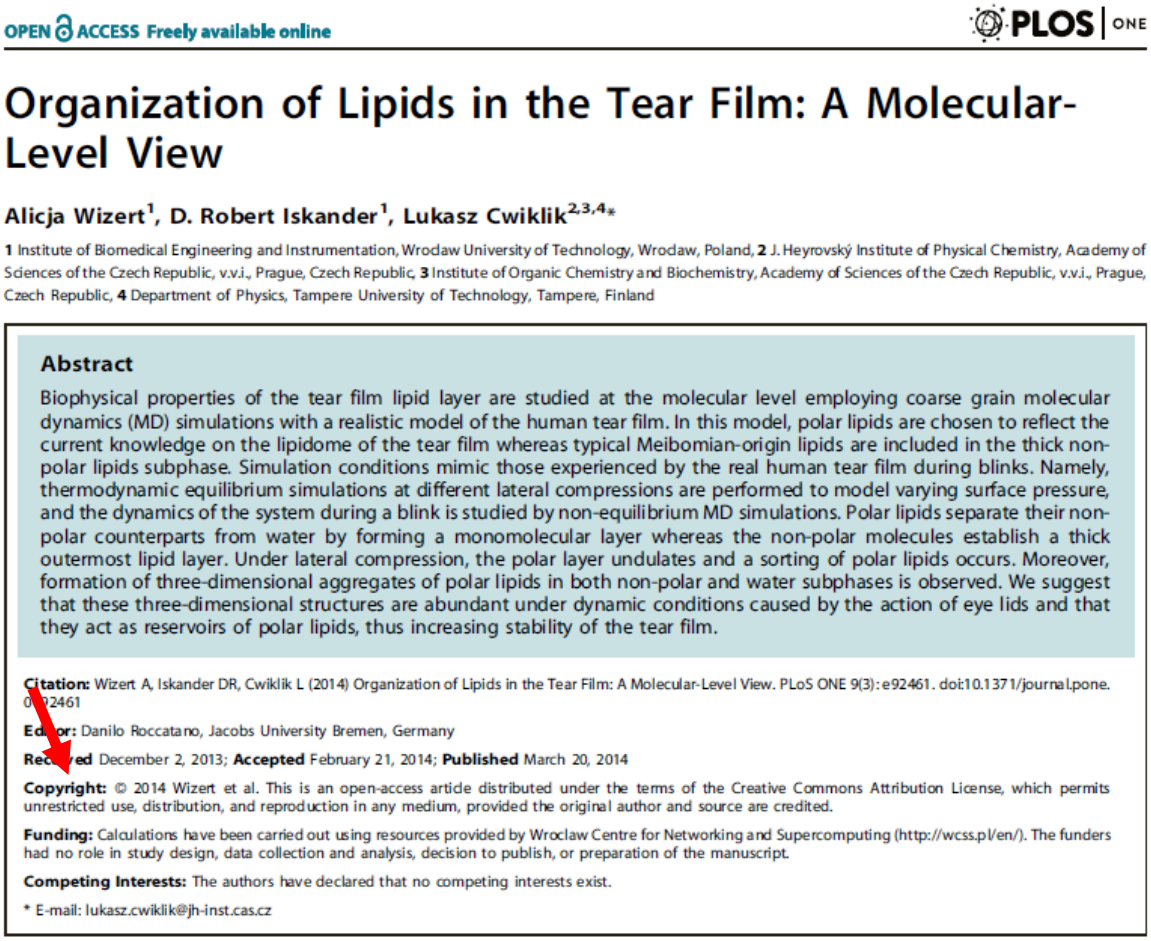

OPEN ACCESS Freely available online

PLOS | ONE

Organization of Lipids in the Tear Film: A Molecular-Level View

Alicja Wizert[1], D. Robert Iskander[1], Lukasz Cwiklik[2,3,4]*

1 Institute of Biomedical Engineering and Instrumentation, Wrocław University of Technology, Wrocław, Poland, **2** J. Heyrovský Institute of Physical Chemistry, Academy of Sciences of the Czech Republic, v.v.i., Prague, Czech Republic, **3** Institute of Organic Chemistry and Biochemistry, Academy of Sciences of the Czech Republic, v.v.i., Prague, Czech Republic, **4** Department of Physics, Tampere University of Technology, Tampere, Finland

Abstract

Biophysical properties of the tear film lipid layer are studied at the molecular level employing coarse grain molecular dynamics (MD) simulations with a realistic model of the human tear film. In this model, polar lipids are chosen to reflect the current knowledge on the lipidome of the tear film whereas typical Meibomian-origin lipids are included in the thick non-polar lipids subphase. Simulation conditions mimic those experienced by the real human tear film during blinks. Namely, thermodynamic equilibrium simulations at different lateral compressions are performed to model varying surface pressure, and the dynamics of the system during a blink is studied by non-equilibrium MD simulations. Polar lipids separate their non-polar counterparts from water by forming a monomolecular layer whereas the non-polar molecules establish a thick outermost lipid layer. Under lateral compression, the polar layer undulates and a sorting of polar lipids occurs. Moreover, formation of three-dimensional aggregates of polar lipids in both non-polar and water subphases is observed. We suggest that these three-dimensional structures are abundant under dynamic conditions caused by the action of eye lids and that they act as reservoirs of polar lipids, thus increasing stability of the tear film.

Citation: Wizert A, Iskander DR, Cwiklik L (2014) Organization of Lipids in the Tear Film: A Molecular-Level View. PLoS ONE 9(3): e92461. doi:10.1371/journal.pone.0092461

Editor: Danilo Roccatano, Jacobs University Bremen, Germany

Received December 2, 2013; **Accepted** February 21, 2014; **Published** March 20, 2014

Funding: Calculations have been carried out using resources provided by Wrocław Centre for Networking and Supercomputing (http://wcss.pl/en/). The funders had no role in study design, data collection and analysis, decision to publish, or preparation of the manuscript.

Competing Interests: The authors have declared that no competing interests exist.

* E-mail: lukasz.cwiklik@jh-inst.cas.cz